Microglial-mediated inflammatory responses and perturbed vasculature in an animal model of inflamed Alzheimer's disease brain

by

Jae Kyu Ryu

B.HSc., Yonsei University, 1999
M.Sc., Ajou University, 2001

A THESIS SUBMITTED IN PARTIAL FULFILMENT OF
THE REQUIREMENTS FOR THE DEGREE OF

DOCTOR OF PHILOSOPHY

in

THE FACULTY OF GRADUATE STUDIES
(Pharmacology)

THE UNIVERSITY OF BRITISH COLUMBIA

(Vancouver)

April 2008

ABSTRACT

Chronic inflammation in response to Aβ peptide deposits is a pathological hallmark of Alzheimer's disease (AD). The inflammatory environment includes populations of reactive and proliferating microglia and astrocytes and perturbed vasculature. However, the association between activated glial cells and cerebrovascular dysfunction remain largely unknown. This study has used $A\beta_{1-42}$ intrahippocampal injection as an animal model of inflamed AD brain to characterize mechanisms of glial-vasculature responses as a basis for chronic inflammation.

Preliminary findings suggested $A\beta_{1-42}$-injected brain demonstrated vascular remodeling including evidence for formation of new blood vessels (angiogenesis). This result led to study of the effects of the anti-angiogenic/anti-inflammatory compound, thalidomide on activated glial cells and perturbations in the vasculature in an $A\beta_{1-42}$ peptide-injected rat model. First, $A\beta_{1-42}$ injection was found to cause perturbations in vasculature including new blood vessel formation and increased BBB leakiness. Second, thalidomide decreased the vascular perturbations and the glial reactivity and conferred neuroprotection. Overall, these results suggest that altered cerebral vasculature is integral to the overall inflammatory response induced by peptide.

Experiments then examined the level of parenchymal plasma proteins in brain tissue from AD and nondemented (ND) individuals. AD, but not ND, brain tissue demonstrated high levels of fibrinogen immunoreactivity (ir). $A\beta_{1-42}$ injection into the rat hippocampus increased the level of parenchymal fibrinogen, which was reduced by treatment with the defibrinogenating agent, ancrod. In addition, ancrod also attenuated microglial activation and prevented neuronal injury. Overall, these results demonstrate that extravasation of blood protein and a leaky BBB are important in promoting and amplifying inflammatory responses and causing neuronal damage in inflamed AD brain.

Microglial chemotactic responses to VEGF (vascular endothelial growth factor) receptor Flt-1 were next studied. Treatment with a monoclonal antibody to Flt-1 (anti-Flt-1 Ab) in the peptide-injected hippocampus diminished microglial reactivity and provided neuroprotection. Secondly, anti-Flt-1 Ab inhibited the $A\beta_{1-42}$-induced migration of human microglia. These results suggest critical functional roles for Flt-1 in mediating microglial chemotaxis and inflammatory responses in AD brain.

The overall conclusion from my work is that Aβ deposits induce microglial reactivity which subsequently causes vascular remodeling resulting in an amplified inflammatory microenvironment which is damaging to bystander neurons.

TABLE OF CONTENTS

LIST OF TABLES

LIST OF FIGURES

LIST OF ABBREVIATIONS

Aβ	amyloid beta-peptide
$A\beta_{1-42}$	42-residue C-terminal variant of amyloid beta peptide
$A\beta_{42-1}$	42-residue C-terminal variant of reverse amyloid beta peptide
ABC	avidin-biotin-peroxidase kit
AD	Alzheimer's disease
ANOVA	analysis of variance
AP	anteriorposterior
ApoE	apolipoprotein E
APP	amyloid precursor protein
BACE1	β-site APP cleaving enzyme 1
BBB	blood-brain barrier
bFGF	basic fibroblast growth factor
BSA	bovine serum albumin
CAA	cerebro-amyloid angiopathy
CMC	carboxymethylcellulose
CNS	central nervous system
COX	cyclooxygenase
CSF	cerebrospinal fluid
CSPGs	chondroitin sulfate proteoglycans
DAB	3,3'-diaminobenzidine
DMEM	Dulbecco's modified Eagle's medium
DV	dorsoventral
EAE	experimental encephalomyelitis
ECM	extracellular matrix
EGFP	enhanced green fluorescent protein
FBS	fetal bovine serum
Flt-1	vascular endothelial growth factor receptor-1
Flt-4	VEGF receptor-3
GCL	granule cell layer
GFAP	glial fibrillary acidic protein
H_2O_2	hydrogen peroxide
HPLC	high-performance liquid chromatography
HSPGs	heparin sulfate proteoglycans
i.p.	intraperitoneal
Iba-1	anti-ionized calcium binding adapter molecule-1
IgG	immunoglobulin G
IL	interleukin
ir	immunoreactivity
KDR/Flk-1	VEGF receptor-2
LPR	lipoprotein receptor-related protein
MC	minocycline
MCP	monocyte chemotactic protein
MIP	macrophage inflammatory protein;
ML	mediallateral
ML	molecular layer

MMLV	Moloney Murine Leukemia Virus
MPTP	1-methyl-4-phenyl-1,2,3,6-tetrahydropyridine
MS	multiple sclerosis
ND	nondemented
NeuN	neuronal nuclei
NGS	normal goat serum
NSAIDs	non-steroidal anti-inflammatory drug products
3-NT	3-nitrotyrosine
PAF	platelet activating factor
PB	phosphate buffer
PBST	phosphate buffered saline with Triton X-100
PS1	presenilin 1
PS2	presenilin 2
RA	rheumatoid arthritis
RAGE	advanced glycation end-products
RECA-1	rat endothelial cell antigen-1, RECA-1
RT	room temperature
SEC	serpin enzyme complex
TGF	transforming growth factor
TNF-α	tumor necrosis factor-α
tPA	tissue plasminogen activator
TU	transducing units
uPA	urokinase plasminogen activator
VEGF	vascular endothelial growth factor
vWF	von Willebrand factor

ACKNOWLEDGEMENTS

I would like to express my sincere gratitude to my supervisor, Dr. James G. McLarnon for his excellent scientific guidance, never-ending support, and all his personal help. His scientific brilliance and profound knowledge have made this thesis possible. I am grateful to my committee members Dr. Lynn Raymond, Dr. Brian Conway, and Dr. Blair Leavitt for their scientific guidance and support into this work.

I would like to make special thanks to: Dr. Seung U. Kim, Dr. Hyun B. Choi, Dr. Sonia Franciosi, Taesup Cho, Dr. Atushi Nagai, Dr. Kozo Hatori, Dr. Min C. Lee, Dr. Byung K. Jin, Dr. Ismail Laher, Dr. David Godin, Wei Wei, Tran Karen, Nattinee Jantaratnotai, Prasongchai Sattayaprasert, Dr. Han S. Jeong, Dr. Jong S. Park for their friendship, invaluable helps in various aspect, and sharing their scientific knowledge.

I would also like to extend my gratitude to Dr. Patrick McGeer and his lab members for their kindness to allow me to use the experimental facilities in his lab and for sharing scientific knowledge and to Dr. Yu Tian Wang and his lab members for collaboration and valuable discussion and to Dr. Douglas Walker for giving us great help on experimental human materials for my work.

I wish to express special thanks to the Faculty, Staff and students in the department of Anesthesiology, Pharmacology, and Therapeutics, UBC.

I would like to recognize my parents and my sister and her family for their love and encouragement throughout my years.

Finally, I wish to express my deepest thanks to my wife Hye Kyoung Kim and my lovely daughter Eunbi Ryu for their love, patience and understanding.

The studies in this thesis were supported by fellowships from a Michael Smith Memorial Fellowship and University Graduate Fellowship and grants from the Pacific Alzheimer Research Foundation, Alzheimer's Association USA, and Alzheimer's Society of Canada.

DEDICATION

I would like to dedicate this thesis to my parents, wife Hye Kyoung and daughter Eunbi.

CO-AUTHORSHIP STATEMENT

The chapters in this thesis contain work that has been previously published or submitted for publication in peer-reviewed journals

Ryu JK and McLarnon JG. Minocycline or iNOS inhibition block 3-nitrotyrosine increases and blood-brain barrier leakiness in amyloid-beta peptide-injected rat hippocampus. This study has been published in Experimental Neurology (presented here as Chapter Two).

Ryu JK and McLarnon JG. Thalidomide inhibition of perturbed vasculature and glial-derived tumor necrosis factor-α in an animal model of inflamed Alzheimer's disease brain. This study has been published in Neurobiology of Disease (presented here as Chapter Three).

Ryu JK and McLarnon JG. A leaky blood-brain barrier and fibrinogen infiltration in inflamed Alzheimer's disease brain. This study has been submitted to Brain (presented here as Chapter Four).

Ryu JK, Choi HB, Cho T, Wang YT and McLarnon JG. Microglial VEGF receptor response is an integral chemotactic component in Alzheimer's disease pathology. This study has been submitted to Journal of Neuroscience (presented here as Chapter Five).

The thesis author Jae Kyu Ryu was the primary researcher for all the results presented in the articles above. Jae Kyu Ryu contributed to design of research, performed animal experiments, analyzed data, and manuscript preparation. Dr. James G. McLarnon identified and designed the research, analyzed data and revised the manuscript. Dr. Hyun B. Choi performed RT-PCR and analyzed data. Taesup Cho conducted rat microglial cell culture. Dr. Yu Tian Wang contributed new reagents/analytic tools. Microglia prepared from AD and ND cases were provided by Dr. Douglas G. Walker (Sun Health Research Institute, AZ, USA). Dr. Patrick McGeer (UBC, BC, Canada) provided tissue sections from AD and ND cases.

CHAPTER 1: INTRODUCTION

1.1 ALZHEIMER'S DISEASE

Alzheimer's disease (AD) is a slowly progressive neurodegenerative disease of the brain, characterized by significant loss of intellectual abilities such as learning and memory. Although memory impairment may result from a variety of causes, AD is the most common cause of memory loss and cognitive impairment. AD individuals present clinical signs including progressive memory loss, difficulty of performing familiar tasks, disturbances in language and perception, and personality changes (Förstl and Kurz, 1999). AD is diagnosed as a neuropathological condition based on the presence of the accumulation of senile plaques, deposits of polymorphous amyloid β-peptide (Aβ) and neurofibrillary tangles consisting of intracellular bundles of self-assembled hyperphosphorylated microtubule-associated proteins (tau) (Kosik et al., 1986; Selkoe, 1994). Aβ peptide is derived from enzymatic degradation of amyloid precursor protein (APP, an integral membrane glycoprotein). APP can be proteolytically processed by different secretase activity (α-, β-, and γ-secretases) via two distinct intracellular metabolic pathways: non-amyloidogenic and amyloidogenic pathways. In the non-amyloidogenic pathway, APP is cleaved within the Aβ sequence by α-secretase, to yield a soluble N-terminal fragment (sAPPα) and an intracellular C-terminal membrane-bound fragment (CTFα) (Oltersdorf et al., 1990). Although the primary function of sAPPα is not known, it has been implicated as a regulator of synaptogenesis, neurite outgrowth and neuronal survival (Turner et al., 2003; Priller et al., 2006). CTFα is further cleaved by γ-secretase, giving rise to a soluble N-terminal fragment (p3) and a membrane-anchored C-terminal fragment (AICD, or APP intracellular domain). The amyloidogenic pathways release amyloid-β (Aβ, a 39- to 42-amino acid peptide) which is derived from APP by sequential processing with β-secretase (β-site APP cleavage enzyme, BACE) and γ-secretase (a multiprotein complex, comprised of presenilin, nicastrin, anterior pharynx defective-1 and presenilin enhancer-2) (Vassar et al., 1999).

The causes of AD are not known, however, phospho-tau of the neurofibrillary tangles and Aβ peptide deposits have received considerable attention as pathological mechanisms for AD. Indeed, numerous studies have shown these histopathological patterns to be present in the brain tissue of AD patients (Glenner, 1989; Akiyama et al., 2000; McGeer and McGeer, 2007). An aggregation of filamentous tau has been suggested to be linked to the neuronal degeneration in AD (Mandelkow and Mandelkow, 1998). An over-expression of human tau mutant in cultured

neurons exhibited degenerative patterns of neurofilaments (Hall et al., 1997), and similar patterns of neurofibrillary degeneration can be produced *in vivo* from chronic human tau fillament aggregation (Hall et al., 2000). Nevertheless, the "tau-hypothesis" has not been supported by much experimental evidence. Recent studies from tetracycline-regulated, mutant human tau transgenic mice demonstrated that neurofibrillary tangles are not able to cause neuronal degeneration in this model (Santacruz et al., 2005). A similar conclusion was reached by Andorfer et al (2005) who investigated non-mutant human tau transgenic mice. Furthermore, no clear evidence of correlation between tau filament formation and microtubule damage was found in brain tissue from AD patients (Cash et al., 2003). These experimental and clinical studies are not consistent with tau as a causative factor in AD pathogenesis.

Considerable evidence suggests that accumulated Aβ is the most important factor in AD pathology. Genetic studies have identified the several inherited specific genes that are associated with an increased risk for developing early- and late-onset familial forms of AD (familial AD, FAD) (Pastor and Goate, 2004). Linkage and cloning analyses indicate that three dominantly inherited genes of the amyloidogenic molecules: amyloid precursor protein (APP, chromosome 21), presenilin 1 (PS1, chromosome 14), and presenilin 2 (PS2, chromosome 1) are associated with early-onset FAD (Goate et al., 1991; Sherrington et al., 1995; Levy-Lahad et al., 1995). Extracellular deposition of β-amyloid protein, the major component of amyloid plaques is consistently present in early-onset AD patients with mutations of the genes encoding APP, PS1, and PS2. This provides evidence for a relationship between the abnormal accumulation of Aβ and the onset of AD (Czech et al., 2000). However, early-onset FAD comprises only about 5% of all AD cases, with most AD cases being late-onset (termed sporadic; developing after age 65). Although no obvious genetic inheritance pattern has been found in sporadic AD, previous studies have identified an increased risk of developing sporadic AD in relation to the apolipoprotein E (ApoE) gene (Corder et al., 1993; Tsai et al., 1994). Further studies found that the APOE e4 allele is associated with an increased number of amyloid plaques, in brain tissue from AD patients (Nagy et al., 1995; Polvikoski et al., 1995). Nevertheless, the e4 variant of the ApoE gene is only involved in 50% of the AD cases (Katzman, 1994). Recent studies on the Aβ processing pathways suggest that inherited variants of the SORL1 neuronal sorting receptor are also associated with an accumulation of Aβ and late-onset AD (Lee et al., 2007; Rogaeva et al., 2007).

Although neuropathological similarities have been observed between AD patient brains such as neurofibrillary tangles and senile plaques in the neocortex, this brain disease does not exhibit

a single type of neurodegenerative disorder. Different contributing factors seem to be involved including inheritance (familial or sporadic), rate of disease progression, age of onset and motor deficit. Recently, clinical and biological studies have provided additional evidence for the presence of subtypes and heterogeneity in AD patients. For example, studies with PET scans have demonstrated that different regional cerebral glucose metabolic activity is associated with heterogeneous patterns of cognitive deficit in AD patients. Neurochemical studies with human AD brains have shown different degrees of neuronal damage in cholinergic, noradrenergic, and serotonergic systems, which could be involved in the heterogeneous cognitive dysfunction seen in AD patients (Reinikainen et al., 1988). AD brains can also exhibit considerable differences in vascular abnormalities (Kalaria, 1996). Heterogeneous behavioral and neuropsychological manifestations are also indicated in AD clinical studies.

Many associations have been noted between AD and various risk factors, with the latter including female gender (Andersen et al., 1999), high blood pressure (Kehoe and Wilcock, 2007), cerebrovascular disease (Stampfer, 2006), diabetes (Irie et al., 2008), head injury (Van Den Heuvel et al., 2007) and elevated blood cholesterol (Sjögren et al., 2006). Population studies, however, have not been able to differentiate between factors which may be causative and those which are merely associative. The most important risk factor for the development of AD is increasing age. The incidence of having AD increases substantially after the age of 65 and AD will affect 50% of those who are over 85 years of age. According to recent studies, 26 million people worldwide have AD today, and that number is expected to be more than 100 million people by 2050 if no effective treatment is found for the disease (Ferri et al., 2005).

Previous studies have shown that both genetic and environmental factors contribute to the accumulation of amyloid plaques in the brains of transgenic AD mice (Price and Sisodia, 1998; Lazarov et al., 2005). In neuropathological examinations, however, the density of amyloid plaques is not strongly correlated with the neuronal loss or severity of cognitive deficits in AD (Gómez-Isla et al., 1996; Giannakopoulos et al., 2003). These findings emphasize the importance of the interaction between other pathological processes in the AD brain. Accumulated amyloid deposits are associated with an up-regulated immune response including activated glial cells, microglia and astrocytes, and vascular pathologies (Kalaria, 1996; McGeer and McGeer, 2003). The specific roles of the immune cells and the altered vascular function in AD pathology are not well understood. Nevertheless, emerging evidence suggests that activated immune responses and an altered vasculature are not just pathological consequences of AD but may also have deleterious effects on disease progression (Humpel and Marksteiner, 2005; Zlokovic, 2005;

Wyss-Coray, 2006). Thus, in AD pathology inflammatory and vascular processes need to be carefully characterized since they may guide the approaches used in AD therapy. These are considered in more detail below.

1.1.1 *Microglia and AD*

Microglia are immune regulatory cells in the central nervous system (CNS) comprising about 10% of the brain's total glial cells. Microglia are of mesodermal origin and belong to the bone marrow-derived myelomonocytic cell line (Cuadros and Navascués, 1998). Microglia are generally divided into two types according to morphologies: ramified and amoeboid microglia. Ramified microglia have small sized soma with numerous long processes extending in various directions. The amoeboid microglia display larger soma size and show retracted processes. In addition, microglia can be immunophenotypically identified by the use of several cell surface antigens, including CD11b, CD11c, CD 14, CD45, CD68, and MHC class II (Guillemin and Brew, 2004). Microglia are able to produce a broad spectrum of inflammatory mediators, such as pro-inflammatory and pro-angiogenic factors (Table 1). The level of these factors secreted from the microglia has been shown to influence the different cellular systems in the CNS, including neurologic and vascular systems (de Vries et al., 1997; Akiyama et al., 2000)

Neuropathological studies of brains from AD patients revealed that amyloid plaques and neurofibrillary tangles are associated with an accumulation of infiltrated microglia (McGeer et al., 1988). Transgenic animal models of AD also provide strong evidence for the presence of reactive microglia around the deposited amyloid plaques (Frautschy et al., 1998; Stalder et al., 1999). β-amyloid-injected models of AD have demonstrated that $A\beta_{1-42}$ injection produces microglial activation (Giovannini et al., 2002; McLarnon et al., 2006). Previous studies have identified a number of microglial receptors, which are activated by β-amyloid including integrin receptor ($\alpha_5\beta_1$), receptor for advanced glycation end-products (RAGE), serpin enzyme complex (SEC), heparin sulfate proteoglycans (HSPGs), and scavenger receptor A (Bamberger and Landreth, 2001). Interestingly, inhibiting microglial binding to fibrillar β-amyloid reveals a reduced microglial reactivity, by the lower production of inflammatory factors, reactive oxygen species and pro-inflammatory cytokine (El Khoury et al., 1996; Bamberger et al., 2003).

Table 1

Microglia-derived pro-inflammatory and pro-angiogenic mediators

Complement proteins
C1~C9
Cytokines
IL-1β, IL-6, TNF-α, TGF-β
Chemokines
IL-8, MIP-1α, MCP-1
Enzyme
COX-2
Proteases
Thrombin, tPA, uPA
Lipid carrier protein
ApoE
Growth factor
VEGF, bFGF

Abbreviations: IL, interleukin; TNF, tumor necrosis factor; TGF, transforming growth factor; MIP, macrophage inflammatory protein; MCP, monocyte chemotactic protein; COX, cyclooxygenase; tPA, tissue plasminogen activator; uPA, urokinase plasminogen activator; ApoE, apolipoprotein E; VEGF, vascular endothelial growth factor; bFGF, basic fibroblast growth factor

Therefore, microglia activation in AD is speculated to be strongly related to deposition of amyloid plaques. In neuropathological studies of AD, as well as animal models of AD, amyloid-associated reactive microglia display up-regulated expression of pro-inflammatory mediators including cytokines IL-1α and β, IL-6, TNF-α; chemokines IL-8, MCP-1, MIP-1; complement; and COX-2 (Akiyama et al., 2000; Wyss-Coray, 2006). *In vitro* study of cultured microglia taken from the brains of AD patients have shown increased levels of chemotactic responses and production of TNF-α and IL-6 in response to β-amyloid stimulation (Strohmeyer et al., 2005). Moreover, the increased level of inflammatory mediators derived from β-amyloid stimulation of microglia has been shown to induce neuronal injury (Combs et al., 2001; Floden et al., 2005). Pro-angiogenic factors derived from activated microglia provide also strong evidence for the involvement of microglia in the alteration of cerebrovasculature. In β-amyloid-injected animal model of AD, upregulation of microglia-mediated angiogenic factors was associated with increased structural changes and permeability of cerebral blood vessels. These results suggested activated microglia were involved in the alteration of vasculature (Zand et al., 2005; Ryu et al., Ryu and McLarnon, 2006, 2007).

1.1.2 *Astrocytes and AD*

Astrocytes are the most numerous type of glial cells in the CNS. They are generally divided into two types according to their morphologies and distribution: protoplasmic astrocytes in grey matter and fibrous astrocytes in white matter. Protoplasmic astrocytes have short, numerously branched processes. Fibrous astrocytes have long, less frequently branched processes (Oberheim et al., 2006). Astrocytes can be immunophenotypically identified by a number of key intermediate filament proteins including glial fibrillary acidic protein (GFAP), vimentin, and nestin. In the developmental stage, immature astrocytes express both vimentin and nestin but following astrocyte maturation, GFAP and vimentin are localized on non-reactive astrocytes (Pekny, 2001).

Astrocytes have many important roles in normal brain function. The cells are involved in regulating the extracellular environment of neurons, providing structural support, neuronal metabolic activity, and modulating synaptic transmission. Recent studies report that astrocytes play an important role in maintaining the cerebrovascular system in the brain (Mulligan and

MacVicar, 2004; Takano et al., 2006). Astrocytes can become activated in response to pathological insults. The up-regulation of intermediate filament proteins and morphological changes are evident in activated astrocytes. In pathological conditions, reactive astrocytes migrate to the site of injury and are involved in glial scar formation (Saadoun et al., 2005).

In AD, increased numbers of astrocytes exhibit up-regulated intermediate filament protein GFAP (Webster et al., 2006). A similar reactivity of astrocytes occurs around peptide deposition areas in transgenic mice AD models (Calingasan et al., 2002; Heneka et al., 2005) and with Aβ injection into rodent brain (Weldon et al., 1998). Consistent with the AD pathological examination, cultured astrocytes become activated in response to peptide treatment (Pike et al., 1994), and release pro-inflammatory mediators (Hu et al., 1998). Although reactive astrocytes in brain injury are involved in repair mechanisms by producing neurotrophic factors (Chen and Swanson, 2003), some reports suggest that activated astrocytes in AD brain express a broad spectrum of inflammatory factors including cytokines, complement proteins, complement inhibitor proteins, protease inhibitors, and nitric oxide synthase (Walker and Beach, 2002). In addition, the increased level of extracellular matrix protein chondroitin sulfate proteoglycans (CSPGs) in astrocytes has been implicated in the inhibition of microglial phagocytosis of senile plaques (DeWitt et al., 1998) and neuronal regenerative processes (Canning et al., 1993; DeWitt and Silver, 1996). In such cases, astrocyte-derived CSPGs may play a deleterious role in the progression of AD pathology.

1.1.3 *Cerebrovascular dysfunction and AD*

The structural and functional integrity of the CNS is maintained by the cerebrovascular system controlling cerebral blood flow and providing a physical and metabolic barrier to harmful substances in the blood. The BBB is comprised of the cerebrovasculature, together with the physical support from astrocytes, having important roles in controlling toxic molecules that might cross into the brain, and in providing the required biochemical and nutrient support for cells in the brain (Abbott et al., 2006). Pathological conditions of the cerebrovasculature in AD may include extracellular deposition of β-amyloid in cerebral vasculature (Chalmers et al., 2003), pathological angiogenic activity (Thirumangalakudi et al., 2006), microvascular injury (Berzin et al., 2000), blood-brain barrier (BBB) leakiness (Bowman et al., 2007), microinfarctions (Kalaria and Skoog, 2002), and cerebral hemorrhages (Jellinger and Mitter-

Ferstl, 2003). In particular, the cerebrovascular pathologies found in AD brain can mediate a reduced cerebral blood flow (Farkas and Luiten, 2001), the extravasation of serum proteins (Behrouz et al, 1991) and inflammatory responses (Miao et al., 2005) which, in turn, may disturb the homeostatic environment required for neuronal survival and increase glial activation.

Recent studies suggest that vascular alterations are important in the pathogenesis of AD and the progression of disease (Iadecola, 2004). Some authors suggest that genetic mutation (ApoE ε4 allele) may be a primary mechanism causing vasculature dysfunction (Premkumar et al., 1996; Chalmers et al., 2003; Fryer et al., 2005). Nevertheless, it remains unclear whether vascular alterations are the pathological consequences, or a contributing factor for the progression of the pathological severity of AD. On the basis of a broad spectrum of data derived from basic science and clinical studies, sporadic AD has been suggested to be a primary vascular disorder (de la Torre, 2000). The evidence for this idea includes a commonality of risk factors, clinical symptoms, and the degenerative pathology seen in vascular dementia and AD. At present; however, the specific relationship between vascular dysfunction and the processes associated with, or the cause of, the progressive neurodegeneration seen in AD, remains largely unresolved.

Detailed epidemiologic analyses have led to the characterization of common risk factors shared between vascular dysfunction and AD (Breteler, 2000). The number of risk factors that are common to vascular dementia and AD are both large and diverse and include cardiac-specific dysfunctions (i.e., stroke) in addition to other factors such as alcoholism, migraine, elevated serum homocysteine and diabetes mellitus (de la Torre, 2004). Pharmacological evidence suggests that the use of agents such as non-steroidal anti-inflammatory drug products (NSAIDs), which have some benefits in AD (Etminan et al., 2003), also have utility in preventing impairment to cerebral vasculature (Grosser and Schröder, 2003).

Another salient point is that many AD individuals show some degree of cerebrovascular dysfunction such as diminished perfusion (Johnson et al., 2005). The argument that cerebral hypoperfusion is a precursor to neurodegeneration in AD has been detailed (Ruitenberg et al., 2005). Briefly, supporting data includes changes in microvasculature, appear prior to AD pathology (Huang et al., 2002) and individuals with Down's syndrome exhibit a similar impairment on cerebral perfusion, however, without the plaques and neurofibrillary tangles which are hallmarks of AD (Aydin et al., 2007). Results from animal studies also indicate that

cerebral hypoperfusion can induce a host of cognitive and behavioral defects in rats (Farkas and Luiten, 2001). Risk factors, such as aging, have also been considered as aiding the progression of vascular impairment leading to the progressive dysfunction seen in AD (Borenstein et al., 2005).

1.2 ANIMAL MODELS OF AD

Over the past few years, the development of AD animal models (with genetic mutation and Aβ peptide injection) has been focused on the accumulation of pathogenic forms of β-amyloid and other pathological changes (i.e., tau hyperphosphorylation, formation of neurofibrillary tangles, and neuronal loss) in the brain (Spires and Hyman, 2005). Possible environmental factors may also be involved in AD development, in combination with genetic factors or the physiological aging process.

1.2.1 *Genetic models of AD*

The inherited familial form of AD exhibits an early onset of disease in a small population of AD cases. The majority of AD cases are sporadic and seem to result from the interaction of multiple genetic and environmental factors. Several inherited specific genes have been identified and found to be associated with an increased risk for developing early- and late-onset familial forms of AD. These genes included APP, presenilins, and other APP-interacting genes (ApoE, lipoprotein receptor-related protein (LPR), and β-site APP cleaving enzyme 1 (BACE1)) (Spires and Hyman, 2005). Since these genes are involved in the generation of amyloid, their mutations could give rise to an increased accumulation of β-amyloid.

Transgenic mice, exhibiting a number of features of AD, were first generated using a platelet-derived growth factor-β promoter for expressing a mutant form of human APP (APP V717F). APP V717F transgenic mice express a β-amyloid pathology (thioflavine S-fluorescent Aβ deposits and formation of amyloid plaques), are associated with astrogliosis and microgliosis, and exhibit synaptic dysfunction (Games et al., 1995). APP695-expressing transgenic mice (Tg 2576), containing the double mutation (K670N/M671L), show age-dependent amyloid deposits associated with marked neuritic dystrophy, as well as microglial

activation and alteration of synaptophysin immunoreactivity (Hsiao et al., 1996). The APP23 transgenic mice, which express human mutated APP under control of a neuron-specific promoter element, demonstrate congophilic amyloid plaques associated with neuritic changes and microglial activation. The APP23 mice also produce hyperphosphorlyated tau protein and develop CA1 neuronal loss (Sturchler-Pierrat et al., 1997). Most importantly, all of these transgenic mice that overexpress APP (APP V717F, Tg 2576, and APP23) do not develop neurofibrillary tangles (NFT), a pathological hallmark of AD (Hsiao et al., 1996). Human mutant PSEN knock-in mice also do not develop NFT or exhibit β-amyloid pathology, even though they have an increased level of Aβ1-42 (Houlden et al., 2000). This finding could indicate that the level of generated Aβ1-42 in the PSEN transgenic mice was not sufficient for the formation of amyloid.

NFT formation has been attempted in tau-based transgenic mice that overexpress a four-repeat form of human tau. Nevertheless, this tau-expressing model develops hyperphosphorylation of tau without any apparent neurofibrillary pathology. The lack of NFT formation in transgenic mice has been resolved in a recent transgenic study using pathogenic mutations in tau cDNA transgenes; however, the tau-based transgenic mice do not exhibit Aβ pathology (Probst et al., 2000). Although different double transgenic mice were used to increase the levels of β-amyloid, NFT formation was not seen (Van Dam and De Deyn, 2006). A triple transgenic mice model (expressing mutant APP, PSEN, and tau) was generated by co-injection of the APP and tau transgenes into a PSEN-1 knock-in line, which demonstrated many of the features of AD, including Aβ pathology, NFT formation, inflammation, and synaptic dysfunction (Oddo et al., 2003).

Although previous studies have found evidence for activated microglia and astrogliosis in transgenic models of AD (Morgan et al., 2005), these mice show only a minimum level of inflammation exclusively localized at sites of amyloid plaque deposition (Wegiel et al., 2001). Neuropathological and chronic inflammatory reactivity, associated with various forms of amyloid deposits in AD brain, is more widespread than just showing association with dense amyloid deposits. These transgenic models would provide suitable experimental conditions for investigating mechanisms of local tissue neuropathology associated with dense amyloid plaques. In any case, previous studies using transgenic AD mice have demonstrated the usefulness of these models for genetic manipulation of inflammation pathways. For example, inflammatory mediators (PGE2 receptor EP2, complement pathway, CD40, and RAGE), with genetic

manipulation, were shown to alter inflammatory processes in these mice (Wyss-Coray, 2006). Moreover, in pharmacological studies of inflammation, the transgenic AD mice were useful in investigating several anti-inflammatory compounds such as NSAIDs (Yan et al., 2003) and minocycline (Fan et al., 2007).

1.2.2 *Cerebrovascular pathology in transgenic mice models of AD*

Cerebrovascular pathologies have been found in the neuropathology of AD. Several clinical studies have demonstrated vascular changes in the brains of AD patients (Farkas and Luiten, 2001). Accumulation of β-amyloid was reported in vessels, in addition to brain parenchyma, and the vessels with amyloid deposits appeared to be more damaged. The exact mechanism by which amyloid plaque accumulation takes place in vessels, to cause cerebral amyloid angiopathy is not clear but evidence indicates that AD patients who carry the APP duplication (Rovelet-Lecrux et al., 2006) or ε4 allele of the ApoE gene have an increased risk of developing CAA (Chalmers et al., 2003). Recent work with a transgenic mouse of cerebral microvascular amyloid show that microvascular amyloid accumulation is accompanied by microglial activation and this vascular-inflammation is correlated with behavioral impairment (Xu et al., 2007). Subsequent work on this model using the anti-inflammatory compound minocycline showed a reduction in microglial activation and cognitive deficits (Fan et al., 2007). Other evidence for vascular changes in the transgenic AD mice that expresses mutant APP is increased levels of vascular density (Schultheiss et al., 2006). A leakiness of the BBB in APP transgenic mice was also observed (Dickstein et al., 2006). In summary, these transgenic AD mice studies provide a unique experimental model to investigate the role of vascular amyloid-derived inflammation in the progression of AD pathology.

1.2.3 *The amyloid peptide injection model of AD*

The increased deposition of amyloid plaques has emerged as a putative risk factor for AD since major components of plaques, i.e., β-amyloid, can cause pathological changes that are relevant to AD. The role of β-amyloid in AD is further elucidated by recent work involving immunization therapy against β-amyloid that can ameliorate the pathological changes in animal

models of AD (Schenk, 2002). Extensive research has been conducted to demonstrate that stimulation of microglia with β-amyloid can produce a broad spectrum of neurotoxic molecules (Akiyama et al., 2000). In this way, injection of β-amyloid can produce β-amyloid-associated pathological changes in the injected brain. β-amyloid of different lengths ($A\beta_{1-40}$, $A\beta_{1-42}$, $A\beta_{25-35}$) is injected into different brain regions, including hippocampus, cortex, or other regions. A single injection or continuous infusion by osmotic pump has been used on rodent brains. The β-amyloid-injected brains showed that some of the features of AD can be produced by administration of the peptide (e.g., neuronal degeneration, extensive inflammatory responses, and cognitive impairment) (Yamada and Nabeshima, 2000). Interestingly, it has been observed that Aβ deposition is induced in 3-month-old APP transgenic mice by intracerebral injection of dilute AD brain extract (Kane et al., 2000). Although intracerebral infusion of β-amyloid does not produce NFT formation or tau phosphorylation, animal models with β–amyloid injection support the hypothesis of a pathogenic role of Aβ.

β-amyloid injection models have been shown to activate inflammatory cells including microglia and astrocytes. This cellular activation leads to upregulation of pro-inflammatory cytokines, such as IL-6, IL-1β, TNF-α, and inflammatory enzymes iNOS and COX-2 (Weldon et al., 1998; Heneka et al., 2002; Clarke et al., 2007; Medeiros et al., 2007). Blockade of peptide-induced immune responses with pharmacological compounds supports the deleterious role of activated glial cells-derived mediators in mediating β-amyloid-induced neurotoxicity (Giovannini et al., 2002; Ryu et al., 2004). These studies suggest that inflammation is an important contributing factor in β-amyloid-induced neurodegeneration. Overall, the β-amyloid injection model provides considerable insight into mechanisms of β-amyloid-induced toxicity.

1.2.4 *Cerebrovascular pathology in amyloid peptide-injected brain*

It has been suggested that cerebrovascular pathology is associated with the vascular deposition of β-amyloid in AD (Jellinger, 2002). Nevertheless, a recent clinical study of AD patients with no history of CAA, showed that the BBB integrity is impaired in correlation with disease progression (Bowman et al., 2007). This evidence implies that parenchymal deposition of β-amyloid is associated with altered vascular function in the AD brain. No clear evidence, however, supports a link between parenchymal amyloid plaque deposition and vascular

alteration in the brain. Previous findings in this laboratory have shown that intrahippocampal β-amyloid injection led to marked angiogenic activity characterized by the up-regulation of the vascular extracellular matrix protein, laminin (Zand et al., 2005). This β-amyloid injection model of AD also showed evidence for enhanced permeability of the BBB, with leakiness to serum proteins (Ryu and McLarnon, 2006). In addition, recent study in $A\beta_{1-42}$-injected rat hippocampus has found that peptide-derived microglial activation can contribute to vascular perturbations (Ryu and McLarnon, 2006). We used pharmacological inhibition of TNF-α with thalidomide (an anti-angiogenic and anti-inflammatory) to inhibit microglial derived vascular alterations (Ryu and McLarnon, 2007). Future studies using this β-amyloid injection model might help to elucidate the detailed mechanisms of activated glial-derived vascular injury stimulated by β-amyloid deposition.

1.3 CEREBROVASCULAR ABNORMALITIES IN AD

Chronic inflammatory responses could constitute a driving force for sustained cerebrovascular perturbations in AD brain. The presence of senile plaques, containing deposits of Aβ peptide, is a characteristic of diseased brains. This peptide is a potent stimulatory agent for activation of microglia. Stimulated microglia are sources of numerous inflammatory mediators including cytokines, chemokines, proteases, excitatory amino acids, and reactive oxygen species. Importantly, the products of stimulated microglia/macrophages also include a host of pro-angiogenic factors including vascular endothelial growth factor (VEGF) (Sunderkötter et al., 1994). Examination of AD brains reveals evidence for ongoing inflammation and inflamed brains have populations of reactive microglia and astrocytes. A critical general question concerns the roles of inflammatory responses and disturbed vascular responses in contributing to the pathophysiology of AD. In a recent study, increased CSF levels of VEGF were measured in AD and vascular dementia brains, in comparison to controls (Tarkowski et al., 2002). The authors concluded that up-regulation of this vascular factor suggests a common underlying pathogenesis for AD and vascular dementia. Evidence suggesting that VEGF is a potential contributory factor in the pathophysiological processes of AD includes its ability to increase vascular permeability (Senger et al., 1986) and also chemoattractive microglial response (Forstreuter et al., 2002). Recent work has also demonstrated the co-localization of VEGF with Aβ peptide plaques in AD brains (Yang et al., 2004). These investigators suggest that excessive VEGF, associated with

plaques, leads to low levels of VEGF in cerebral hypoperfusion and ultimately, to neurodegeneration. Abundant VEGF immunostaining was reported to be localized to astrocytes in cases of cerebrovascular disease and AD (Kalaria et al., 1998).

1.3.1 *Inflammation and vascular remodeling*

Several recent studies have suggested that vascular remodeling including angiogenic activity and increased permeabillity of BBB could contribute to the pathological processes evident in AD brain (Vagnucci and Li, 2003). The authors indicate that a diversity of agents, with effects to reduce inflammatory components (the risk of AD), are all inhibitors of angiogenesis. Thus, several mechanisms may account for angiogenesis as being an inducer of inflammatory reaction for neurodegeneration, such as: vascular endothelial cell production of amyloid precursor protein leading to a progressive build-up of Aβ peptide, with accumulation of immune cells (Xu et al., 2007) and the direct cerebral microvessel secretion of putative pro-inflammatory factors (Suo et al., 1998; Stanimirovic and Satoh, 2000). Also, putative mechanisms may be involved that could initiate and sustain angiogenesis in AD brain, such as during inflammation. Examination of AD brains shows that the increased angiogenic marker laminin are associated with the deposition of amyloid plaques and reactive microglia (Fig. 1-1).

Another possible initiating process is hypoperfusion in aged brain, which leads to hypoxia and the subsequent activation of a diversity of angiogenic stimulatory factors. A gene profiling study examined the expression of angiogenic factors in AD brains, and found the up-regulation of a host of pro-angiogenic and pro-inflammatory genes in disease (Pogue and Lukiw, 2004). This enhancement of angiogenic factors could possibly act as a compensatory mechanism for cerebral hypoperfusion in AD. The subsequent angiogenesis could then serve as an integral component, leading to the progression, and possible severity, of the immune responses of AD.

AD brains show considerable evidence of inflammation with vascular remodeling often a prominent component of inflamed lesions (Perlmutter et al., 1991; Farkas and Luiten, 2001). Inflamed brains also exhibit marked increases in proliferation and activation of microglia and astrocytes. Because of microglial-mediated inflammatory responses and the proximity of astrocytes to the BBB, glia are suggested to contribute to angiogenic activity. Furthermore, reactive glia are observed to be co-localized with cerebral microvessels in AD brains (Perlmutter

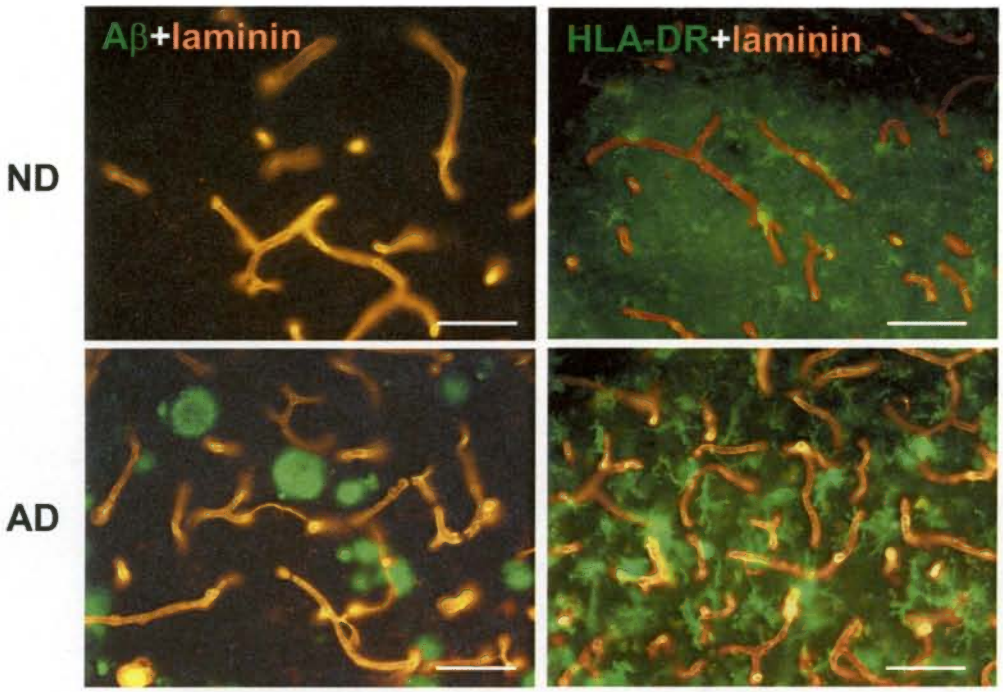

Figure 1-1. Photomicrographs of human frontal cortical sections immunostained for vascular matrix protein laminin combined with amyloid plaques and HLA-DR+ microglia. Laminin antibody was used for the indicative of angiogenic activity (a part of vascular remodeling). Frontal cortical sections were obtained from nondemented person (upper panels) and from an AD patient (lower panels). Scale bars = 50 μm. Note that markedly increased laminin immunoreactivity associated with deposition of amyloid plaques and HLA-DR+ microglia in AD brain sections compared with ND sections.

et al., 1992; Uchihara et al., 1997). Glial-mediated inflammatory responses are particularly suitable for stimulatory actions that could promote neovascularization (Sunderkötter et al., 1994). For example, glia, activated by stimuli such as hypoxia, can secrete a diversity of angiogenic agents including VEGF, bFGF, TNF-α, MMPs, and IL-8 (Xiong et al., 1998; Crowther et al., 2001). In a study using a mouse model of retinal neovascularization, it was concluded that underlying processes included contributions by TNF-α, mediated by inflammatory responses from activated microglia (Yoshida et al., 2004). Reactive oxygen species also have potent pro-angiogenic and pro-inflammatory actions on tissue and can contribute to processes in disease pathology (Tojo et al., 2005; Kim et al., 2006). Even though the mechanisms of angiogenic activity for pro-inflammatory mediators are not well known, recent work suggests that inflammatory cytokine-induced angiogenesis is required to induce the activation of an inducible COX-2 (Kuwano et al., 2004). Evidence also suggests that angiogenic activity and inflammatory responses can damage neurons. In an *in vitro* study, a loss of cortical or cerebellar neurons was seen after direct exposure to AD microvessels or conditioned medium from vessels (Grammas et al., 1999). Subsequent reports from this same laboratory suggested several inflammatory mediators from cerebral microcirculation in the AD brain as being putative mediators of neuronal damage (Grammas and Ovase, 2001, 2002). These mediators included the chemokine, MCP-1, the pro-inflammatory cytokine, IL-1β and TNF-α. Direct vasoactivity of Aβ on cerebral microvessels has been attributed to the activation of a pro-inflammatory pathway involving COX-2 and p38 MAPK (Paris et al., 2000). Overall, the results are consistent with a dysfunctional vasculature producing neurotoxic inflammatory products. Chronic inflammatory conditions are sustained by the stimulated glial release of a host of pro-angiogenic factors leading to neovascularization and progressive damage to neurons.

1.3.2 *Inflammation and damage to the BBB in AD*

One of the prominent cerebrovascular pathologies of AD is the leakiness of BBB. Recent work has reported increased albumin concentration in the cerebrospinal fluid (CSF) of patients with AD, resulting from an alteration in BBB permeability (Algotsson and Winblad, 2007; Bowman et al., 2007). The BBB alteration assumed different degrees of severity, in the pathological stages of AD, and was often observed prior to the onset of cognitive impairment of patients with AD (Bowman et al., 2007). Pathological examination of the brains of patients with

AD indicated that the amyloid plaque that is deposited on vessels had a structural alteration of endothelial cells and a degeneration of smooth muscle cells (Farkas and Luiten, 2001). The detection of blood-derived serum proteins in AD brain sections also provided evidence for the leakiness of the BBB in AD (Tomimoto et al., 1996).

β-amyloid deposition has been considered as a causative factor in the BBB alteration. Consistent with this notion, transgenic AD mice, expressing mutant human APP gene, develop cerebro-amyloid angiopathy (CAA) and associated BBB damage at an early stage (Ujiie et al., 2003). Recent clinical studies; however, show that all patients with AD that have BBB damage may not have any signs of CAA (Bowman et al., 2007). In this patient population, BBB disruption was not associated with genetic mutations of the genes responsible for AD. Although the direct effect of β-amyloid on endothelial cell function cannot be excluded, activation of immune cells can provide an alternative explanation for the BBB damage in patients with AD. Furthermore, since physiological function of the BBB includes a number of homeostatic processes, any alteration of the BBB in AD brain would likely influence glial function. Our results and the work of others on the pathological AD brain indicate that accumulated activated microglia and astrocytes are located at the site of BBB damage in patients with AD, compared with controls (Fiala et al., 2002; Ryu et al, 2006). A broad spectrum of pro-inflammatory factors, derived from activated glial cells could increase the endothelial cell susceptibility in the presence of amyloid plaques at the pathological site. In AD brains, the level of pro-inflammatory mediators, including: cytokines, chemokines, ROS, and NO are increased by the activated microglia and reactive astrocytes that are found around the amyloid plaque and vasculature in AD (Akiyama et al., 2000). *In vitro* studies of cultured endothelial cells, and the glial-derived pro-inflammatory mediators have been shown to damage or alter endothelial cell function (Mark et al., 2001; Argaw et al., 2006). Furthermore, impaired cerebrovasculature can provide a route for the entry of blood-derived components including: serum proteins, blood-borne immune cells, and circulating pro-inflammatory mediators (Abbott et al., 2006). These factors are not normally found in the normal brain with an intact cerebrovascular barrier, but in pathological conditions such as AD, factors may enter the parenchymal regions of brain and stimulate brain inflammation of microglial activation and astrogliosis, leading to the production of more neurotoxic molecules causing neuronal damage and further cerebrovascular injury. The degeneration of the cerebrovasculature also causes decreased levels of CSF, leading to a lack of blood-derived factors, which are required for maintaining the neuronal homeostatic environment

(Zlokovic, 2005). Under such pathological vascular conditions, damaged neurons produce a broad spectrum of signaling molecules, including chemokines (Ubogu et al., 2006). Several lines of evidence show that these chemotactic molecules can recruit immune cells and cause further inflammatory responses (Weiss et al., 1998; Davalos et al., 2005). Thus, vascular alteration can indirectly influence glial activation through the pathological neuronal conditions. These results described above provide a framework for the putative β-amyloid scheme linking vascular impairment and inflammatory reaction to neuronal damage (Fig. 1-2).

Evidence suggests that the cerebrovasculature plays an important role in regulating the level of β-amyloid in the brain (Deane and Zlokovic, 2007). The β-amyloid clearance mechanism involves several transport binding proteins, including: apolipoprotein E, apoJ, transthyretin, lipoproteins, α_2-macroglobulin, and LDL receptor-related protein-1 (Holtzman and Zlokovic, 2007). Because an increase in levels of β-amyloid concentration in the brain has been demonstrated in AD transgenic mice that exhibited impairment of these transport binding proteins (Shibata et al., 2000; Sagare et al., 2007), conceivably, cerebrovascular damage is responsible for the accumulation of β-amyloid, to cause the significant inflammation responses associated with amyloid deposits.

1.4 CURRENT TREATMENTS IN AD

A number of therapeutic approaches have been taken to inhibit inflammation in AD (Wyss-Coray, 2006). Inhibition of immune responses has been used in experimental animal models of AD, including transgenic mice and β-amyloid peptide-injected animals (Yan et al., 2003; Ryu et al., 2004). The general results from animal studies indicate that anti-inflammatory drugs show significant action to protect neurons. In contrast to the experimental animal results, clinical treatments of AD patients using a number of anti-inflammatory compounds (i.e., the glucocorticoid prednisone, the anti-malarial immunomodulating drug hydroxychloroquine, the selective COX-2 inhibitors celecoxib and rofecoxib) have shown little or no beneficial effects in preventing or delaying disease progression (Aisen et al., 2000; Sainati et al., 2000; Van Gool et al., 2001; Thal et al., 2005).

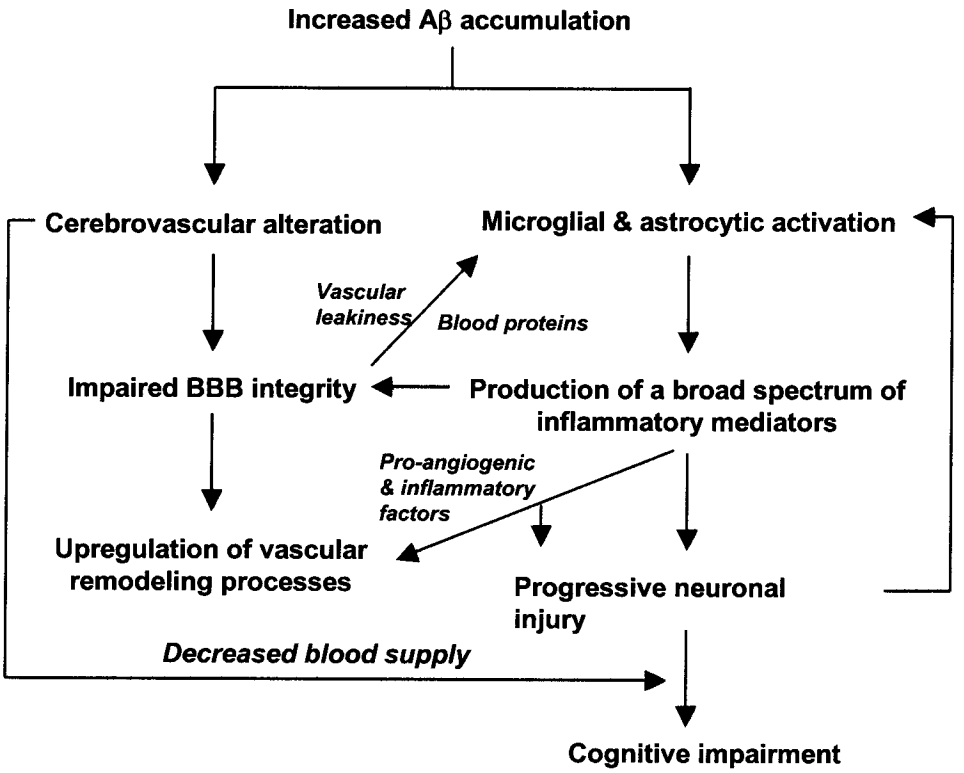

Figure 1-2. The sequence of pathological events in neuronal degeneration associated with cerebrovascular pathology and inflammatory reaction in AD.

Effects of NSAIDs (non-steroidal anti-inflammatory drugs) in AD have been extensively studied (Weggen et al., 2007). In a current long-term follow-up (7-year) study of patients at risk for AD, treatment with NSAIDs revealed an important therapeutically effective time course. In the trial, patients who were exposed to NSAIDs for two or more years before onset of dementia had less chance of developing AD pathology (in t' Veld et al., 2001). Results from other clinical trials using NSAIDs have also reported some benefits in cognitive function with these compounds (McGeer and McGeer, 2007). Overall, however, the inhibition of inflammation using anti-inflammatory compounds has shown limited utility as a treatment in AD. The underlying reasons for limited efficacy are not known but may involve the complexity in multifactorial cellular pathways underlying inflammatory responses in AD brains. The work presented in this thesis suggests the importance of pharmacological modulation of microglial-vasculature processes as a relevant future strategy to attenuate chronic inflammation in AD brain.

Cholinesterase inhibitors are used in the treatment of AD. The rationale for their use came from earlier observations that the cognitive decline seen in AD was associated with reduced levels of the neurotransmitter acetylcholine due to loss of cholinergic neurons. However, trials with anti-cholinesterase compounds (rivastigmine, donepezil, galantamine) showed that these compounds produce small benefits to improve cognition of patients with mild to moderate dementia (Raschetti et al., 2007). In recent years, interest in the possible role of excitotoxicity in AD pathology has led to several clinical trials with memantine, a N-methyl-D-asparate (NMDA) antagonist. One randomized controlled trial using this compound has demonstrated moderate effects to improve cognitive performance (Bakchine and Loft, 2007). Ongoing studies with memantine should lead to a better understanding of the NMDA receptor as a target for drugs in AD brain.

Epidemiological studies have linked cholesterol-lowering compounds, such as statins, to lower rates in the incidence of AD in the elderly (Jick et al., 2000; Wolozin et al., 2007). Clinical studies using the statins have been initiated to treat AD patients and early results suggest these compounds delay the appearance of cognitive decline (Sparks et al., 2005) and reduce neuropathological changes in AD patients (Li et al., 2007). The potential therapeutic mechanisms of statins in AD are not well understood but recent studies have found that these compounds can regulate APP processing and Aβ generation (Pedrini et al., 2005). Further

studies are required to determine if cholesterol-lowering compounds will be useful therapy in AD.

Active and passive amyloid vaccinations have been used to treat AD (Schenk et al., 1999; Lemere et al., 2006;). Results have shown these procedures capable of initiating microglial phagocytic responses resulting in decreased Aβ plaque burden. However, the procedures also caused an increase in inflammatory responses in some individuals resulting in the development of meningoencephalitis (Nicoll et al., 2003; Ferrer et al., 2004). To overcome limitations of amyloid vaccination, differing doses of Aβ peptide-anti-Aβ peptide adjuvants and Aβ gene vaccination are currently being explored.

1.5 RESEARCH HYPOTHESIS

Chronic inflammation is a critical component in the pathology of AD. The hypothesis of the proposed research is that Aβ intrahippocampal injection stimulates a chronic inflammatory microenvironment in brain which is characterized by populations of mobile and reactive microglia, a perturbed vasculature, including enhanced expression of angiogenic factors and a leaky BBB, and a diminished viability of neurons. It is postulated that activated microglia initiate vascular remodeling and that abnormalities in vasculature, such as extravasation of plasma proteins into parenchyma, help sustain inflammatory reactivity resulting in damage to bystander neurons. Pharmacological inhibition of microglial and vascular inflammatory responses is posited as a rational therapeutic approach to diminish neuronal damage in AD brain.

1.6 SUMMARY OF PROPOSED RESEARCH OBJECTIVES

The overall thesis objective was to examine roles of microglia in modulating vascular processes and neuronal viability in an amyloid beta-peptide ($A\beta_{1-42}$)-injected animal model of inflamed Alzheimer's disease (AD) brain and how glial-vascular interactions contribute to chronic inflammation in AD. In addition to *in vivo* studies, my work also includes analysis of AD and nondemented (ND) brain tissue and *in vitro* analysis of microglial functional inflammatory responses. The specific objectives are listed below.

1. To investigate levels of 3-nitrotyrosine (3-NT, a marker for peroxynitrite formation) and intactness of blood-brain barrier (BBB) in $A\beta_{1-42}$-injected rat hippocampus. To examine effects of the broad spectrum anti-inflammatory agent, minocycline or the iNOS inhibitor, 1400W on glial-derived 3-NT and BBB damage in $A\beta_{1-42}$-injected rat hippocampus.

2. To investigate the effects of the anti-angiogenic/anti-inflammatory compound thalidomide on microglial responses and association of microgliosis with vascular perturbations in $A\beta_{1-42}$-injected rat hippocampus. To determine effects of thalidomide on the pro-inflammatory/angiogenic factor, tumor necrosis factor-α (TNF-α) expression in $A\beta_{1-42}$-injected rat hippocampus and in $A\beta_{1-42}$-stimulated adult human microglia.

3. To assess extravasation of the blood protein fibrinogen through a perturbed BBB in inflammatory conditions related to AD. These conditions include fibrinogen leakiness in tissue obtained from AD brains (versus control tissue from ND individuals) and rat hippocampus injected with $A\beta_{1-42}$ (versus controls saline and reverse peptide injection). To examine effects of the defibrinogenating agent ancrod and microglial inhibitor anti-Mac-1 antibody as a modulator of fibrinogen-associated inflammation *in vivo*.

4. To investigate microglial expression and function of VEGF (vascular endothelial growth factor) receptor-1 (Flt-1) in $A\beta_{1-42}$-injected rat hippocampus, in peptide-stimulated human adult microglia and in brain tissue obtained from AD patients. To determine Flt-1-dependent microglial chemotaxis *in vitro* (using a transwell migration assay) and *in vivo* (using transplanted enhanced green fluorescent protein (EGFP)-labelled microglia). Pharmacological modulation of chemotaxis will be examined using anti-Flt-1 antibody treatment to alter mobility of microglia.
The specific objectives 1 to 4 are presented in thesis chapters 2 to 5.

1.7 REFERENCES

Abbott NJ, Rönnbäck L, Hansson E. 2006. Astrocyte-endothelial interactions at the blood-brain barrier. Nat Rev Neurosci 7:41-53.

Aisen PS, Davis KL, Berg JD, Schafer K, Campbell K, Thomas RG, Weiner MF, Farlow MR, Sano M, Grundman M, Thal LJ. 2000. A randomized controlled trial of prednisone in Alzheimer's disease. Alzheimer's Disease Cooperative Study. Neurology 54:588-593.

Akiyama H, Barger S, Barnum S, Bradt B, Bauer J, Cole GM, Cooper NR, Eikelenboom P, Emmerling M, et al., 2000. Inflammation and Alzheimer's disease. Neurobiol Aging 21:383-421.

Algotsson A, Winblad B. 2007. The integrity of the blood-brain barrier in Alzheimer's disease. Acta Neurol Scand 115:403-408.

Andersen K, Launer LJ, Dewey ME, Letenneur L, Ott A, Copeland JR, Dartigues JF, Kragh-Sorensen P, Baldereschi M, et al. 1999. Gender differences in the incidence of AD and vascular dementia: The EURODEM Studies. EURODEM Incidence Research Group. Neurology 53:1992-1997.

Andorfer C, Acker CM, Kress Y, Hof PR, Duff K, Davies P. 2005. Cell-cycle reentry and cell death in transgenic mice expressing nonmutant human tau isoforms. J Neurosci 25:5446-5454.

Argaw AT, Zhang Y, Snyder BJ, Zhao ML, Kopp N, Lee SC, Raine CS, Brosnan CF, John GR. 2006. IL-1beta regulates blood-brain barrier permeability via reactivation of the hypoxia-angiogenesis program. J Immunol 177:5574-5584.

Aydin M, Kabakus N, Balci TA, Ayar A. 2007. Correlative study of the cognitive impairment, regional cerebral blood flow, and electroencephalogram abnormalities in children with Down's syndrome. Int J Neurosci 117:327-336.

Bakchine S, Loft H. 2007. Memantine treatment in patients with mild to moderate Alzheimer's disease: results of a randomised, double-blind, placebo-controlled 6-month study. J Alzheimers Dis 11:471-479.

Bamberger ME, Harris ME, McDonald DR, Husemann J, Landreth GE. 2003. A cell surface receptor complex for fibrillar beta-amyloid mediates microglial activation. J Neurosci 23:2665-2674.

Bamberger ME, Landreth GE. 2001. Microglial interaction with beta-amyloid: implications for the pathogenesis of Alzheimer's disease. Microsc Res Tech 54:59-70.

Behrouz N, Defossez A, Delacourte A, Mazzuca M. 1991. The immunohistochemical evidence of amyloid diffuse deposits as a pathological hallmark in Alzheimer's disease. J Gerontol 46:B209-212.

Berzin TM, Zipser BD, Rafii MS, Kuo-Leblanc V, Yancopoulos GD, Glass DJ, Fallon JR, Stopa EG. 2000. Agrin and microvascular damage in Alzheimer's disease. Neurobiol Aging 21:349-355.

Borenstein AR, Wu Y, Mortimer JA, Schellenberg GD, McCormick WC, Bowen JD, McCurry S, Larson EB. 2005. Developmental and vascular risk factors for Alzheimer's disease. Neurobiol Aging. 26:325-334.

Bowman GL, Kaye JA, Moore M, Waichunas D, Carlson NE, Quinn JF. 2007. Blood-brain barrier impairment in Alzheimer disease: stability and functional significance. Neurology 68:1809-1814.

Breteler MM. 2000. Vascular involvement in cognitive decline and dementia. Epidemiologic evidence from the Rotterdam Study and the Rotterdam Scan Study. Ann N Y Acad Sci 903:457-465.

Calingasan NY, Erdely HA, Altar CA. 2002. Identification of CD40 ligand in Alzheimer's disease and in animal models of Alzheimer's disease and brain injury. Neurobiol Aging 23:31-39.

Canning DR, McKeon RJ, DeWitt DA, Perry G, Wujek JR, Frederickson RC, Silver J. 1993. beta-Amyloid of Alzheimer's disease induces reactive gliosis that inhibits axonal outgrowth. Exp Neurol 124:289-298.

Cash AD, Aliev G, Siedlak SL, Nunomura A, Fujioka H, Zhu X, Raina AK, Vinters HV, Tabaton M, Johnson AB, Paula-Barbosa M, Avíla J, Jones PK, Castellani RJ, Smith MA, Perry G. 2003. Microtubule reduction in Alzheimer's disease and aging is independent of tau filament formation. Am J Pathol 162:1623-1627.

Chalmers K, Wilcock GK, Love S. 2003. APOE epsilon 4 influences the pathological phenotype of Alzheimer's disease by favouring cerebrovascular over parenchymal accumulation of A beta protein. Neuropathol Appl Neurobiol 29:231-238.

Chen G, Chen KS, Kobayashi D, Barbour R, Motter R, Games D, Martin SJ, Morris RG. 2007. Active beta-amyloid immunization restores spatial learning in PDAPP mice displaying very low levels of beta-amyloid. J Neurosci 27:2654-2662.

Chen Y, Swanson RA. 2003. Astrocytes and brain injury. J Cereb Blood Flow Metab 23:137-149.

Clarke RM, O'Connell F, Lyons A, Lynch MA. 2007. The HMG-CoA reductase inhibitor, atorvastatin, attenuates the effects of acute administration of amyloid-beta1-42 in the rat hippocampus in vivo. Neuropharmacology 52:136-145.

Combs CK, Karlo JC, Kao SC, Landreth GE. 2001. beta-Amyloid stimulation of microglia and monocytes results in TNFalpha-dependent expression of inducible nitric oxide synthase and neuronal apoptosis. J Neurosci 21:1179-1188.

Crowther M, Brown NJ, Bishop ET, Lewis CE. 2001. Microenvironmental influence on macrophage regulation of angiogenesis in wounds and malignant tumors. J Leukoc Biol 70:478-490.

Cuadros MA, Navascués J. 1998. The origin and differentiation of microglial cells during development. Prog Neurobiol 56:173-189.

Czech C, Tremp G, Pradier L. 2000. Presenilins and Alzheimer's disease: biological functions and pathogenic mechanisms. Prog Neurobiol 60:363-384.

Davalos D, Grutzendler J, Yang G, Kim JV, Zuo Y, Jung S, Littman DR, Dustin ML, Gan WB. 2005. ATP mediates rapid microglial response to local brain injury in vivo. Nat Neurosci 8:752-758.

de la Torre JC. 2000. Cerebral hypoperfusion, capillary degeneration, and development of Alzheimer disease. Alzheimer Dis Assoc Disord Suppl 1:S72-81.

de la Torre JC. 2004. Is Alzheimer's disease a neurodegenerative or a vascular disorder? Data, dogma, and dialectics. Lancet Neurol 3:184-190.

de Vries HE, Kuiper J, de Boer AG, Van Berkel TJ, Breimer DD. 1997. The blood-brain barrier in neuroinflammatory diseases. Pharmacol Rev 49:143-155.

Deane R, Zlokovic BV. 2007. Role of the blood-brain barrier in the pathogenesis of Alzheimer's disease. Curr Alzheimer Res 4:191-197.

DeWitt DA, Perry G, Cohen M, Doller C, Silver J. 1998. Astrocytes regulate microglial phagocytosis of senile plaque cores of Alzheimer's disease. Exp Neurol 149:329-340.

DeWitt DA, Silver J. 1996. Regenerative failure: a potential mechanism for neuritic dystrophy in Alzheimer's disease. Exp Neurol 142:103-110.

Dickstein DL, Biron KE, Ujiie M, Pfeifer CG, Jeffries AR, Jefferies WA. 2006. Abeta peptide immunization restores blood-brain barrier integrity in Alzheimer disease. FASEB J 20:426-433.

El Khoury J, Hickman SE, Thomas CA, Cao L, Silverstein SC, Loike JD. 1996. Scavenger receptor-mediated adhesion of microglia to beta-amyloid fibrils. Nature 382:716-719.

Etminan M, Gill S, Samii A. 2003. Effect of non-steroidal anti-inflammatory drugs on risk of Alzheimer's disease: systematic review and meta-analysis of observational studies. BMJ 327:128.

Fan R, Xu F, Previti ML, Davis J, Grande AM, Robinson JK, Van Nostrand WE. 2007. Minocycline reduces microglial activation and improves behavioral deficits in a transgenic model of cerebral microvascular amyloid. J Neurosci 27:3057-3063.

Farkas E, Luiten PG. 2001. Cerebral microvascular pathology in aging and Alzheimer's disease. Prog Neurobiol 64:575-611.

Ferrer I, Boada Rovira M, Sánchez Guerra ML, Rey MJ, Costa-Jussá F. 2004. Neuropathology and pathogenesis of encephalitis following amyloid-beta immunization in Alzheimer's disease. Brain Pathol 14:11-20.

Ferri CP, Prince M, Brayne C, Brodaty H, Fratiglioni L, Ganguli M, Hall K, Hasegawa K, Hendrie H, Huang Y, Jorm A, Mathers C, Menezes PR, Rimmer E, Scazufca M. 2005. Alzheimer's Disease International. Global prevalence of dementia: a Delphi consensus study. Lancet 366:2112-2117.

Fiala M, Liu QN, Sayre J, Pop V, Brahmandam V, Graves MC, Vinters HV. 2002. Cyclooxygenase-2-positive macrophages infiltrate the Alzheimer's disease brain and damage the blood-brain barrier. Eur J Clin Invest 32:360-371.

Floden AM, Li S, Combs CK. 2005. Beta-amyloid-stimulated microglia induce neuron death via synergistic stimulation of tumor necrosis factor alpha and NMDA receptors. J Neurosci 25:2566-2575.

Förstl H, Kurz A. 1999. Clinical features of Alzheimer's disease. Eur Arch Psychiatry Clin Neurosci 249:288-290.

Forstreuter F, Lucius R, Mentlein R. 2002. Vascular endothelial growth factor induces chemotaxis and proliferation of microglial cells. J Neuroimmunol 132:93-98.

Frautschy SA, Yang F, Irrizarry M, Hyman B, Saido TC, Hsiao K, Cole GM. 1998. Microglial response to amyloid plaques in APPsw transgenic mice. Am J Pathol 152:307-317.

Fryer JD, Simmons K, Parsadanian M, Bales KR, Paul SM, Sullivan PM, Holtzman DM. 2005. Human apolipoprotein E4 alters the amyloid-beta 40:42 ratio and promotes the formation of cerebral amyloid angiopathy in an amyloid precursor protein transgenic model. J Neurosci 25:2803-2810.

Games D, Adams D, Alessandrini R, Barbour R, Berthelette P, Blackwell C, Carr T, Clemens J, Donaldson T, Gillespie F, et al. 1995. Alzheimer-type neuropathology in transgenic mice overexpressing V717F beta-amyloid precursor protein. Nature.373:523-527.

Giannakopoulos P, Herrmann FR, Bussière T, Bouras C, Kövari E, Perl DP, Morrison JH, Gold G, Hof PR. 2003. Tangle and neuron numbers, but not amyloid load, predict cognitive status in Alzheimer's disease. Neurology 60:1495-1500.

Giovannini MG, Scali C, Prosperi C, Bellucci A, Vannucchi MG, Rosi S, Pepeu G, Casamenti F. 2002. Beta-amyloid-induced inflammation and cholinergic hypofunction in the rat brain in vivo: involvement of the p38MAPK pathway. Neurobiol Dis 11:257-274.

Glenner GG. 1989. The pathobiology of Alzheimer's disease. Annu Rev Med 40:45-51.

Goate A, Chartier-Harlin MC, Mullan M, Brown J, Crawford F, Fidani L, Giuffra L, Haynes A, Irving N, James L, et al. 1991. Segregation of a missense mutation in the amyloid precursor protein gene with familial Alzheimer's disease. Nature 349:704-706.

Gómez-Isla T, Price JL, McKeel DW Jr, Morris JC, Growdon JH, Hyman BT. 1996. Profound loss of layer II entorhinal cortex neurons occurs in very mild Alzheimer's disease. J Neurosci 16:4491-4500.

Grammas P, Moore P, Weigel PH. 1999. Microvessels from Alzheimer's disease brains kill neurons in vitro. Am J Pathol 154:337-342.

Grammas P, Ovase R. 2001. Inflammatory factors are elevated in brain microvessels in Alzheimer's disease. Neurobiol Aging 22:837-842.

Grammas P, Ovase R. 2002. Cerebrovascular transforming growth factor-beta contributes to inflammation in the Alzheimer's disease brain. Am J Pathol 160:1583-1587.

Grosser N, Schröder H. 2003. Aspirin protects endothelial cells from oxidant damage via the nitric oxide-cGMP pathway. Arterioscler Thromb Vasc Biol 23:1345-1351.

Guillemin GJ, Brew BJ. 2004. Microglia, macrophages, perivascular macrophages, and pericytes: a review of function and identification. J Leukoc Biol 75:388-397

Hall GF, Chu B, Lee G, Yao J. 2000. Human tau filaments induce microtubule and synapse loss in an in vivo model of neurofibrillary degenerative disease. J Cell Sci 113:1373-1387.

Hall GF, Yao J, Lee G. 1997. Human tau becomes phosphorylated and forms filamentous deposits when overexpressed in lamprey central neurons in situ. Proc Natl Acad Sci U S A 94:4733-4738.

Heneka MT, Galea E, Gavriluyk V, Dumitrescu-Ozimek L, Daeschner J, O'Banion MK, Weinberg G, Klockgether T, Feinstein DL. 2002. Noradrenergic depletion potentiates beta-

amyloid-induced cortical inflammation: implications for Alzheimer's disease. J Neurosci 22:2434-2442.

Heneka MT, Sastre M, Dumitrescu-Ozimek L, Dewachter I, Walter J, Klockgether T, Van Leuven F. 2005. Focal glial activation coincides with increased BACE1 activation and precedes amyloid plaque deposition in APP[V717I] transgenic mice. J Neuroinflammation 2:22.

Holtzman DM, Zlokovic B. 2007. Role of A β Transport and Clearance in the Pathogenesis and Treatment of Alzheimer's Disease. Alzheimer's Disease Advances in Genetics, Molecular and Cellular Biology. Sangram S. Sisodia and Rudolph E. Tanzi. Springer US.

Houlden H, Baker M, McGowan E, Lewis P, Hutton M, Crook R, Wood NW, Kumar-Singh S, Geddes J, et al. 2000. Variant Alzheimer's disease with spastic paraparesis and cotton wool plaques is caused by PS-1 mutations that lead to exceptionally high amyloid-beta concentrations. Ann Neurol 48:806-808.

Hsiao K, Chapman P, Nilsen S, Eckman C, Harigaya Y, Younkin S, Yang F, Cole G. 1996. Correlative memory deficits, Abeta elevation, and amyloid plaques in transgenic mice. Science 274:99-102.

Hu J, Akama KT, Krafft GA, Chromy BA, Van Eldik LJ. 1998. Amyloid-beta peptide activates cultured astrocytes: morphological alterations, cytokine induction and nitric oxide release. Brain Res 785:195-206.

Huang C, Wahlund LO, Svensson L, Winblad B, Julin P. 2002. Cingulate cortex hypoperfusion predicts Alzheimer's disease in mild cognitive impairment. BMC Neurol 2:9.

Humpel C, Marksteiner J. 2005. Cerebrovascular damage as a cause for Alzheimer's disease. Curr Neurovasc Res 2:341-347.

Iadecola C. 2004. Neurovascular regulation in the normal brain and in Alzheimer's disease. Nat Rev Neurosci 5:347-360.

in t' Veld BA, Ruitenberg A, Hofman A, Launer LJ, van Duijn CM, Stijnen T, Breteler MM, Stricker BH. 2001. Nonsteroidal antiinflammatory drugs and the risk of Alzheimer's disease. N Engl J Med 345:1515-1521.

Irie F, Fitzpatrick AL, Lopez OL, Kuller LH, Peila R, Newman AB, Launer LJ. 2008. Enhanced Risk for Alzheimer Disease in Persons With Type 2 Diabetes and APOE {varepsilon}4: The Cardiovascular Health Study Cognition Study. Arch Neurol 65:89-93.

Jellinger KA, Mitter-Ferstl E. 2003. The impact of cerebrovascular lesions in Alzheimer disease--a comparative autopsy study. J Neurol 250:1050-1055.

Jellinger KA. Alzheimer disease and cerebrovascular pathology: an update. J Neural Transm. 2002 May;109:813-836.

Jick H, Zornberg GL, Jick SS, Seshadri S, Drachman DA. 2000. Statins and the risk of dementia. Lancet. 356:1627-1631.

Johnson NA, Jahng GH, Weiner MW, Miller BL, Chui HC, Jagust WJ, Gorno-Tempini ML, Schuff N. 2005. Pattern of cerebral hypoperfusion in Alzheimer disease and mild cognitive impairment measured with arterial spin-labeling MR imaging: initial experience. Radiology 234:851-859.

Kalaria RN, Cohen DL, Premkumar DR, Nag S, LaManna JC, Lust WD. 1998. Vascular endothelial growth factor in Alzheimer's disease and experimental cerebral ischemia. Brain Res Mol Brain Res 62:101-105.

Kalaria RN, Skoog I. 2002. Overlap with Alzheimer's disease. In T. Erkinjuntti and S. Gauthier (Eds.), Vascular cognitive impairment. Philadelphia: Dunitz. pp.145-166.

Kalaria RN. 1996. Cerebral vessels in ageing and Alzheimer's disease. Pharmacol Ther 72:193-214.

Kane MD, Lipinski WJ, Callahan MJ, Bian F, Durham RA, Schwarz RD, Roher AE, Walker LC. 2000. Evidence for seeding of beta-amyloid by intracerebral infusion of Alzheimer brain extracts in beta -amyloid precursor protein-transgenic mice. J Neurosci 20:3606-3611.

Katzman R. 1994. Apolipoprotein E and Alzheimer's disease. Curr Opin Neurobiol 4:703-707.

Kehoe PG, Wilcock GK. 2007. Is inhibition of the renin-angiotensin system a new treatment option for Alzheimer's disease? Lancet Neurol 6:373-378.

Kim YM, Kim KE, Koh GY, Ho YS, Lee KJ. 2006. Hydrogen peroxide produced by angiopoietin-1 mediates angiogenesis. Cancer Res 66:6167-6174.

Kosik KS, Joachim CL, Selkoe DJ. 1986. Microtubule-associated protein tau (tau) is a major antigenic component of paired helical filaments in Alzheimer disease. Proc Natl Acad Sci U S A 83:4044-4048.

Kuwano T, Nakao S, Yamamoto H, Tsuneyoshi M, Yamamoto T, Kuwano M, Ono M. 2004. Cyclooxygenase 2 is a key enzyme for inflammatory cytokine-induced angiogenesis. FASEB J 18:300-310.

Lazarov O, Robinson J, Tang YP, Hairston IS, Korade-Mirnics Z, Lee VM, Hersh LB, Sapolsky RM, Mirnics K, Sisodia SS. 2005. Environmental enrichment reduces Abeta levels and amyloid deposition in transgenic mice. Cell 120:701-713.

Lee JH, Cheng R, Schupf N, Manly J, Lantigua R, Stern Y, Rogaeva E, Wakutani Y, Farrer L, St George-Hyslop P, Mayeux R. 2007. The association between genetic variants in SORL1 and Alzheimer disease in an urban, multiethnic, community-based cohort. Arch Neurol 64:501-506.

Lemere CA, Maier M, Jiang L, Peng Y, Seabrook TJ. 2006. Amyloid-beta immunotherapy for the prevention and treatment of Alzheimer disease: lessons from mice, monkeys, and humans. Rejuvenation Res 9:77-84.

Levy-Lahad E, Wasco W, Poorkaj P, Romano DM, Oshima J, Pettingell WH, Yu CE, Jondro PD, Schmidt SD, Wang K, et al. 1995. Candidate gene for the chromosome 1 familial Alzheimer's disease locus. Science 269:973-977.

Li G, Larson EB, Sonnen JA, Shofer JB, Petrie EC, Schantz A, Peskind ER, Raskind MA, Breitner JC, Montine TJ. 2007. Statin therapy is associated with reduced neuropathologic changes of Alzheimer disease. Neurology 69:878-85.

Mandelkow EM, Mandelkow E. 1998. Tau in Alzheimer's disease. Trends Cell Biol 8:425-427.

Mark KS, Trickler WJ, Miller DW. 2001. Tumor necrosis factor-alpha induces cyclooxygenase-2 expression and prostaglandin release in brain microvessel endothelial cells. J Pharmacol Exp Ther 297:1051-1058.

McGeer EG, McGeer PL. 2003. Inflammatory processes in Alzheimer's disease. Prog Neuropsychopharmacol Biol Psychiatry. 27:741-749.

McGeer PL, Itagaki S, Boyes BE, McGeer EG. 1988. Reactive microglia are positive for HLA-DR in the substantia nigra of Parkinson's and Alzheimer's disease brains. Neurology 38:1285-1291.

McGeer PL, McGeer EG. 2007. NSAIDs and Alzheimer disease: epidemiological, animal model and clinical studies. Neurobiol Aging 28:639-647.

McLarnon JG, Ryu JK, Walker DG, Choi HB. 2006. Upregulated expression of purinergic P2X(7) receptor in Alzheimer disease and amyloid-beta peptide-treated microglia and in peptide-injected rat hippocampus. J Neuropathol Exp Neurol 65:1090-1097.

Medeiros R, Prediger RD, Passos GF, Pandolfo P, Duarte FS, Franco JL, Dafre AL, Di Giunta G, Figueiredo CP, Takahashi RN, Campos MM, Calixto JB. 2007. Connecting TNF-alpha signaling pathways to iNOS expression in a mouse model of Alzheimer's disease: relevance for the behavioral and synaptic deficits induced by amyloid beta protein. J Neurosci 27:5394-5404.

Miao J, Vitek MP, Xu F, Previti ML, Davis J, Van Nostrand WE. 2005. Reducing cerebral microvascular amyloid-beta protein deposition diminishes regional neuroinflammation in vasculotropic mutant amyloid precursor protein transgenic mice. J Neurosci 25:6271-6277.

Morgan D, Gordon MN, Tan J, Wilcock D, Rojiani AM. 2005. Dynamic complexity of the microglial activation response in transgenic models of amyloid deposition: implications for Alzheimer therapeutics. J Neuropathol Exp Neurol 64:743-753.

Mulligan SJ, MacVicar BA. 2004. Calcium transients in astrocyte endfeet cause cerebrovascular constrictions. Nature 431:195-199

Nagy Z, Esiri MM, Jobst KA, Johnston C, Litchfield S, Sim E, Smith AD. 1995. Influence of the apolipoprotein E genotype on amyloid deposition and neurofibrillary tangle formation in Alzheimer's disease. Neuroscience 69:757-761.

Nicoll JA, Wilkinson D, Holmes C, Steart P, Markham H, Weller RO. 2003. Neuropathology of human Alzheimer disease after immunization with amyloid-beta peptide: a case report. Nat Med 9:448-452.

Oberheim NA, Wang X, Goldman S, Nedergaard M. 2006. Astrocytic complexity distinguishes the human brain. Trends Neurosci 29:547-553.

Oddo S, Caccamo A, Shepherd JD, Murphy MP, Golde TE, Kayed R, Metherate R, Mattson MP, Akbari Y, LaFerla FM. 2003. Triple-transgenic model of Alzheimer's disease with plaques and tangles: intracellular Abeta and synaptic dysfunction. Neuron 39:409-421.

Oltersdorf T, Ward PJ, Henriksson T, Beattie EC, Neve R, Lieberburg I, Fritz LC. 1990. The Alzheimer amyloid precursor protein. Identification of a stable intermediate in the biosynthetic/degradative pathway. J Biol Chem. 265:4492-4497.

Paris D, Town T, Mori T, Parker TA, Humphrey J, Mullan M. 2000. Soluble beta-amyloid peptides mediate vasoactivity via activation of a pro-inflammatory pathway. Neurobiol Aging 21:183-197

Pastor P, Goate AM. 2004. Molecular genetics of Alzheimer's disease. Curr Psychiatry Rep 6:125-133.

Pedrini S, Carter TL, Prendergast G, Petanceska S, Ehrlich ME, Gandy S. 2005. Modulation of statin-activated shedding of Alzheimer APP ectodomain by ROCK. PLoS Med 2:e18.

Pekny M. 2001. Astrocytic intermediate filaments: lessons from GFAP and vimentin knock-out mice. Prog Brain Res 132:23-30.

Perlmutter LS, Barrón E, Saperia D, Chui HC. 1991. Association between vascular basement membrane components and the lesions of Alzheimer's disease. J Neurosci Res 30:673-681.

Perlmutter LS, Scott SA, Barrón E, Chui HC. 1992. MHC class II-positive microglia in human brain: association with Alzheimer lesions. J Neurosci Res 33:549-558.

Pike CJ, Cummings BJ, Monzavi R, Cotman CW. 1994. Beta-amyloid-induced changes in cultured astrocytes parallel reactive astrocytosis associated with senile plaques in Alzheimer's disease. Neuroscience 63:517-531.

Pogue AI, Lukiw WJ. 2004. Angiogenic signaling in Alzheimer's disease. Neuroreport15:1507-1510.

Polvikoski T, Sulkava R, Haltia M, Kainulainen K, Vuorio A, Verkkoniemi A, Niinistö L, Halonen P, Kontula K. 1995. Apolipoprotein E, dementia, and cortical deposition of beta-amyloid protein. N Engl J Med 333:1242-1247.

Premkumar DR, Cohen DL, Hedera P, Friedland RP, Kalaria RN. 1996. Apolipoprotein E-epsilon4 alleles in cerebral amyloid angiopathy and cerebrovascular pathology associated with Alzheimer's disease. Am J Pathol 148:2083-2095.

Price DL, Sisodia SS. 1998. Mutant genes in familial Alzheimer's disease and transgenic models. Annu Rev Neurosci 21:479-505.

Priller C, Bauer T, Mitteregger G, Krebs B, Kretzschmar HA, Herms J. 2006. Synapse formation and function is modulated by the amyloid precursor protein. J Neurosci 26:7212-7221.

Probst A, Götz J, Wiederhold KH, Tolnay M, Mistl C, Jaton AL, Hong M, Ishihara T, Lee VM, Trojanowski JQ, Jakes R, Crowther RA, Spillantini MG, Bürki K, Goedert M. 2000. Axonopathy and amyotrophy in mice transgenic for human four-repeat tau protein. Acta Neuropathol (Berl) 99:469-481.

Raschetti R, Albanese E, Vanacore N, Maggini M. 2007. Cholinesterase inhibitors in mild cognitive impairment: a systematic review of randomised trials. PLoS Med 4:e338.

Reinikainen KJ, Paljärvi L, Huuskonen M, Soininen H, Laakso M, Riekkinen PJ. 1988. A post-mortem study of noradrenergic, serotonergic and GABAergic neurons in Alzheimer's disease. J Neurol Sci. 84:101-116.

Rogaeva E, Meng Y, Lee JH, Gu Y, Kawarai T, Zou F, Katayama T, Baldwin CT, Cheng R, et al. 2007. The neuronal sortilin-related receptor SORL1 is genetically associated with Alzheimer disease. Nat Genet 39:168-177.

Rovelet-Lecrux A, Hannequin D, Raux G, Le Meur N, Laquerrière A, Vital A, Dumanchin C, Feuillette S, Brice A, Vercelletto M, Dubas F, Frebourg T, Campion D. 2006. APP locus duplication causes autosomal dominant early-onset Alzheimer disease with cerebral amyloid angiopathy. Nat Genet 38:24-26.

Ruitenberg A, den Heijer T, Bakker SL, van Swieten JC, Koudstaal PJ, Hofman A, Breteler MM. 2005. Cerebral hypoperfusion and clinical onset of dementia: the Rotterdam Study. Ann Neurol 57:789-794.

Ryu JK, Franciosi S, Sattayaprasert P, Kim SU, McLarnon JG. 2004. Minocycline inhibits neuronal death and glial activation induced by beta-amyloid peptide in rat hippocampus. Glia 48:85-90.

Ryu JK, McLarnon JG. 2006. Minocycline or iNOS inhibition block 3-nitrotyrosine increases and blood-brain barrier leakiness in amyloid beta-peptide-injected rat hippocampus. Exp Neurol 198:552-557.

Ryu JK, McLarnon JG. 2007. Thalidomide inhibition of perturbed vasculature and glial-derived tumor necrosis factor-alpha in an animal model of inflamed Alzheimer's disease brain. Neurobiol Dis doi:10.1016/j.nbd.2007.08.019.

Ryu JK, Wei W, Tran K, Choi H, McLarnon JG. 2006. Fibrinogen increases inflammatory responses and neuronal degeneration in amyloid beta-injected rat hippocampus. Soc Neurosci Abstr FF20.

Saadoun S, Papadopoulos MC, Watanabe H, Yan D, Manley GT, Verkman AS. 2005. Involvement of aquaporin-4 in astroglial cell migration and glial scar formation. J Cell Sci 118:5691-5698.

Sagare A, Deane R, Bell RD, Johnson B, Hamm K, Pendu R, Marky A, Lenting PJ, Wu Z, Zarcone T, Goate A, Mayo K, Perlmutter D, Coma M, Zhong Z, Zlokovic BV. 2007. Clearance of amyloid-beta by circulating lipoprotein receptors. Nat Med 13:1029-1031.

Sainati SM, Ingram DM, Talwalker S, Geis GS. 2000. Results of a double-blind, randomized, placebocontrolled study of celecoxib in the treatment of progression of Alzheimer's disease, Proceedings of the Sixth International Stockholm/Springfield Symposium on Advances in Alzheimer Therapy **180**, Stockholm, Sweden.

Santacruz K, Lewis J, Spires T, Paulson J, Kotilinek L, Ingelsson M, Guimaraes A, DeTure M, Ramsden M, et al. 2005. Tau suppression in a neurodegenerative mouse model improves memory function. Science 309:476-481.

Schenk D, Barbour R, Dunn W, Gordon G, Grajeda H, Guido T, Hu K, Huang J, Johnson-Wood K, Khan K, Kholodenko D, Lee M, Liao Z, Lieberburg I, Motter R, Mutter L, Soriano F, Shopp G, Vasquez N, Vandevert C, Walker S, Wogulis M, Yednock T, Games D, Seubert P. 1999. Immunization with amyloid-beta attenuates Alzheimer-disease-like pathology in the PDAPP mouse. Nature. 400:173-177.

Schenk D. 2002. Amyloid-beta immunotherapy for Alzheimer's disease: the end of the beginning. Nat Rev Neurosci 3:824-828.

Schultheiss C, Blechert B, Gaertner FC, Drecoll E, Mueller J, Weber GF, Drzezga A, Essler M. 2006. In vivo characterization of endothelial cell activation in a transgenic mouse model of Alzheimer's disease. Angiogenesis 9:59-65.

Selkoe DJ. 1994. Amyloid beta-protein precursor: new clues to the genesis of Alzheimer's disease. Curr Opin Neurobiol 4:708-716.

Senger DR, Perruzzi CA, Feder J, Dvorak HF. 1986. A highly conserved vascular permeability factor secreted by a variety of human and rodent tumor cell lines. Cancer Res 46:5629-5632.

Sherrington R, Rogaev EI, Liang Y, Rogaeva EA, Levesque G, Ikeda M, Chi H, Lin C, Li G, Holman K, et al. 1995. Cloning of a gene bearing missense mutations in early-onset familial Alzheimer's disease. Nature 375:754-760.

Shibata M, Yamada S, Kumar SR, Calero M, Bading J, Frangione B, Holtzman DM, Miller CA, Strickland DK, Ghiso J, Zlokovic BV. 2000. Clearance of Alzheimer's amyloid-ss(1-40) peptide from brain by LDL receptor-related protein-1 at the blood-brain barrier. J Clin Invest 106:1489-1499.

Sjögren M, Mielke M, Gustafson D, Zandi P, Skoog I. 2006. Cholesterol and Alzheimer's disease--is there a relation? Mech Ageing Dev 127:138-147.

Sparks DL, Sabbagh MN, Connor DJ, Lopez J, Launer LJ, Browne P, Wasser D, Johnson-Traver S, Lochhead J, Ziolwolski C. 2005. Atorvastatin for the treatment of mild to moderate Alzheimer disease: preliminary results. Arch Neurol 62:753-757.

Spires TL, Hyman BT. 2005. Transgenic models of Alzheimer's disease: learning from animals. NeuroRx 2:423-437.

Stalder M, Phinney A, Probst A, Sommer B, Staufenbiel M, Jucker M. 1999. Association of microglia with amyloid plaques in brains of APP23 transgenic mice. Am J Pathol 154:1673-1684.

Stampfer MJ. 2006. Cardiovascular disease and Alzheimer's disease: common links. J Intern Med 260:211-223.

Stanimirovic D, Satoh K. 2000. Inflammatory mediators of cerebral endothelium: a role in ischemic brain inflammation. Brain Pathol 10:113-126.

Strohmeyer R, Kovelowski CJ, Mastroeni D, Leonard B, Grover A, Rogers J. 2005. Microglial responses to amyloid beta peptide opsonization and indomethacin treatment. J Neuroinflammation 2:18.

Sturchler-Pierrat C, Abramowski D, Duke M, Wiederhold KH, Mistl C, Rothacher S, Ledermann B, Bürki K, Frey P, Paganetti PA, Waridel C, Calhoun ME, Jucker M, Probst A, Staufenbiel M, Sommer B. 1997. Two amyloid precursor protein transgenic mouse models with Alzheimer disease-like pathology. Proc Natl Acad Sci U S A. 94:13287-13292.

Sunderkötter C, Steinbrink K, Goebeler M, Bhardwaj R, Sorg C. 1994. Macrophages and angiogenesis. J Leukoc Biol 55:410-422.

Suo Z, Tan J, Placzek A, Crawford F, Fang C, Mullan M. 1998. Alzheimer's beta-amyloid peptides induce inflammatory cascade in human vascular cells: the roles of cytokines and CD40. Brain Res 807:110-117.

Takano T, Tian GF, Peng W, Lou N, Libionka W, Han X, Nedergaard M. 2006. Astrocyte-mediated control of cerebral blood flow. Nat Neurosci 9:260-267.

Tarkowski E, Issa R, Sjögren M, Wallin A, Blennow K, Tarkowski A, Kumar P. 2002. Increased intrathecal levels of the angiogenic factors VEGF and TGF-beta in Alzheimer's disease and vascular dementia. Neurobiol Aging 23:237-243.

Thal LJ, Ferris SH, Kirby L, Block GA, Lines CR, Yuen E, Assaid C, Nessly ML, Norman BA, Baranak CC, Reines SA; Rofecoxib Protocol 078 study group. 2005. A randomized, double-blind, study of rofecoxib in patients with mild cognitive impairment. Neuropsychopharmacology 30:1204-1215.

Thirumangalakudi L, Samany PG, Owoso A, Wiskar B, Grammas P. 2006. Angiogenic proteins are expressed by brain blood vessels in Alzheimer's disease. J Alzheimers Dis 10:111-118.

Tojo T, Ushio-Fukai M, Yamaoka-Tojo M, Ikeda S, Patrushev N, Alexander RW. 2005. Role of gp91phox (Nox2)-containing NAD(P)H oxidase in angiogenesis in response to hindlimb ischemia. Circulation 111:2347-2355.

Tomimoto H, Akiguchi I, Suenaga T, Nishimura M, Wakita H, Nakamura S, Kimura J. 1996. Alterations of the blood-brain barrier and glial cells in white-matter lesions in cerebrovascular and Alzheimer's disease patients. Stroke 27:2069-2074.

Turner PR, O'Connor K, Tate WP, Abraham WC. 2003. Roles of amyloid precursor protein and its fragments in regulating neural activity, plasticity, and memory. Prog Neurobiol 70:1-32.

Ubogu EE, Cossoy MB, Ransohoff RM. 2006. The expression and function of chemokines involved in CNS inflammation. Trends Pharmacol Sci 27:48-55.

Uchihara T, Akiyama H, Kondo H, Ikeda K. 1997. Activated microglial cells are colocalized with perivascular deposits of amyloid-beta protein in Alzheimer's disease brain. Stroke 28:1948-1950.

Ujiie M, Dickstein DL, Carlow DA, Jefferies WA. 2003. Blood-brain barrier permeability precedes senile plaque formation in an Alzheimer disease model. Microcirculation 10:463-470.

Vagnucci AH Jr, Li WW. 2003. Alzheimer's disease and angiogenesis. Lancet 361:605-608.

Van Dam D, De Deyn PP. 2006. Drug discovery in dementia: the role of rodent models. Nat Rev Drug Discov 5:956-970.

Van Den Heuvel C, Thornton E, Vink R. 2007. Traumatic brain injury and Alzheimer's disease: a review. Prog Brain Res 161:303-316.

Van Gool WA, Weinstein HC, Scheltens P, Walstra GJ. 2001. Effect of hydroxychloroquine on progression of dementia in early Alzheimer's disease: an 18-month randomised, double-blind, placebo-controlled study. Lancet 358:455-460.

Vassar R, Bennett BD, Babu-Khan S, Kahn S, Mendiaz EA, Denis P, Teplow DB, Ross S, Amarante P, Loeloff R, Luo Y, Fisher S, Fuller J, Edenson S, Lile J, Jarosinski MA, Biere AL, Curran E, Burgess T, Louis JC, Collins F, Treanor J, Rogers G, Citron M. 1999. Beta-secretase cleavage of Alzheimer's amyloid precursor protein by the transmembrane aspartic protease BACE. Science. 286:735-741.

Walker DG, Beach TG. 2002. Microglial and astrocytic reactions in Alzheimer's disease. In: De Vellis JS , editor. *Neuroglia in the aging brain.* Totowa, NJ: Humana Press. pp. 339-363.

Webster B, Hansen L, Adame A, Crews L, Torrance M, Thal L, Masliah E. 2006. Astroglial activation of extracellular-regulated kinase in early stages of Alzheimer disease. J Neuropathol Exp Neurol 65:142-151.

Weggen S, Rogers M, Eriksen J. 2007. NSAIDs: small molecules for prevention of Alzheimer's disease or precursors for future drug development? Trends Pharmacol Sci 28:536-543.

Wegiel J, Wang KC, Imaki H, Rubenstein R, Wronska A, Osuchowski M, Lipinski WJ, Walker LC, LeVine H. 2001. The role of microglial cells and astrocytes in fibrillar plaque evolution in transgenic APP(SW) mice. Neurobiol Aging 22:49-61.

Weiss JM, Downie SA, Lyman WD, Berman JW. 1998. Astrocyte-derived monocyte-chemoattractant protein-1 directs the transmigration of leukocytes across a model of the human blood-brain barrier. J Immunol 161:6896-6903.

Weldon DT, Rogers SD, Ghilardi JR, Finke MP, Cleary JP, O'Hare E, Esler WP, Maggio JE, Mantyh PW. 1998. Fibrillar beta-amyloid induces microglial phagocytosis, expression of inducible nitric oxide synthase, and loss of a select population of neurons in the rat CNS in vivo. J Neurosci 18:2161-2173.

Wolozin B, Wang SW, Li NC, Lee A, Lee TA, Kazis LE. 2007. Simvastatin is associated with a reduced incidence of dementia and Parkinson's disease. BMC Med 5:20.

Wyss-Coray T. 2006. Inflammation in Alzheimer disease: driving force, bystander or beneficial response? Nat Med 12:1005-1015.

Xiong M, Elson G, Legarda D, Leibovich SJ. 1998. Production of vascular endothelial growth factor by murine macrophages: regulation by hypoxia, lactate, and the inducible nitric oxide synthase pathway. Am J Pathol 153:587-598.

Xu F, Grande AM, Robinson JK, Previti ML, Vasek M, Davis J, Van Nostrand WE. 2007. Early-onset subicular microvascular amyloid and neuroinflammation correlate with behavioral deficits in vasculotropic mutant amyloid beta-protein precursor transgenic mice. Neuroscience 146:98-107.

Yamada K, Nabeshima T. 2000. Animal models of Alzheimer's disease and evaluation of anti-dementia drugs. Pharmacol Ther 88:93-113.

Yan Q, Zhang J, Liu H, Babu-Khan S, Vassar R, Biere AL, Citron M, Landreth G. 2003. Anti-inflammatory drug therapy alters beta-amyloid processing and deposition in an animal model of Alzheimer's disease. J Neurosci 23:7504-7509.

Yang SP, Bae DG, Kang HJ, Gwag BJ, Gho YS, Chae CB. 2004. Co-accumulation of vascular endothelial growth factor with beta-amyloid in the brain of patients with Alzheimer's disease. Neurobiol Aging 25:283-290.

Yoshida S, Yoshida A, Ishibashi T. 2004. Induction of IL-8, MCP-1, and bFGF by TNF-alpha in retinal glial cells: implications for retinal neovascularization during post-ischemic inflammation. Graefes Arch Clin Exp Ophthalmol 242:409-413.

Zand L, Ryu JK, McLarnon JG. 2005. Induction of angiogenesis in the beta-amyloid peptide-injected rat hippocampus. Neuroreport 16:129-132.

Zlokovic BV. 2005. Neurovascular mechanisms of Alzheimer's neurodegeneration. Trends Neurosci 28:202-208.

CHAPTER 2: MINOCYCLINE OR INOS INHIBITION BLOCK 3-NITROTYROSINE INCREASES AND BLOOD-BRAIN BARRIER LEAKINESS IN AMYLOID-BETA PEPTIDE-INJECTED RAT HIPPOCAMPUS[1]

2.1 INTRODUCTION

Inflammation has been suggested as a contributing factor in the pathological processes of Alzheimer's disease (AD) (Akiyama et al., 2000). Results from analysis of postmortem AD brains (McGeer and McGeer, 2003) and transgenic animal models of AD (Heneka et al., 2005) show upregulation of inflammatory components in AD brain compared with age-matched controls. Importantly, a diversity of pharmacological agents sharing a commonality in reducing risk of AD, show anti-inflammatory effects with long-term application (Aisen et al., 2002). In vitro, results from a number of studies have reported enhanced inflammatory responses in $A\beta_{1-42}$-stimulated microglia (Combs et al., 2001; Lue et al., 2001; Xie et al., 2002).

Alterations in properties of the cerebrovasculature have been suggested as contributing to the pathogenesis in AD (Vagnucci and Li, 2003; Zlokovic et al., 2005). Indeed, impaired cerebral circulation, vascular inflammation and BBB dysfunction have been identified in the brains of AD patients (Farkas and Luiten, 2001). The functional importance of cerebrovasculature in AD is based on its ability to maintain a homeostatic environment, crucial to the viability of neurons (Hawkins and Davis, 2005). Inflammatory responses, mediated by activated glia, could play an important role in perturbing cerebrovascular functions in AD.

We have previously demonstrated that blockade of $A\beta_{1-42}$-derived microglial activation by minocycline, a second-generation tetracycline derivative with anti-inflammatory and neuroprotective properties (Domercq and Matute, 2004) can enhance neuronal survival in the rat hippocampus (Ryu et al., 2004a). In the present study we report that the peptide-injected hippocampus exhibits marked elevation of nitrotyrosine (3-NT), an indicator for peroxynitrite formation, and increased leakiness of the BBB. Minocycline, or the iNOS inhibitor 1400W, have then been examined for effects to inhibit glial-derived 3-NT and maintain the integrity of the BBB.

---

[1]A version of this chapter has been published. Ryu, J.K. and McLarnon, J.G. (2006) Minocycline or iNOS inhibition block 3-nitrotyrosine increases and blood-brain barrier leakiness in amyloid-beta peptide-injected rat hippocampus. Exp Neurol. 198:552-557.

2.2 MATERIALS AND METHODS

2.2.1 Animal care and surgery

All animal experiments were approved by the Committee on Animal Care of the University of British Columbia. Adult male Sprague Dawley rats (Charles River Labs, St. Constant, Quebec; 260–280 g) were anesthetized with ketamine hydrochloride (72 mg/kg, i.p.) and xylazine (9 mg/kg, i.p.) and then mounted in a stereotaxic apparatus (David Kopf Instruments, Tujunga, CA). Rats (n = 4 per group) received unilateral stereotaxic injection of $A\beta_{1-42}$ or reverse peptide $A\beta_{42-1}$ (1 nmol in 2 μl; California Peptide Research, Napa, CA) into dentate gyrus of hippocampus (AP: -3.6 mm, ML: -1.8 mm, DV: -3.2 mm) as described previously (Ryu et al., 2004a). Nonlesioned animals served as control. Minocycline (Sigma, St. Louis, MO) was injected intraperitoneally at 50 mg/kg immediately following and 12 hr after $A\beta_{1-42}$ injection and then 25 mg/kg daily for 7 days (Ryu et al., 2004a) (n = 4). 1400W (Sigma) was dissolved in saline and injected subcutaneouly at a dose of 10 mg/kg immediately following and 12 hr after $A\beta_{1-42}$ injection and then daily for 7 days (Parmentier et al., 1999) (n = 4). Control rats and rats injected with $A\beta_{1-42}$, but not $A\beta_{42-1}$, were administered with minocycline or 1400W. All animals were sacrificed at 7 days.

2.2.2 Immunohistochemistry

The preparation of tissue (40 μm serial coronal sections) and immunohistochemical procedures followed published procedures (Ryu et al., 2004b). Briefly, free-floating sections were incubated overnight at 4°C with the primary antibodies; rabbit anti-3-nitrotyrosine (indicative of peroxynitrite formation, 1:500, Upstate Biotechnology, Lake Placid, NY). Sections were then incubated at room temperature (RT) with biotinylated secondary antibody (1:500; Vector, Burlingame, CA), avidin-biotin-peroxidase kit (ABC, 1:200, Vector), and 3,3′-diaminobenzidine (Sigma). As positive control for 3-NT staining, sections were preincubated with 24 mM peroxynitrite and processed as above. Specificity of 3-NT antibody was confirmed by incubating the primary antibody with a 10 mM nitrotyrosine. The permeability of BBB was assessed using IgG immunohistochemistry with brain sections incubated at RT with rat anti-IgG (1:500; Vector), ABC, and DAB (Sigma).

2.2.3 Double immunofluorescence staining

For double immunofluorescence staining (Ryu et al., 2004b), sections were incubated (24 hr at 4°C) with a mixture of two primary antibodies: mouse anti-CR3 (OX-42, indicative of microglia/macrophages, 1:500; Serotec, Oxford), mouse anti-GFAP (indicative of astrocytes, 1:1000, Sigma) or mouse anti-NeuN (indicative of neurons, 1:500, Chemicon, Temecula, CA) in combination with 3-NT (1:500; Upstate Biotechnology). Sections were then incubated with fluorescence-conjugated goat secondary antibodies (Alexa Fluor antibodies; Molecular Probes, Eugene, OR) at RT for 2 hr in the dark.

2.2.4 Quantitative analysis of immunohistochemical staining

Three hippocampal sections (AP: -3.6 mm, equally spaced 80 μm intervals) were used for quantitative analysis. For 3-NT and IgG immunoreactivity, gray scale pixel values were measured in the dentate gyrus using Northern Eclipse software (Empix Imaging) as described previously (Ryu et al., 2004a). The number of 3-NT expressing microglia/macrophages, astrocytes and neurons in the dentate gyrus were counted using a 40X objective under a Zeiss Axioplan-2 fluorescence microscope with Northern Eclipse software (Empix Imaging) (Ryu et al., 2004b).

2.2.5 Statistical Analysis

All quantitative analyses were carried out in a blinded manner with values expressed as means ± SEM. Statistical significance was assessed using analysis of variance (ANOVA), followed by Student-Newman-Keuls multiple comparison test (GraphPad Prism 3.0). Significance was set at $p < 0.05$.

2.3 RESULTS

Initial experiments examined the induction of 3-nitrotyrosine (3-NT) at 7 d following $A\beta_{1-42}$ injection into rat hippocampus. As shown in Fig. 2-1A, numbers of 3-NT-positive cells were significantly increased with $A\beta_{1-42}$ injection relative to nonlesioned control. Both minocycline or iNOS inhibitor 1400W treatments were effective in reducing numbers of 3-NT-positive cells in $A\beta_{1-42}$-injected brain. Little or no induction of 3-NT was found in the hippocampus after injection of reverse peptide $A\beta_{42-1}$ (Fig. 2-1A), or minocycline or 1400W alone (data not shown). Quantitative analysis (Fig. 2-1B) showed $A\beta_{1-42}$ injection increased 3-NT immunoreactivity (ir) 194-fold relative to nonlesioned control and this increase was significantly reduced in minocycline (by 56%) or 1400W (by 66%) administered animals. As shown in Fig. 2-1B, 3-NT ir was very low with reverse peptide ($A\beta_{42-1}$) injection or in animals receiving minocycline or 1400W in the absence of $A\beta_{1-42}$.

We next assessed the effects of minocycline or 1400W on $A\beta_{1-42}$-induced 3-NT induction in specific cell types; microglia/macrophages, astrocytes and neurons. Representative results from double immunofluorescence analysis (Fig. 2-2A and B) showed that at 7 d following $A\beta_{1-42}$ injection into rat brain, 3-NT ir in OX-42-positive microglia/macrophages (Fig. 2-2A, top row and second column) and GFAP-positive astrocytes (Fig. 2-2B, top row and second column) was considerably increased relative to nonlesioned control. Both minocycline and 1400W treatments were effective in attenuating expressions of 3-NT in both microglia/macrophages and astrocytes (Fig. 2-2A and B). Injection of $A\beta_{42-1}$ (bottom low and second column) or minocycline or 1400W alone (data not shown) had little or no effect to alter the 3-NT expression in glial cells. In addition, no 3-NT ir was observed in NeuN-positive neurons at 7 days post-$A\beta_{42-1}$ injection (data not shown).

Overall, intrahippocampal $A\beta_{1-42}$ injection significantly increased 3-NT expression in microglia/macrophages (by 31-fold) and astrocytes (by 58-fold) compared with nonlesioned control (Fig. 2-2C). In $A\beta_{1-42}$-injected hippocampus, administration of minocycline significantly reduced 3-NT expressions in glia (by 57% for microglia/macrophages and by 22% for astrocytes) relative to $A\beta_{1-42}$ alone. 1400W treatment also inhibited induction of 3-NT in microglia/macrophages (by 70%) and astrocytes (by 38%) relative to $A\beta_{1-42}$ alone; actions of the iNOS inhibitor were significant.

Figure 2-1. Effects of minocycline and 1400W on $A\beta_{1-42}$-mediated 3-NT induction. (A) Representative photomicrographs of 3-NT-immunoreactive cells in the dentate gyrus from nonlesioned control, $A\beta_{1-42}$-injection at 7 days in the absence and presence of minocycline (MC) or 1400W, and for $A\beta_{42-1}$ injection. Scale bar = 30 μm. (B) Quantification of 3-NT immunoreactivity; data are mean ± SEM (n=4). $*p < 0.05$ vs. nonlesioned control. $**p < 0.05$ vs. $A\beta_{1-42}$-injected rats.

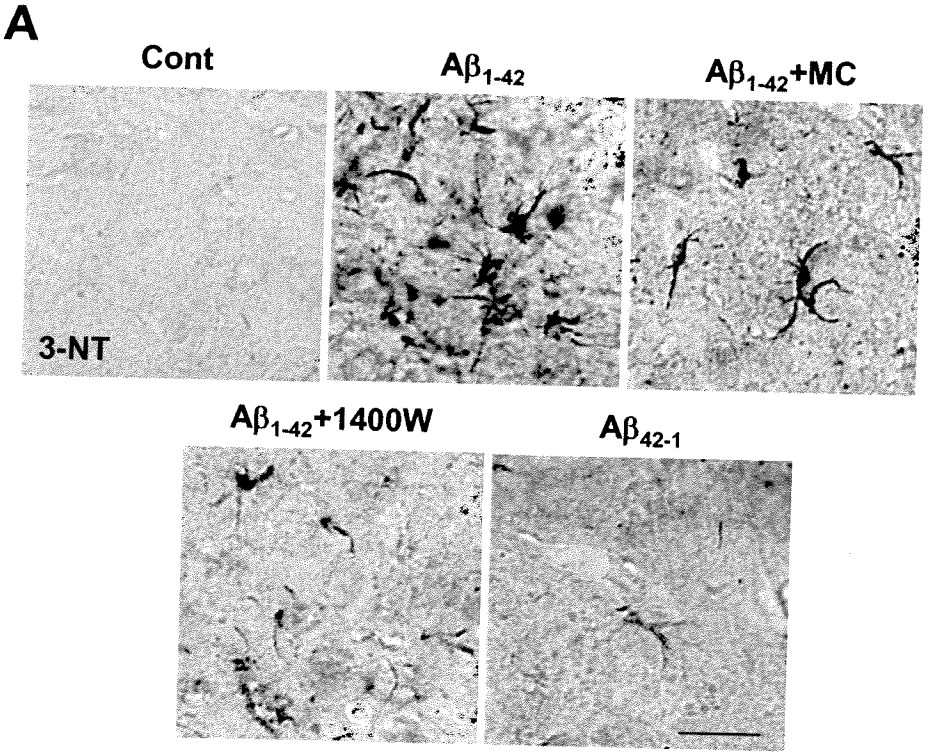
A
Cont
Aβ1-42
Aβ1-42+MC
3-NT
Aβ1-42+1400W
Aβ42-1

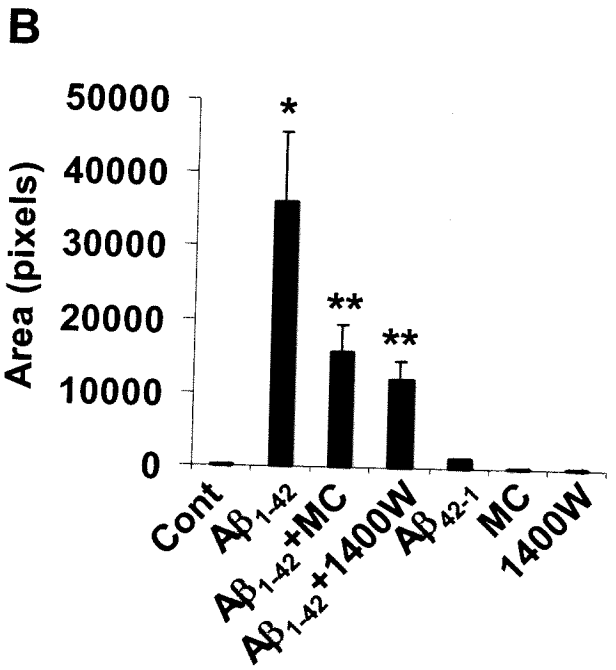
B
Area (pixels)
50000
40000
30000
20000
10000
0
*
**
**
Cont
Aβ1-42
Aβ1-42+MC
Aβ1-42+1400W
Aβ42-1
MC
1400W

Figure 2-2. Effects of minocycline and 1400W on $A\beta_{1-42}$-induced 3-NT induction in activated glial cells. (A) Double immunofluorescence staining of 3-NT (green) with OX-42-positive microglia/macrophages (red) or (B) GFAP-positive astrocytes (red) in the dentate gyrus obtained from nonlesioned control animals, $A\beta_{1-42}$-injected rats for 7 days in the absence or presence of minocycline (MC) or 1400W, and rats injected with $A\beta_{42-1}$ alone. Scale bars = 20 μm. (C) Quantification of the number of microglia/macrophages or astrocytes expressing 3-NT. Data are mean ± SEM (n=4). $*p < 0.05$ vs. nonlesioned control. $**p < 0.05$ vs. $A\beta_{1-42}$-injected rats.

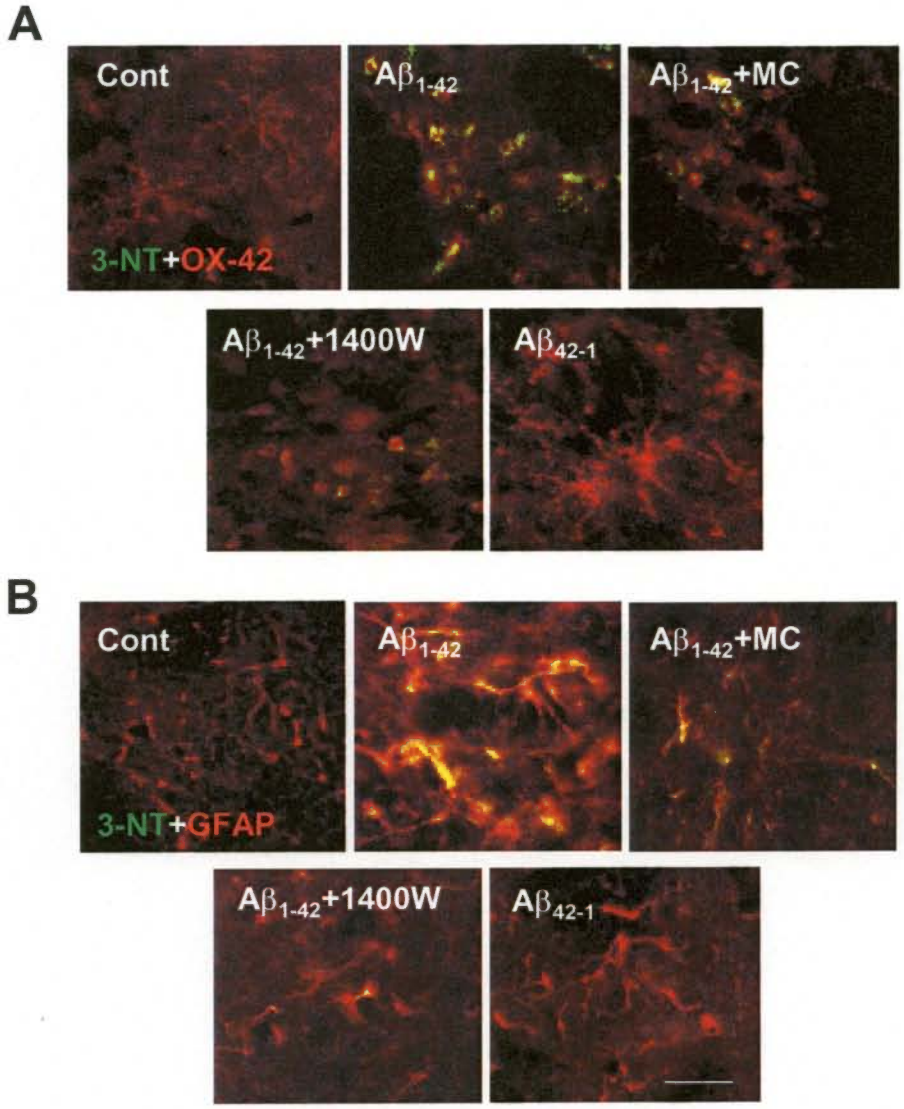
A
Cont
3-NT+OX-42
Aβ1-42
Aβ1-42+MC
Aβ1-42+1400W
Aβ42-1
B
Cont
3-NT+GFAP
Aβ1-42
Aβ1-42+MC
Aβ1-42+1400W
Aβ42-1
C
Microglia
Astrocytes
3-NT+ cells/mm2
80
60
40
20
0
*
**
**
Cont
Aβ1-42
Aβ1-42+MC
Aβ1-42+1400W
Aβ42-1
MC
1400W

Intrahippocampal injections with any of $A\beta_{42-1}$, minocycline or 1400W had little effect on number of 3-NT immunoreactive glial cells compared to control (Fig. 2-2C).

An important aspect of this study was to examine properties of vasculature in $A\beta_{1-42}$-injected hippocampus. Immunohistochemical staining showed prominent 3-NT ir located in proximity to cerebral blood vessels (indicated by V) with $A\beta_{1-42}$ injection for microglia/macrophages (top row) and astrocytes (bottom row) compared with nonlesioned control (first and second columns, Fig. 2-3A). Injection of minocycline (third column) or 1400W (fourth column) with $A\beta_{1-42}$ considerably reduced 3-NT ir in the vicinity of blood vessels. No induction of 3-NT was found in animal brains injected with $A\beta_{42-1}$ (Fig. 2-3A, fifth column), or minocycline or 1400W separately (data not shown).

We also measured BBB permeability in $A\beta_{1-42}$-injected hippocampus using immunohistochemical analysis with IgG antibody. Figure 2-3B (top row) presents representative (low magnification) IgG-stained hippocampal regions showing no IgG ir for nonlesioned control but high levels of IgG staining in the dentate gyrus of $A\beta_{1-42}$-injected hippocampus. This increased IgG staining was markedly diminished by minocycline or 1400W treatment and absent with $A\beta_{42-1}$ injection. The regions denoted by asterisks (top row, Fig. 2-3B) are presented at higher magnification (lower row, Fig. 2-3B). The results show a high degree of IgG infiltration in regions adjacent to blood vessels (V) at 7 days after $A\beta_{1-42}$ injection (Fig. 2-3B, bottom row and second column) relative to nonlesioned control (Fig. 2-3B, bottom row and first column). However, IgG ir in the vicinity of blood vessels (marked as V) was markedly reduced in the hippocampus of rats receiving minocycline (third column) or 1400W (fourth column) with $A\beta_{1-42}$. Little or no IgG ir was evident in the hippocampus of animals injected with $A\beta_{42-1}$ (Fig. 2-3B, bottom row and fifth column) or either of minocycline or 1400W alone (data not shown). Quantification in the level of IgG ir is presented in Fig. 2-3C with minocycline and 1400W showing significant reductions of IgG ir (by 59% for minocycline and by 73% for 1400W relative to control). Minocycline or 1400W alone, in the absence of $A\beta_{1-42}$, showed little or no IgG ir. Reverse peptide $A\beta_{42-1}$ had only a small effect on IgG ir.

Figure 2-3. Effects of minocycline and 1400W on $A\beta_{1-42}$-induced BBB leakiness. (A) Double immunofluorescence staining of 3-NT (green) and OX-42-positive microglia/macrophages (red) or GFAP-positive astrocytes (red) in the vicinity of blood vessels (labelled V): nonlesioned control, $A\beta_{1-42}$-injected animals at 7 days in the absence or presence of minocycline (MC) or 1400W, and rats injected with $A\beta_{42-1}$. Scale bars = 30 μm. (B) IgG immunoreactivity in the hippocampus of nonlesioned control and lesioned hippocampus obtained from $A\beta_{1-42}$-injected rats at 7 days in the absence or presence of MC or 1400W and rats injected with $A\beta_{42-1}$ (top row). Highly magnified photomicrographs of IgG immunoreactivity around blood vessels (V) are presented (bottom row, corresponding to region indicated by asterisk (*) in top row). Scale bars = 1 mm (top row) and 50 μm (bottom row). (C) Quantification of IgG immunoreactivity; data are mean ± SEM (n=4). $*p < 0.05$ vs. nonlesioned control. $**p < 0.05$ vs. $A\beta_{1-42}$-injected rats.

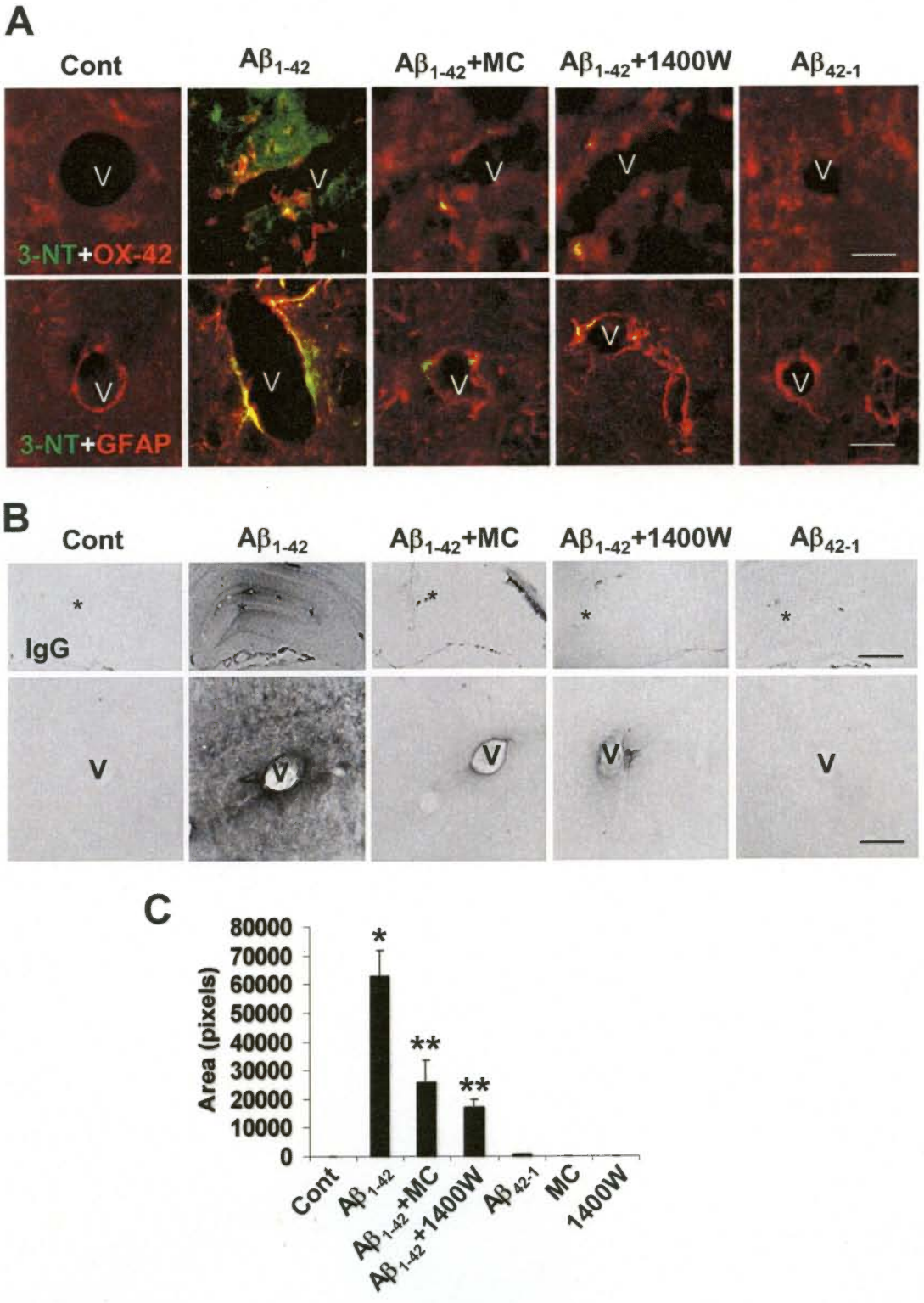
A
Cont
Aβ1-42
Aβ1-42+MC
Aβ1-42+1400W
Aβ42-1
3-NT+OX-42
3-NT+GFAP
V
B
Cont
Aβ1-42
Aβ1-42+MC
Aβ1-42+1400W
Aβ42-1
IgG
V
C
Area (pixels)
80000
70000
60000
50000
40000
30000
20000
10000
0
*
**
**
Cont
Aβ1-42
Aβ1-42+MC
Aβ1-42+1400W
Aβ42-1
MC
1400W

2.4 DISCUSSION

In this study we demonstrate for the first time that administration of minocycline or a selective iNOS inhibitor decreases 3-NT induction in activated microglia/macrophages and reactive astrocytes following intrahippocampal $A\beta_{1-42}$ injection. Of particular importance was the finding that activated glial cells expressing 3-NT were spatially associated with blood vessels. IgG permeability through BBB was markedly increased with $A\beta_{1-42}$ injection indicative of leakiness of this barrier. Both minocycline or iNOS inhibition were highly effective in restoring the integrity of the BBB.

The present results suggest that $A\beta_{1-42}$ injection is associated with a spectrum of inflammatory responses including changes in functional properties of BBB. Furthermore, reactive nitrogen species, induced by stimulation of both microglia/macrophages and astrocytes, appears to play a role in mediating perturbations in BBB. The decreased 3-NT ir in glial cells in response to minocycline treatment may be due to the ability of this compound to reduce the activity of oxidative enzymes such as COX-2, NADPH-oxidase and iNOS; involvement of the latter factor is also indicated by the efficacy of 1400W to reduce 3-NT. Findings from high-performance liquid chromatography (HPLC) (Hensley et al., 1998) and immunohistochemical (Smith et al., 1997) analysis and proteonomic studies (Castegna et al., 2003) of AD brain have demonstrated increased levels of nitrotyrosine in affected brain regions. Previous work has reported minocycline-induced inhibition of 3-NT production is correlated with reduction of glial oxidative enzyme activity in 1-methyl-4-phenyl-1,2,3,6-tetrahydropyridine (MPTP) (Wu et al., 2002) or LPS-injected animals (Tomas-Camardiel et al., 2004).

Our results show similar spatial patterns of 3-NT and clusters of IgG immunostaining in the vicinity of blood vessels suggesting the possibility that glial cell-derived nitrogen species such as peroxynitrite may be involved in the alteration of blood vascular function. Administration of minocycline or 1400W decreased 3-NT induction in glial cells in the vicinity of blood vessels (Fig. 2-3A) and decreased the permeability of the BBB to IgG (Fig. 2-3B). These observations are consistent with a reduction in glial activation leading to a diminished peroxynitrite formation and increase in the intactness of the BBB. Recent studies have reported that peroxynitrite is capable of causing alterations in BBB integrity (Knepler et al., 2001; Tan et al., 2004). Although the specific pathological roles of BBB dysfunction in the pathogenesis of AD are not known, previous studies have indicated alterations in BBB permeability may increase risk of neuronal damage in AD (de Vries et al., 1997).

The present results suggest the utility of future studies to correlate the effects of changes in BBB functional properties with neuronal viability and to examine pharmacological modulation of BBB for neuroprotection in $A\beta_{1-42}$-injected brain. Minocycline, which exhibits anti-angiogenic properties (Tamargo et al., 1991), is a candidate therapeutic compound to inhibit inflammation and cerebrovascular alterations in AD.

2.5 REFERENCES

Aisen, P.S., 2002. The potential of anti-inflammatory drugs for the treatment of Alzheimer's disease. Lancet Neurol. 1, 279-284.

Akiyama, H., Barger, S., Barnum, S., Bradt, B., Bauer, J., Cole, G.M., et al., 2000. Inflammation and Alzheimer's disease. Neurobiol. Aging 21, 383-421.

Castegna, A., Thongboonkerd, V., Klein, J.B., Lynn, B., Markesbery, W.R., Butterfield, D.A., 2003. Proteomic identification of nitrated proteins in Alzheimer's disease brain. J. Neurochem. 85, 1394-1401.

Combs, C.K., Karlo, J.C., Kao, S.C., Landreth, G.E., 2001. beta-Amyloid stimulation of microglia and monocytes results in TNFalpha-dependent expression of inducible nitric oxide synthase and neuronal apoptosis. J. Neurosci. 21, 1179-1188.

de Vries, H.E., Kuiper, J., de Boer, A.G., Van Berkel, T.J., Breimer, D.D., 1997. The blood-brain barrier in neuroinflammatory diseases. Pharmacol. Rev. 49, 143-155.

Domercq, M., Matute, C., 2004. Neuroprotection by tetracyclines. Trends Pharmacol. Sci. 25, 609-612.

Farkas, E., Luiten, P.G., 2001. Cerebral microvascular pathology in aging and Alzheimer's disease. Prog. Neurobiol. 64, 575-611.

Hawkins, B.T., Davis, T.P., 2005. The blood-brain barrier/neurovascular unit in health and disease. Pharmacol. Rev. 57, 173-185.

Heneka, M.T., Sastre, M., Dumitrescu-Ozimek, L., Hanke, A., Dewachter, I., Kuiperi, C., et al., 2005. Acute treatment with the PPARgamma agonist pioglitazone and ibuprofen reduces glial inflammation and Abeta1-42 levels in APPV717I transgenic mice. Brain 128, 1442-1453.

Hensley, K., Maidt, M.L., Yu, Z., Sang, H., Markesbery, W.R., Floyd, R.A., 1998. Electrochemical analysis of protein nitrotyrosine and dityrosine in the Alzheimer brain indicates region-specific accumulation. J. Neurosci. 18, 8126-8132.

Knepler, J.L. Jr., Taher, L.N., Gupta, M.P., Patterson, C., Pavalko, F., Ober, M.D., Hart, C.M., 2001. Peroxynitrite causes endothelial cell monolayer barrier dysfunction. Am. J. Physiol. Cell Physiol. 281, C1064-1075.

Lue, L.F., Rydel, R., Brigham, E.F., Yang, L.B., Hampel, H., Murphy, G.M.Jr., et al., 2001. Inflammatory repertoire of Alzheimer's disease and nondemented elderly microglia in vitro. Glia 35, 72-79.

McGeer, E.G., McGeer, P.L., 2003. Inflammatory processes in Alzheimer's disease. Prog. Neuropsychopharmacol. Biol. Psychiatry 27, 741-749.

Parmentier, S., Bohme, G.A., Lerouet, D., Damour, D., Stutzmann, J.M., Margaill, I., Plotkine, M., 1999. Selective inhibition of inducible nitric oxide synthase prevents ischaemic brain injury. Br. J. Pharmacol. 127, 546-552.

Ryu, J.K., Franciosi, S., Sattayaprasert, P., Kim, S.U., McLarnon, J.G., 2004a. Minocycline inhibits neuronal death and glial activation induced by beta-amyloid peptide in rat hippocampus. Glia 48, 85-90.

Ryu, J.K., Kim, S.U., McLarnon, J.G., 2004b. Blockade of quinolinic acid-induced neurotoxicity by pyruvate is associated with inhibition of glial activation in a model of Huntington's disease. Exp. Neurol. 187, 150-159.

Smith, M.A., Richey Harris, P.L., Sayre, L.M., Beckman, J.S., Perry, G., 1997. Widespread peroxynitrite-mediated damage in Alzheimer's disease. J. Neurosci. 17, 2653-2657.

Tamargo, R.J., Bok, R.A., Brem, H., 1991. Angiogenesis inhibition by minocycline. Cancer Res. 51, 672-675.

Tan, K.H., Harrington, S., Purcell, W.M., Hurst, R.D., 2004. Peroxynitrite mediates nitric oxide-induced blood-brain barrier damage. Neurochem. Res. 29, 579-587.

Tomas-Camardiel, M., Rite, I., Herrera, A.J., de Pablos, R.M., Cano, J., Machado, A., Venero, J.L., 2004. Minocycline reduces the lipopolysaccharide-induced inflammatory reaction, peroxynitrite-mediated nitration of proteins, disruption of the blood-brain barrier, and damage in the nigral dopaminergic system. Neurobiol. Dis. 16, 190-201.

Vagnucci, A.H.Jr., Li, W.W., 2003. Alzheimer's disease and angiogenesis. Lancet 361, 605-608.

Wu, D.C., Jackson-Lewis, V., Vila, M., Tieu, K., Teismann, P., Vadseth, C., et al., 2002. Blockade of microglial activation is neuroprotective in the 1-methyl-4-phenyl-1,2,3,6-tetrahydropyridine mouse model of Parkinson disease. J. Neurosci. 22, 1763-1771.

Xie, Z., Wei, M., Morgan, T.E., Fabrizio, P., Han, D., Finch, C.E., Longo, V.D., 2002. Peroxynitrite mediates neurotoxicity of amyloid beta-peptide1-42- and lipopolysaccharide-activated microglia. J. Neurosci. 22, 3484-3492.

Zlokovic, B.V., 2005. Neurovascular mechanisms of Alzheimer's neurodegeneration. Trends Neurosci. 28, 202-208.

CHAPTER 3: THALIDOMIDE INHIBITION OF PERTURBED VASCULATURE AND GLIAL-DERIVED TUMOR NECROSIS FACTOR-α IN AN ANIMAL MODEL OF INFLAMED ALZHEIMER'S DISEASE BRAIN[2]

3.1 INTRODUCTION

Alzheimer's disease (AD) is an age-dependent brain disorder characterized by the progressive degeneration of neurons in brain regions involved in learning, memory and cognitive function. Chronic inflammatory processes are associated with the pathogenesis of AD with affected brain areas containing deposits of amyloid-beta (Aβ) peptide, neurofibrillary tangles and activated microglia, the immune responding cells of brain (McGeer and McGeer, 1999; Akiyama et al., 2000; Hardy and Selkoe, 2002). Stimulation of microglia by Aβ has been considered as a critical component of inflammatory responses in AD (Akiyama et al., 2000; Rogers et al., 2002) with an assemblage of inflammatory mediators released from peptide-activated cells (Lue et al., 2001). Importantly, products of microglia may be involved in neurodegeneration (Banati et al., 1993; Combs et al., 1999, 2001; Mrak and Griffin, 2005; Franciosi et al., 2006).

The use of anti-inflammatory agents such as NSAIDS has shown some clinical benefits in treatment of AD individuals (Breitner et al., 1995; McGeer and McGeer, 2006). However, the overall effectiveness of such medications has generally been limited (Eikelenboom and van Gool, 2004) possible indicating that inhibition of multiple processes resulting from activation of microglia may be required in order to optimally block inflammatory responses. An interesting possibility, not well-studied in terms of pharmacological modulation, is that activated microglia could signal changes in properties of vascular processes as a critical component of an inflammatory response. Such actions could lead to altered responses of endothelial cells and perturbations to the blood-brain barrier (BBB) which in turn could stimulate and shape microglial responses sustaining a chronic inflammatory environment in AD brain. Results from previous work have indicated altered properties of BBB in inflamed AD brain including evidence for increased vascular permeability (Prat et al., 2001; Ujiie et al., 2003), hypoperfusion (de la Torre, 2000, 2002; Zlokovic, 2005), angiogenic activity (Vagnucci and Li, 2003),

[2]A version of this chapter has been published. Ryu, J.K. and McLarnon, J.G. (2008) Thalidomide inhibition of perturbed vasculature and glial-derived tumor necrosis factor-α in an animal model of inflamed Alzheimer's disease brain. Neurobiol Dis. 29:254-266.

upregulation of pro-angiogenic factors (Tarkowski et al., 2002; Pogue and Lukiw, 2004) and endothelial cell damage (Grammas et al., 2006). In this laboratory, we have reported increased angiogenic activity (Zand et al., 2005) and leakiness of BBB (Ryu and McLarnon, 2006) in Aβ-injected rat hippocampus.

The present study has investigated microglial responses and association of microgliosis with vascular perturbations in $A\beta_{1-42}$-injected hippocampus. Thalidomide has been used as a pharmacological modulator since the compound exhibits anti-inflammatory actions (Corral and Kaplan, 1999) and effects on vascular processes (Bartlett et al., 2004). Although multiple thalidomide actions in tissue have been reported (see Discussion), one particular mechanism for the compound is inhibition of the pro-inflammatory factor TNF-α (Moreira et al., 1993). In this work we have addressed the possibility that anti-inflammatory effects of thalidomide to block TNF-α from activated microglia may be associated with effects of the agent to alter vascular processes. Since TNF-α is a potent angiogenic agent (Sunderkotter et al., 1994), we hypothesized that inhibition of the pro-inflammatory cytokine could be effective in modulating vascular remodeling in peptide-injected brain. Our findings indicate altered cerebral vasculature as an integral component of inflammatory responses with thalidomide an effective inhibitor of microglial-derived TNF-α leading to neuroprotection in a model of inflamed AD brain.

3.2 MATERIALS AND METHODS

3.2.1 Animal care and surgery

All animal procedures were approved by the University of British Columbia Animal Care Ethics Committee, adhering to guidelines of the Canadian Council on Animal Care. Male Sprague-Dawley rats (280-300 g) were obtained from Charles River Laboratories (St. Constant, Quebec). Animals were anesthetized with intraperitoneal (i.p.) injection of a mixture of ketamine hydrochloride (72 mg/kg; Bimeda-MTC, Cambridge, Ontario, Canada) and xylazine hydrochloride (9 mg/kg; Bayer Inc., Etobicoke, Ontario, Canada) and placed in a stereotaxic apparatus (David Kopf Instruments, Tujunga, CA). Stereotaxic unilateral injection of beta-amyloid (Aβ) peptide (see below) was performed as previously described (Ryu et al., 2004; Franciosi et al., 2006) using a 10 μl Hamilton syringe fitted with a 26-gauge needle. Injection coordinates were chosen according to the atlas of Paxinos and Watson (2005): anteriorposterior (AP): -3.3 mm, mediallateral (ML): -1.6 mm, dorsoventral (DV): -3.2 mm, from bregma. All efforts were made to minimize animal suffering and to reduce the number of animals used.

3.2.2 Preparation and application of amyloid-beta peptide and thalidomide

Peptides (full length $A\beta_{1-42}$ or reverse peptide $A\beta_{42-1}$; California Peptide, Napa, CA) were prepared following published procedures (Lue et al., 2001; Franciosi et al., 2005, 2006). The compounds were first dissolved in 35% acetonitrile (Sigma) and further diluted to 500 μM with incremental additions of PBS with vortexing. The peptide solution was subsequently incubated at 37°C for 18 hr to promote fibrilization and aggregation and stored at -20°C. Peptides (2 nmol in 1 μl) were slowly injected (0.2 μl/min) into the dentate gyrus of hippocampus for a duration of 7 d.

The preparation of thalidomide followed published work (Kenyon et al., 1997). Thalidomide (Biomol, Plymouth Meeting, PA) was emulsified in 0.5% carboxymethylcellulose in PBS (CMC) and administered i.p. at a dose of 100 mg/kg at the time of $A\beta_{1-42}$ injection followed by daily injection of 100 mg/kg for 7 days. Control animals were injected with CMC vehicle. The dose and treatment protocol for thalidomide in this study was well tolerated by the animals and has been previously reported to be effective in inhibition of angiogenic activity (Kenyon et al., 1997; Kaicker et al., 2003).

3.2.3 Immunofluorescence and Immunohistochemistry

At seven days post-injection, the animals were transcardially perfused with heparinized cold saline followed by 4% paraformaldehyde in 0.1 M phosphate buffer (0.1 M PB, pH 7.4) under anesthesia. Brains were removed from the skull, postfixed in the same fixative overnight and then placed in 30% sucrose for cryoprotection. The brains were then rapidly frozen in powdered dry ice and stored at -70°C. Coronal sections (40 μm) were cut on a cryostat throughout the hippocampus and stored in cryoprotectant solution. Free-floating sections were processed for single immunofluorescence staining as described previously (Ryu et al., 2007). Briefly, sections were incubated in PBS containing 1% bovine serum albumin (BSA; Sigma, St. Louis, MO), 10% normal goat serum (NGS) and 0.2% Triton X-100 (Sigma) for 1 hr. Sections were then incubated overnight at 4°C with the following primary antibodies: mouse anti-endothelial cell antigen (RECA-1, a marker for endothelial cells, 1:1000; Serotec Ltd, Kidlington, Oxford, UK), rabbit anti-laminin (laminin, a marker for vascular basement membrane protein, 1:1000; Sigma), goat anti-tumor necrosis factor-alpha (TNF-α, 1:500; Cedarlane Laboratories Ltd. Hornby, ON, Canada), rabbit anti-ionized calcium binding adapter molecule-1 (Iba-1, a marker for microglia, 1:500; Wako Chemicals, Richmond, VA), mouse anti-glial fibrillary acidic protein (GFAP, a marker for astrocytes, 1:1000; Sigma), or mouse anti-neuronal nuclei (NeuN, a marker for neurons, 1:1000; Chemicon, Temecula, CA). Sections were rinsed in PBS with 0.5% BSA and incubated with Alexa Fluor 488-conjugated goat anti-rabbit IgG (1:200; Invitrogen Canada Inc., Burlington, Ontario, Canada), Alexa Fluor 594-conjugated goat anti-mouse IgG (1:200; Invitrogen) or Alexa Fluor 594-conjugated donkey anti-goat IgG (1:200; Invitrogen) at room temperature (RT) for 2 hr in the dark.

Double immunofluorescence staining was performed as described previously (Ryu et al., 2004). Free-floating sections were incubated overnight at 4°C with a mixture of two primary antibodies: RECA (1:500; Serotec) in combination with laminin (1:1000; Sigma) or Iba-1 (1:1000; Wako); TNF-α (1:500; Cedarlane Laboratories Ltd) in combination with Iba-1 (1:1000; Wako) or rabbit anti-GFAP (1:1000; Sigma). Sections were then incubated in a mixture of Alexa Fluor 488 and Alexa Fluor 594 conjugated secondary antibodies (1:200; Invitrogen) at RT for 2 hr in the dark. For the detection of RECA or Iba-1 associated with altered vasculature, hippocampal sections in which the vessels were labeled by perfusion of FITC-albumin (Sigma, 10 mg/kg, intracardial injection; Cavaglia et al., 2001) were incubated overnight with primary antibody to RECA (1:1000; Serotec) or Iba-1 (1:1000; Wako), followed by incubation of Alexa Fluor conjugated secondary antibody (1:200; Invitrogen).

3.2.4 Quantitative analysis of immunohistochemical staining

Three coronal hippocampal sections were used for immunohistochemical analysis (Ryu et al., 2004). In order to ensure consistency within and between groups, matched hippocampal tissue sections were always processed and all microscopy parameters were kept constant throughout the experiments. Digitized images of immunostained sections were acquired using a Zeiss Axioplan-2 light microscope equipped with a DVC camera (Diagnostic Instruments, Sterling Heights, MI). These images were then analyzed using Northern Eclipse software (Empix Imaging, Mississauga, Ontario, Canada). In each stained section, the hippocampal subregion boudaries were outlined (Fig. 1A, upper left panel). The granule cell layer (GCL) region was defined as the superior blade of the dentate gyrus. The molecular layer (ML) region was defined as the area between GCL border and the hippocampal fissure. Four fields within the GCL and ML regions were then selected in each section (magnification of 40×). Vascular area density (the fraction of the total given area occupied by the vascular wall and lumen) and vessel diameter (measured as the outside diameter of longitudinal vascular images) was measured on RECA-immunostained sections (n = 5 rats per group). For FITC-albumin (measure of vascular permeability) and laminin (measure of vascular basement membrane and angiogenic activity) staining, intensity of pixels above a predetermined threshold level of staining intensity was measured (n = 5 rats per group). The measurements of microglial activation (Iba-1 marker), astrogliosis (GFAP marker), inflammatory/angiogenic factor expression (TNF-α), and neuronal survival (NeuN marker) were made on immunostained sections by counting the number of immunoreactive cells (n = 5 rats per group). All quantitative analyses were performed in a blind manner.

3.2.5 Consideration of vascular fluorescence markers used in this study

RECA-1: Anti-RECA-1 has been developed as a cell-specific monoclonal antibody to rat endothelial cell surface antigen (Duijvestijn et al., 1992). In this work, the specificity of anti-RECA-1 was shown by immunofluorescence staining of paraformaldehyde-fixed rat tissue sections. Anti-RECA-1 antibody reacted with all vascular endothelium in the rat tissues but not with other cell types. The affinity of this antibody to rat endothelial cells was further demonstrated by intravenous injection of RECA-1 antibody localization with rat endothelial cells (Ghabriel et al., 2000). Other evidence has shown anti-RECA-1 antibody association with rat vascular endothelium under different physiological and pathological brain conditions (Cao et al., 2004; Gursoy-Ozdemir et al., 2004; Hellsten et al., 2005).

Laminin: Anti-Laminin is an affinity isolated antigen specific antibody developed as a glycoprotein-specific probe to laminin from the basement membrane. Previous immunohistochemical and immunoelectron microscopy work provided clear evidence of localization of laminin in endothelial basement membrane but not in pericytes or other cell types (Sobel et al., 1998). Recent double immunofluorescent staining of laminin with several vascular markers also demonstrated laminin is strongly associated with blood vessels (Hellsten et al., 2005).

Albumin: FITC-albumin is an albumin labeled with fluorescein isothiocyanate for use in perfusion studies in animals. Therefore, permeability of the blood-brain barrier can be evaluated by the detection of extravasated FITC-albumin after systemic injection (Cavaglia et al., 2001). A previous study (Pietra and Johns, 1996) has examined fluorescent and immunoelectron microscopy staining of FITC-albumin in leaky arterial endothelium. The results showed considerable agreement in staining patterns of localization of FITC-albumin in the perivascular interstitial space using the two different methods.

3.2.6 Reverse Transcription-PCR in vitro in adult human microglia

Human microglia were provided by Douglas G. Walker (Laboratory of Neuroinflammation, Sun Health Research Institute, Sun City, AZ) and cultured as described previously (McLarnon et al., 2006; Walker et al., 2006). Cells were maintained in Dulbecco's modified Eagle's medium (DMEM; Life Technologies, Gaithersburg, MD) supplemented with 10% fetal bovine serum (FBS, Hyclone, Logan, UT) and 50 μg/ml gentamicin. Human microglia were plated on 12-well multiplates and incubated in serum free media for 48 hr to reduce cell activation (Walker et al., 2006). Cell treatments (for 8 hr) included $A\beta_{1-42}$ (5 μM), preincubation with thalidomide (50 μg/ml) for 1 hr before $A\beta_{1-42}$ exposure, thalidomide alone, PBS control and reverse peptide $A\beta_{42-1}$ (5 μM). Total RNA was isolated from microglial cultures using TRIzol Reagent (Invitrogen) according to the manufacture's protocol. RNA was reverse transcribed (RT) to cDNA using Moloney Murine Leukemia Virus (MMLV) reverse transcriptase (Invitrogen). For negative control, MMLV reverse transcriptase was omitted. The PCR primers (human TNF-α and GAPDH) used in this study were described previously (Franciosi et al., 2006). PCR was performed under the following conditions: initial denaturation at 95°C for 6 min followed by 35 cycles of denaturation at 95°C for 45 s, annealing at 55-60°C for 1 min and extension at 72°C for 1 min. A final extension at 72°C for 10 min was included. The amplified DNAs were identified using 1.5% agarose gels containing ethidium bromide (EtBr) and visualized under UV light.

3.2.7 Statistical Analysis

Values are expressed as means ± SEM. Statistical significance was assessed by ANOVA, followed by Newman-Keuls multiple comparison test (GraphPad Prism 3.0). Significance was set at $p < 0.05$.

3.3 RESULTS

3.3.1 Effects of thalidomide on $A\beta_{1-42}$-induced neovasculature

Previous work has reported the formation of newly formed blood vessels in $A\beta_{1-42}$ injected rat hippocampus (Zand et al., 2005). In this study we have used two different experimental designs to examine anti-angiogenic activity of thalidomide in this animal model of inflamed AD brain. In one procedure single staining immunohistochemistry was used to measure immunoreactive (ir) areas of the specific endothelial cell marker RECA-1 and in a subsequent study single staining of laminin, together with double staining of laminin with RECA-1, was used to characterize changes in vasculature. Since RECA-1 ir is a measure of both new and pre-existing blood vessels, the interpretation of our data in terms of neovascularization is discussed below.

Thalidomide modulation of ir for RECA-1: The hippocampal area used for analysis is indicated in Figure 3-1A (upper left panel) and spans the granular cell layer (GL) and molecular layer (ML). Vascularization was measured at a single time point (7 d post-peptide injection) and representative RECA-1 immunostaining is presented in Figure 3-1A for controls (PBS, upper middle panel and reverse peptide $A\beta_{42-1}$, upper right panel). Both controls showed a low level of staining with a pattern of diffuse and thin blood vessels. This morphological appearance of RECA-1 (+)ve vessels in controls was different from that observed following $A\beta_{1-42}$ injection (lower left panel) which was characterized by the presence of thick tubular-like structures. We attributed these large tubular structures to indicate areas of angiogenic activity induced by peptide injection (see Discussion). Administration of thalidomide was effective in reducing $A\beta_{1-42}$-induced RECA-1 ir (lower middle panel) and was featured by the general absence of the tubular-shaped large vessels. Thalidomide injection alone (lower right panel) showed a pattern of RECA-1 ir very similar to that observed with controls.

Quantification of total RECA-1 ir areas (Fig. 3-1B) and diameters of vessels (Fig. 3-1C) were used as measures of vascular angiogenic activity. Overall, RECA-1 ir was significantly increased in $A\beta_{1-42}$-injected dentate gyrus by 292% and 211% relative to PBS and reverse peptide injections, respectively (n = 5 animals). Treatment with thalidomide, in the presence of $A\beta_{1-42}$, significantly reduced the percentage of RECA-1 (+)ve area by 43%, compared with $A\beta_{1-42}$ application alone.

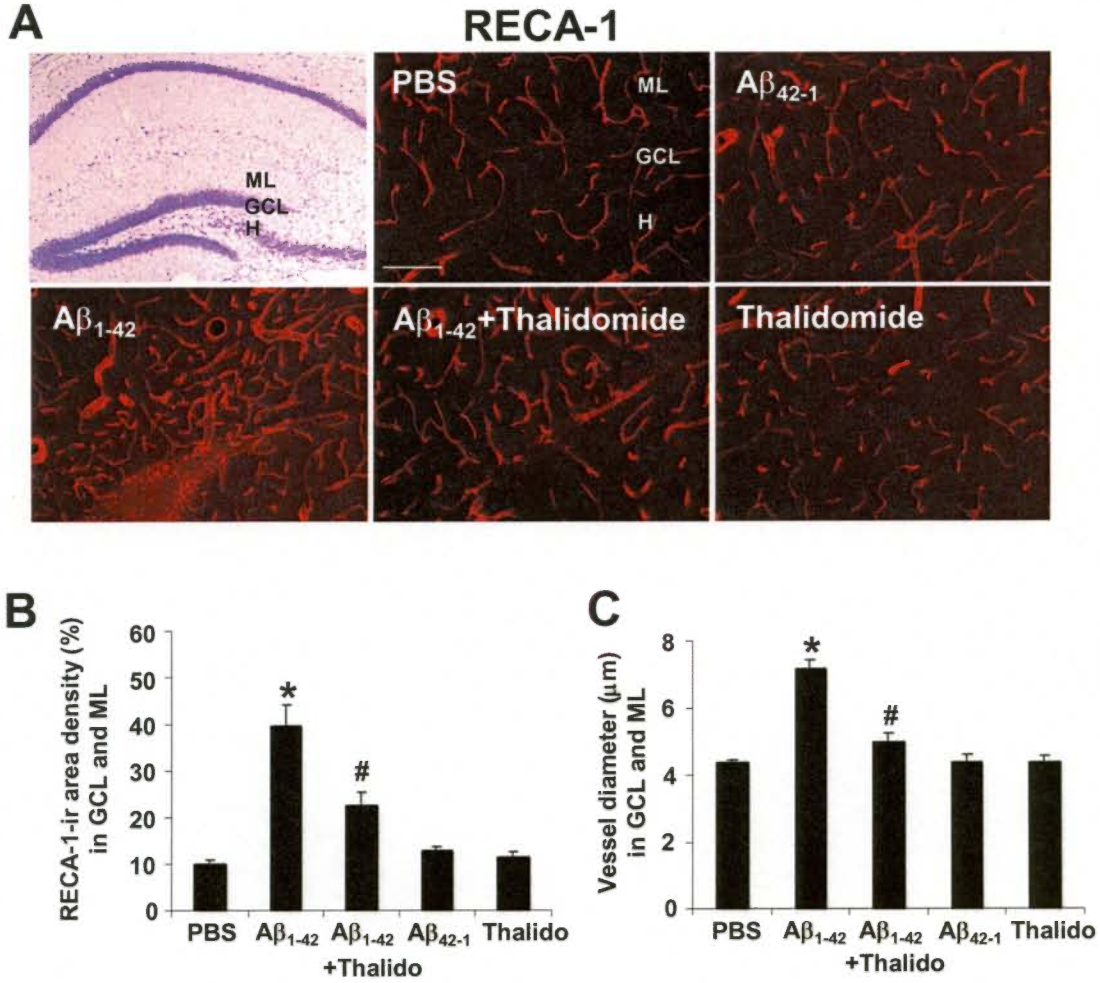

Figure 3-1. Effects of thalidomide on cerebrovascular responses in $A\beta_{1-42}$-injected rat hippocampus. (A) Representative hippocampal section stained with cresyl violet showing the regions of interest for measurements GCL, granular cell layer; ML, molecular layer and H, hilus (upper left panel). Representative immunofluorescence staining of RECA (+)ve vessels in the hippocampal GCL and ML subregions at 7 d post-injection for the following: controls (PBS and reverse peptide, $A\beta_{42-1}$; upper middle and right panels, respectively), $A\beta_{1-42}$ (lower left panel), $A\beta_{1-42}$ with thalidomide (lower middle panel) and thalidomide alone (lower right panel). Scale bar: 300 μm. (B) Quantification of RECA-1 area density for the different injections. (C) Vessel diameter for the treatments. Thalido, thalidomide. $^{*}P < 0.05$ compared with PBS-injected group. Data are mean ± SEM (n = 5 rats per group). $^{\#}P < 0.05$ compared with $A\beta_{1-42}$-injected group.

Similar extents of RECA-1 ir were measured with injections of PBS, reverse peptide or thalidomide applied alone. Vessel diameter was increased with $A\beta_{1-42}$ injection, by respective values of 64% and 63%, compared with PBS and reverse peptide (Fig. 3-1C). In peptide-injected hippocampus, vessel diameter was significantly reduced (by 30%) in the presence of thalidomide. Control injections or thalidomide applied separately yielded very similar mean values for diameters of vessels.

Thalidomide modulation of ir for laminin and laminin plus RECA-1: Laminin is a protein marker for extracellular matrix (ECM) and has been used in vascular remodeling to identify the formation of new blood vessels (Casella et al., 2002; Zand et al., 2005). Representative laminin ir for the different injections is presented in Figure 3-2A and shows minimal immunostaining for controls (PBS or reverse peptide; upper left and middle panels of Fig. 3-2A) or with thalidomide applied alone (upper right panel). Neovascularization was indicated by the high levels of laminin ir following 7 d of $A\beta_{1-42}$ injection (lower left panel) with effects of thalidomide treatment to reduce marker expression in peptide-injected brain (lower right panel). In total (n = 5 animals), in the presence of thalidomide, laminin ir in $A\beta_{1-42}$–injected hippocampus was reduced by 52% (Fig. 3-2B).

Double immunofluorescence staining was then used to investigate areas of overlap between laminin and RECA-1 ir (Fig. 3-2C). At 7 d following peptide injection (left panel) considerable areas of laminin ir (green staining) appeared coincident (merged yellow staining) with RECA-1 ir (red staining). Thalidomide injection with peptide (right panel) effectively diminished the extents of merged (yellow) staining. Overall, the results indicate localized regions of angiogenic activity in $A\beta_{1-42}$-injected brain which were reduced in size if thalidomide was administered with peptide.

3.3.2 Effects of thalidomide on leakiness of BBB

The increased angiogenic activity in peptide-injected dentate gyrus could be associated with an increased permeability of BBB. Indeed, leakiness of BBB following intra-hippocampal peptide injection has recently been demonstrated and associated with enhanced levels of the nitrogen product, peroxynitrite, produced by activated glial cells

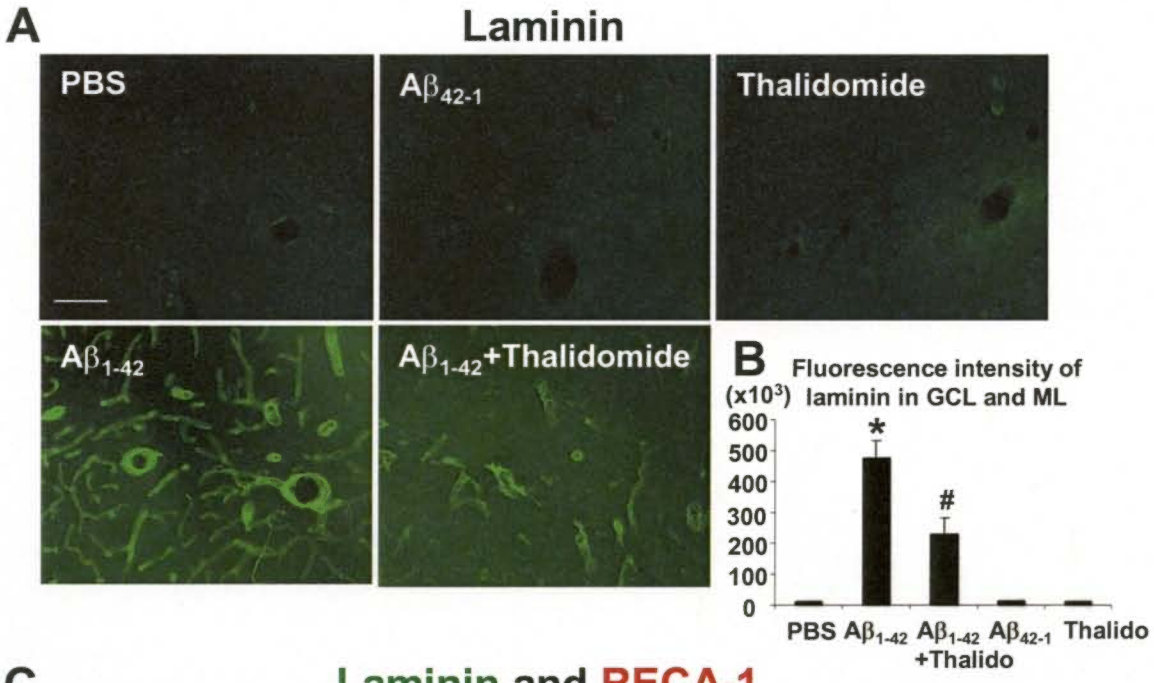

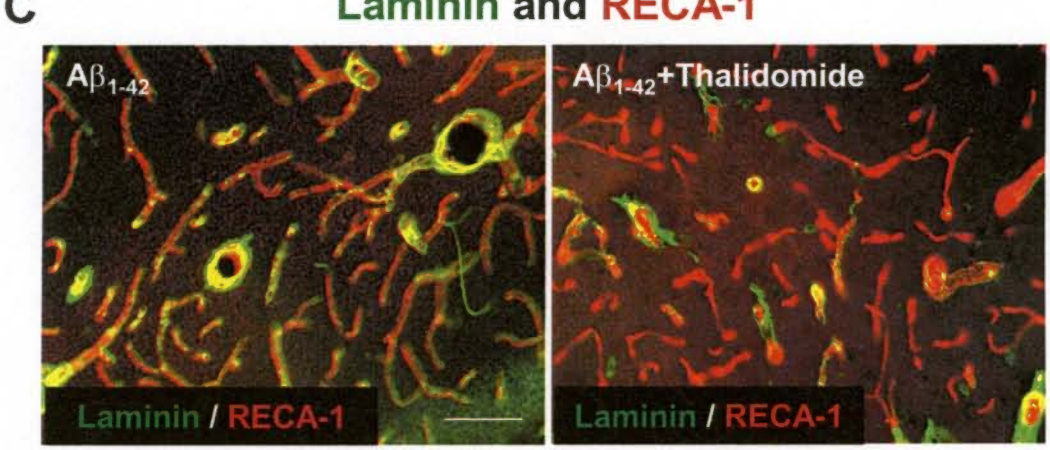

Figure 3-2. Effect of thalidomide on laminin and RECA-1 immunoreactivity (ir) in $A\beta_{1-42}$-injected hippocampus (7 d post-injection). (A) Representative immunofluorescence images of laminin (+)ve vascular basement membrane in the hippocampal ML subregion with intrahippocampal injections with PBS (upper left panel), reverse peptide (upper middle panel), thalidomide alone (upper right panel), $A\beta_{1-42}$ (lower left panel), and $A\beta_{1-42}$ with thalidomide (lower right panel). Scale bar: 300 µm. (B) Quantification of fluorescence intensity of laminin (+)ve vascular basement membrane at 7 d after peptide injection. Thalido, thalidomide. Data are mean ± SEM (n = 5 rats per group). $^{*}P < 0.05$ vs. PBS-injected group. $^{\#}P < 0.05$ vs. $A\beta_{1-42}$-injected group. Scale bar: 300 µm. (C) Typical laminin and RECA-1 ir for $A\beta_{1-42}$ (left panel) and $A\beta_{1-42}$ with thalidomide (right panel) treatments.

(Ryu and McLarnon, 2006). Extravasation of the blood protein albumin was used as a measure of vascular permeability. Representative fluorescence images of FITC-albumin for control injections, with PBS or reverse peptide, are presented in Figure 3-3A (upper left and middle panels, all injections for 7 d). Injection of thalidomide alone (upper right panel) showed a similar FITC-albumin staining pattern as for controls. The patterns of staining were similar to that observed with RECA-1 (Fig. 3-1A) showing outlines of thin blood vessels. However, a very different profile was evident with $A\beta_{1-42}$ injection (Fig. 3-3A, lower left panel) where localized diffuse areas of FITC-albumin leakage were apparent (see arrows in panel) in regions adjacent to blood vessels. In addition, FITC-albumin-labeled vessels were large and tubular in shape in contrast to controls. Fluorescence images for thalidomide injection with peptide (lower right panel) exhibited few regions of diffuse FITC-albumin.

The extent of diffuse FITC-albumin-derived fluorescence was used as a measure of vascular permeability. Semi-quantitative analysis (n = 5 animals) showed little evidence for the presence of diffuse FITC-albumin in controls or with thalidomide alone (Fig. 3-3B). However, considerable increased areas of diffuse FITC-albumin leakage were observed following $A\beta_{1-42}$ injection (by 14-fold compared to PBS control). Thalidomide treatment was found to significantly reduce FITC-albumin leakage area in the hippocampus (57% decrease relative to $A\beta_{1-42}$).

Double staining with FITC-albumin and RECA-1 was also done using higher magnification photomicrographs to denote vasculature changes following peptide injection with and without thalidomide. Typical patterns of immunofluorescence staining for FITC-albumin and RECA-1 are shown in Figure 3-3C in the absence (left panel) and presence (right panel) of thalidomide treatment. Considerable areas of overlaps for the two markers were evident in both cases with peptide injection alone characterized by larger diameter vessels and diffused FITC-albumin-derived fluorescence compared to $A\beta_{1-42}$ with thalidomide application.

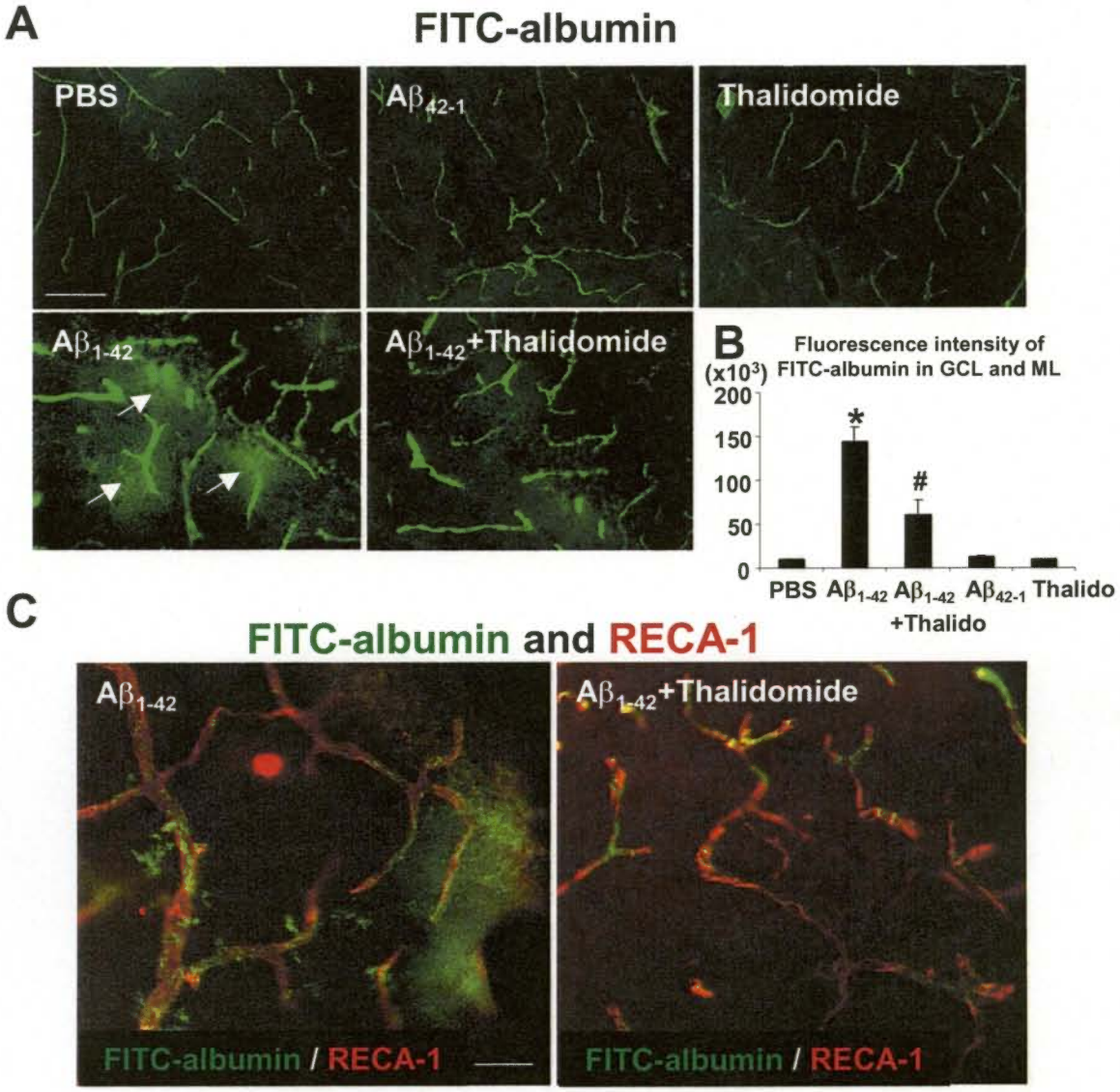

Figure 3-3. Effect of thalidomide on FITC-albumin in $A\beta_{1-42}$-injected hippocampus (7 d injection). (A) Representative images of FITC-albumin in the hippocampal ML subregion with intra-hippocampal injections of PBS (upper left panel), reverse peptide (upper middle panel), $A\beta_{1-42}$ (lower left panel), $A\beta_{1-42}$ with thalidomide (lower right panel) and thalidomide alone (upper right panel). The arrows show examples of albumin leakage from vessels in peptide-injected hippocampus. Scale bar: 300 µm. (B) Quantitative analysis of FITC-albumin fluorescence intensity; Thalido, thalidomide. Data are mean ± SEM (n = 5 rats per group). $^{*}P < 0.05$ vs. PBS-injected group. $^{\#}P < 0.05$ vs. $A\beta_{1-42}$-injected group. (C) Double immunofluorescence images for FITC-albumin and RECA (+)ve vessels show thalidomide treatment (right panel) reduces $A\beta_{1-42}$-induced vascular leakage (left panel). Scale bar: 100 µm.

3.3.3 Effects of thalidomide on microgliosis and astrogliosis

Glial cell responses to peptide injection could serve functional roles as signals for changes in vasculature including angiogenic activity and an increased vascular permeability. Experiments were designed to initially investigate co-localization of vasculature markers (RECA-1 and FITC-albumin) with microglia, a result predicted from previous work (Ryu and McLarnon, 2006). Subsequently, microglial and astrocytic responses to peptide injections and thalidomide treatment were studied and quantified. Additional studies then examined involvement of the glial cells in producing a potent vascular modulatory factor, TNF-α.

Association of vascular markers with microglia: Representative double staining is shown for microglia with RECA-1 and FITC-albumin at 7 d after peptide injection (left panels, Fig. 3-4). Well-defined areas of association of Iba-1 (+)ve microglia with both vascular markers were evident (indicated by merged yellow staining). The effects of thalidomide treatment in $A\beta_{1-42}$-injected hippocampus are also presented (right panels, Fig. 3-4). In the presence of thalidomide, numbers of microglia were considerably reduced and regions of merged staining with RECA-1 or FITC-albumin were markedly attenuated.

Thalidomide modulation of microgliosis: Representative immunohistochemical staining (7 d post-injections) for Iba-1 (microglial marker) is presented in Figure 3-5. Control (PBS, upper left panel) and reverse peptide ($A\beta_{42-1}$, upper right panel) injections were associated with a low level of Iba-1 ir. Injection of $A\beta_{1-42}$ caused a proliferative response of microglia (middle, left panel) which was considerably attenuated if animals also received thalidomide treatment (middle, right panel). Immunoreactivity of the microglial marker with thalidomide alone was similar to control level (lower panel). Morphologically, microglia in $A\beta_{1-42}$-injected brain showed predominant ameboid shapes with roundish cell bodies and retracted processes indicative of an activated state (inset, middle left panel). Cells in PBS-injected hippocampus displayed a resting state profile of ramified shapes with thin bodies and long fine processes (inset, upper left panel). Interestingly, microglia showed an admixture with both types of morphology in the hippocampus following application of thalidomide with $A\beta_{1-42}$ (inset, middle right panel). Quantification of data (Fig. 3-5B) from n = 5 animals showed that $A\beta_{1-42}$ markedly increased the number of Iba-1 (+)ve microglia (by 560%), relative to PBS injection. Thalidomide treatment significantly reduced Iba-1 ir (by 39%) compared to peptide injection. The number of microglia with thalidomide treatment alone was not significantly different from controls (PBS or $A\beta_{42-1}$ injections).

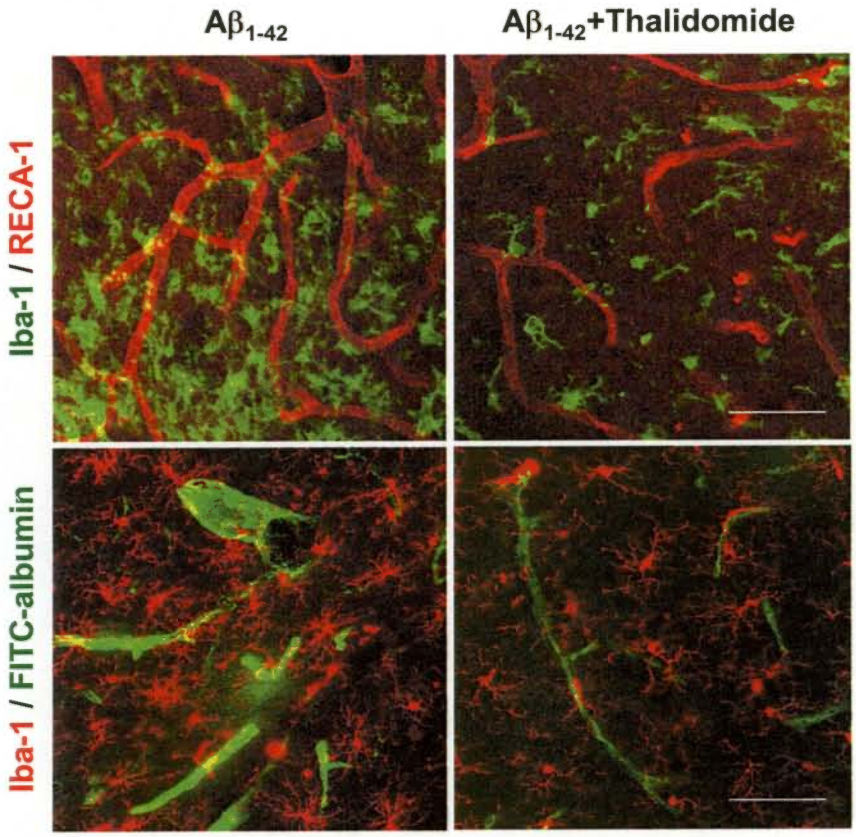

Figure 3-4. Effect of thalidomide on microglial-vasculature responses in $A\beta_{1-42}$-injected hippocampus (7 d injection). Representative double immunofluorescence imaging is shown for $A\beta_{1-42}$-injection (left panels) and $A\beta_{1-42}$-injection with thalidomide (right panels) for Iba-1 (+)ve microglia and RECA-1 (+)ve vessels (upper panels) and Iba-1 (+)ve microglia and FITC-albumin (lower panels) in the hippocampal ML subregion. Scale bars: 100 µm. Note that Iba-1-immunolabeled microglial cells were visualized with goat anti-rabbit secondary antibody (IgG) conjugated to Alexa Fluor 488 (green) or Alexa Fluor 555 (red).

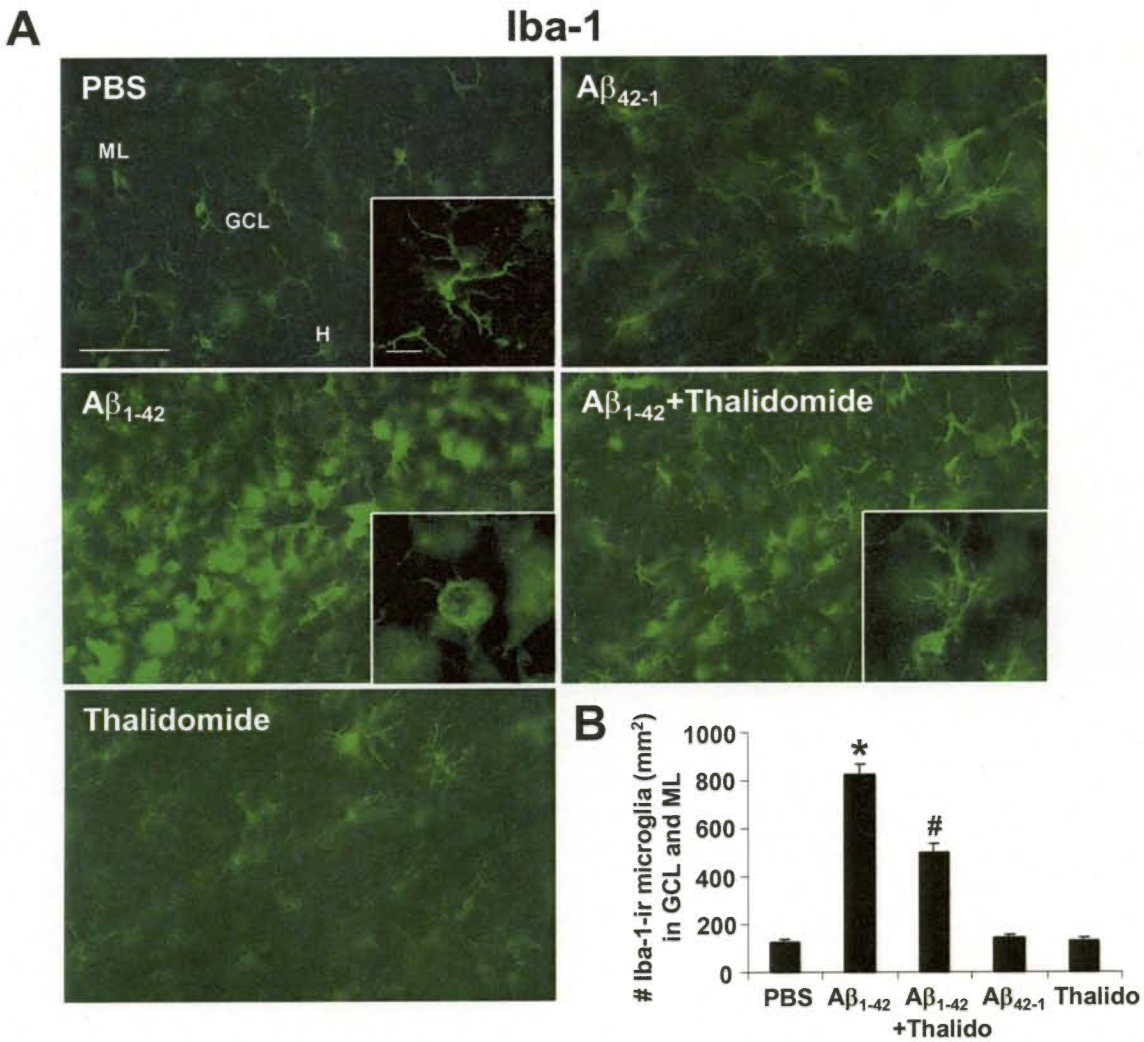

Figure 3-5. Effect of thalidomide on microgliosis in $A\beta_{1-42}$-injected hippocampus (7 d injection). (A) Representative immunofluorescence staining for Iba-1 (+)ve microglia in the hippocampal GCL and ML subregions with injection of PBS or $A\beta_{42-1}$ (upper panels), $A\beta_{1-42}$ or $A\beta_{1-42}$ with thalidomide (middle panels) and thalidomide alone (lower panel). Scale bar: 120 µm. The insets in panels show high magnification of Iba-1 staining; scale bar: 10 µm. GCL, granular cell layer; ML, molecular layer; H, hilus. (B) Quantification of the number of Iba-1 (+)ve microglia. Thalido, thalidomide. Data are mean ± SEM (n = 5 rats per group). $^{*}P < 0.05$ compared with PBS-injected group. $^{\#}P < 0.05$ compared with $A\beta_{1-42}$-injected group.

Thalidomide modulation of astrogliosis: Representative results for astrocytic ir (GFAP marker) are presented in Figure 3-6A. GFAP ir was uniformly low in controls with hippocampal injections of PBS or reverse peptide (upper panels). However, injection with $A\beta_{1-42}$ caused an increase in numbers of astrocytes (middle left panel) which was partially attenuated in animals receiving thalidomide treatment with peptide injection (middle, right panel). Overall (n = 5 animals), GFAP ir was increased by 205% with $A\beta_{1-42}$, compared with PBS, injection (Fig. 3-6B). Thalidomide application with peptide had a small (36%), but significant, effect to decrease astrogliosis. Levels of GFAP ir were similar between injections of PBS, reverse peptide and thalidomide alone.

3.3.4 Effects of thalidomide on the pro-inflammatory/angiogenic factor, TNF-α

The pronounced effects of $A\beta_{1-42}$ injection to cause marked microglial and moderate astrocytic inflammatory responses and the induction of changes in expression of vasculature properties and markers prompted studies to examine putative underlying signaling factors. One plausible candidate derived from activated glia, is the pro-inflammatory and pro-angiogenic cytokine TNF-α (Sunderkotter et al., 1994).

Thalidomide modulation of TNF-α in microglia and astrocytes: Typical patterns of TNF-α ir are presented in Figure 3-7A and indicate markedly elevated expressions of the cytokine at 7 d after $A\beta_{1-42}$ injection (lower left panel) compared with PBS-injected control (upper left panel). Thalidomide treatment was effective in reducing TNF-α ir in the $A\beta_{1-42}$-injected hippocampus (lower right panel, Fig 3-7A). Overall (Fig. 3-7B), the TNF-α ir in the granule cell layer of dentate gyrus was elevated in $A\beta_{1-42}$-injected hippocampus (by 25.9-fold) compared to PBS control (n = 5). A significant reduction in TNF-α ir (by 47%), relative to $A\beta_{1-42}$ alone, was found if peptide injection included treatment with thalidomide. Reverse peptide or thalidomide alone, had no effect to alter levels of the pro-inflammatory cytokine relative to PBS control.

Cellular association of TNF-α with glia were also examined using double immunofluorescence staining. Extents of association of TNF-α ir with microglia (Iba-1 marker) and astrocytes (GFAP marker) were determined in 7 d peptide-injected hippocampus. Representative double staining for TNF-α with the cell-specific markers are illustrated in Figure 3-7C. The results show that TNF-α ir was primarily observed in microglia (left panel, Fig. 3-7C) with a small extent of the cytokine associated with astrocytes (right panel, Fig. 3-7C).

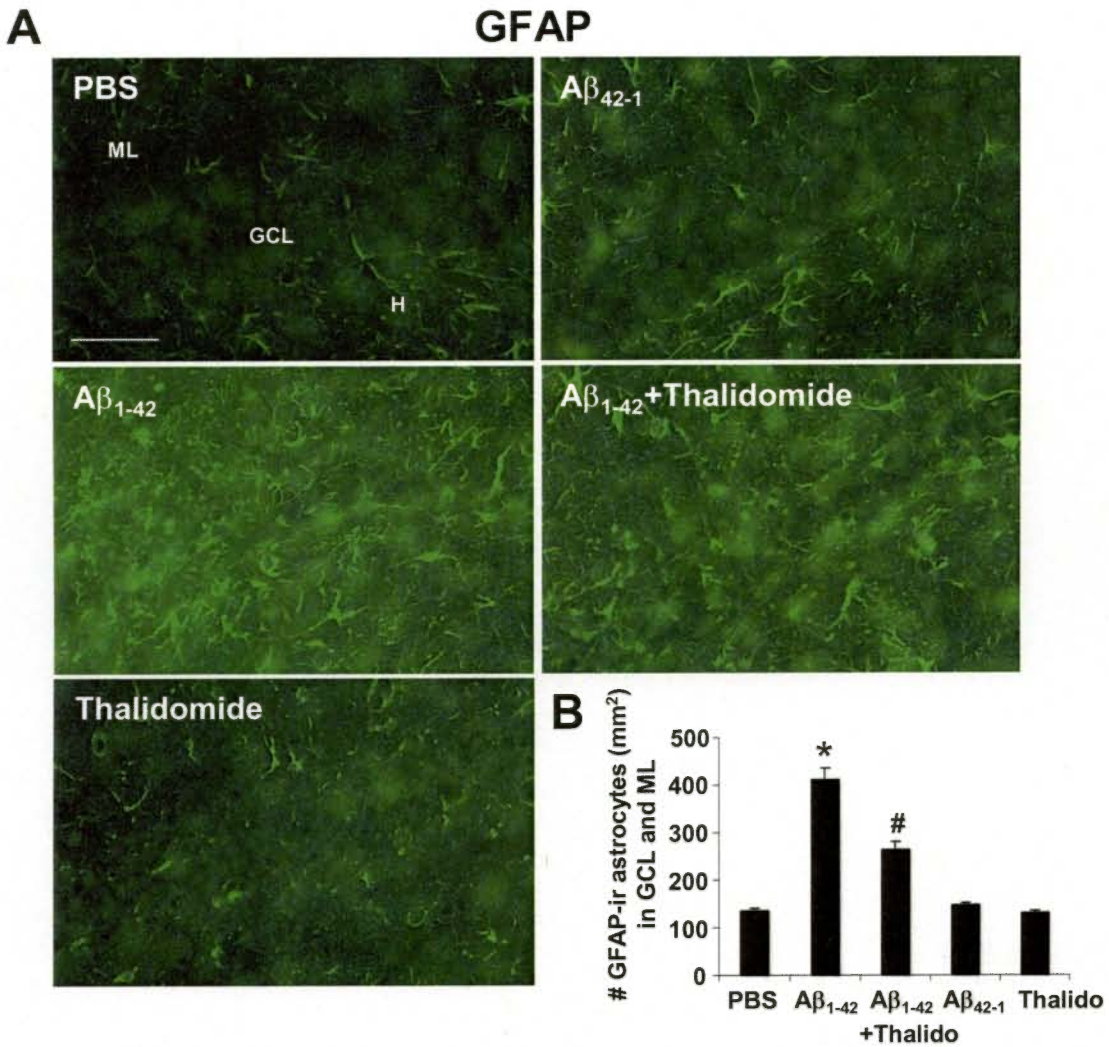

Figure 3-6. Effect of thalidomide on astrogliosis in $A\beta_{1-42}$-injected rat hippocampus (7 d injection). (A) Representative immunofluorescence imaging for GFAP (+)ve astrocytes in the hippocampal GCL and ML subregions with injection of PBS or $A\beta_{42-1}$(upper panels), $A\beta_{1-42}$ or $A\beta_{1-42}$ with thalidomide (middle panels) and thalidomide alone (lower panel). Scale bar: 120 μm. GCL, granular cell layer; ML, molecular layer; H, hilus. (B) Quantitative analysis for the number of GFAP (+)ve astrocytes. Thalido, thalidomide. Data are mean ± SEM (n = 5 rats per group). $^{*}P < 0.05$ compared with PBS-injected group. $^{\#}P < 0.05$ compared with $A\beta_{1-42}$-injected group.

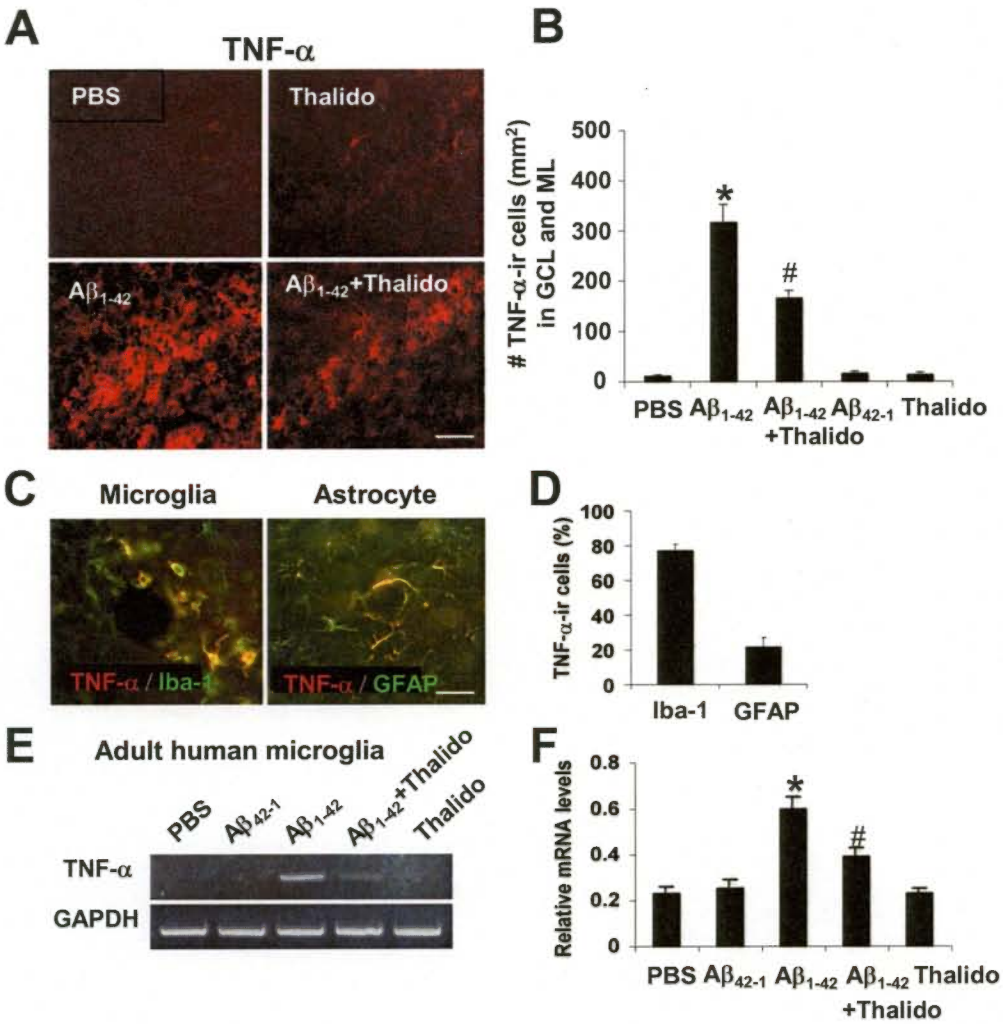

Figure 3-7. Effect of thalidomide on TNF-α in $A\beta_{1-42}$-injected rat hippocampus (7 d injection) and on peptide-stimulated human microglia. (A) Representative immunofluorescence for TNF-α ir after injection of PBS (upper left panel), thalidomide alone (upper right panel), $A\beta_{1-42}$ (lower left panel) or $A\beta_{1-42}$ with thalidomide (lower right panel). Scale bar: 80 µm. (B) Quantitative analysis for the number of TNF-α (+)ve cells; Thalido, thalidomide. Data are mean ± SEM (n = 5 rats per group). $^{*}P < 0.05$ vs. PBS. $^{\#}P < 0.05$ vs. $A\beta_{1-42}$. (C) Double immunofluorescence staining for TNF-α (+)ve microglia (left panel) and TNF-α (+)ve astrocytes (right panel) in $A\beta_{1-42}$-injected hippocampus. Scale bar: 30 µm. (D) The bar graph shows percentage of TNF-a (+)ve cells coexpressed with Iba-1 or GFAP. (E) Representative expression of TNF-a after human adult microglial 8 hr exposure to PBS, reverse peptide $A\beta_{42-1}$ (5 mM), $A\beta_{1-42}$ (5 mM) and $A\beta_{1-42}$ with thalidomide (at 50 mg/ml, 1 hr pretreatment prior to peptide stimulation) and thalidomide alone. GAPDH was used as an internal standard control. (F) Relative mRNA levels for TNF-a with the different treatments (n = 3 independent samples per group). $^{*}P < 0.05$ vs. PBS. $^{\#}P < 0.05$ vs. $A\beta_{1-42}$.

Quantification of double-stained cells (Fig. 3-7D) showed that 77% of TNF-α (+)ve cells were coexpressed with Iba-1 and 21% with GFAP; a small amount of cytokine ir was not associated with either glial cell. These results suggest that in $A\beta_{1-42}$-injected rat hipppcampus, TNF-α is mainly produced from microglia.

In vitro effects of thalidomide on TNF-α in $A\beta_{1-42}$-stimulated adult human microglia:

We also investigated thalidomide efficacy in modulating TNF-α expression in peptide-stimulated adult human microglia. Cultured microglia were treated with $A\beta_{1-42}$ (5 μM for 8 hr) in the presence or absence of thalidomide (50 μg/ml). RT-PCR analysis was performed with representative results shown in Figure 3-7E. Human microglia exposed to $A\beta_{1-42}$ exhibited increased levels of TNF-α gene expression relative to controls (PBS or $A\beta_{42-1}$) with thalidomide treatment inhibiting peptide-induced expression of TNF-α (Fig. 3-7E). Low levels of gene expression for TNF-α were observed with thalidomide applied alone.

The results from semi-quantitative analysis of RT-PCR band intensities are presented in Figure 3-7F (n = 3 independent samples per group). Overall, the expression of TNF-α was increased by 159% in human microglia stimulated with $A\beta_{1-42}$ compared with PBS-treated cells. Thalidomide treatment significantly inhibited TNF-α (by 35%) when added with $A\beta_{1-42}$ peptide.

3.3.5 Effects of thalidomide on neuronal viability

An important question in this study was the possibility that thalidomide could also exhibit neuroprotective effects in peptide-injected hippocampus. This point was investigated using NeuN antibody as a marker for viable neurons. Representative photomicrographs of NeuN ir are presented in Figure 3-8A and show a considerable reduction in the number of neurons in the granular cell layer of dentate gyrus following $A\beta_{1-42}$ injection (middle left panel). Thalidomide was effective in protecting neurons from the neurotoxic effects of $A\beta_{1-42}$ (middle right panel). Numbers of neurons with injection of PBS (upper left panel), reverse peptide $A\beta_{42-1}$ (upper right panel) and thalidomide alone (lower panel) were similar and showed an intact granular cell layer.

Quantitative analysis (Fig. 3-8B; n = 5 animals) revealed that $A\beta_{1-42}$ injection diminished NeuN (+)ve neurons in the superior blade of dentate gyrus (by 45%) compared to control PBS injection. The number of viable neurons was significantly increased (by 29%) when thalidomide treatment accompanied $A\beta_{1-42}$ injection. No significant neuronal loss was measured with either $A\beta_{42-1}$ or thalidomide alone, compared with PBS, injection.

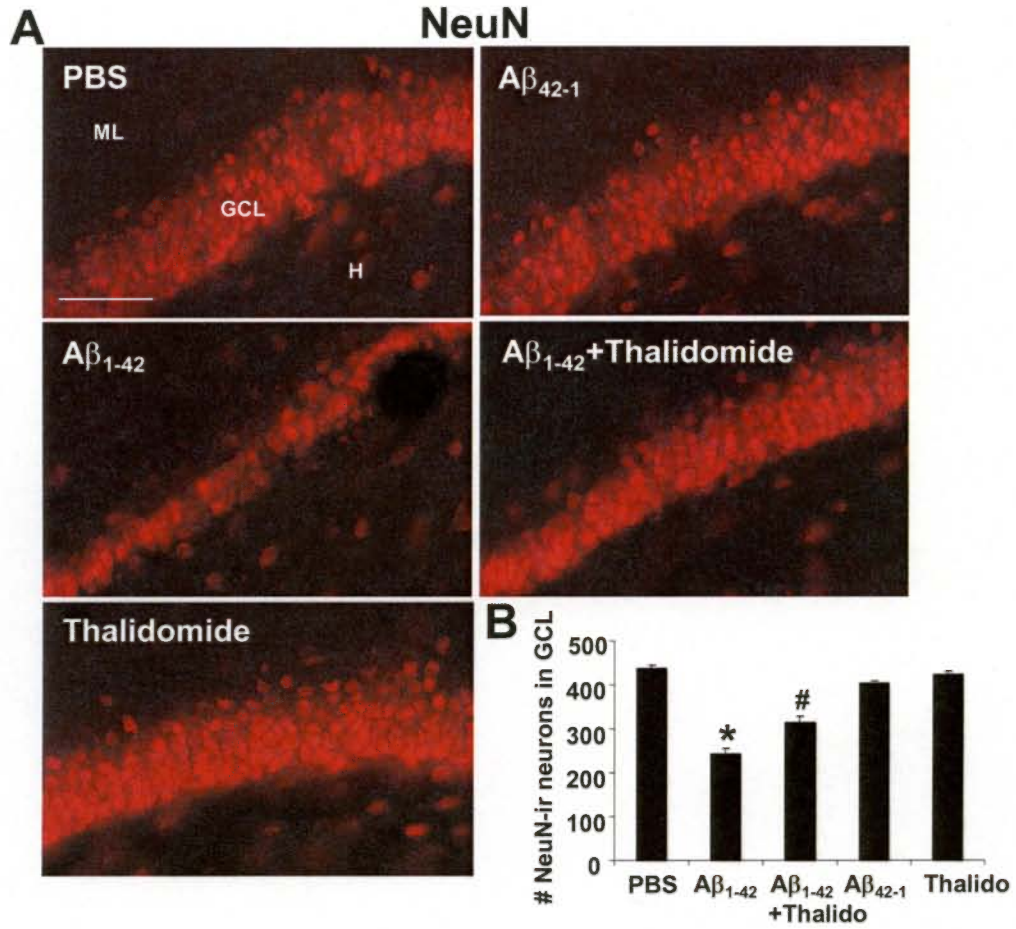

Figure 3-8. Effect of thalidomide on neuronal loss in $A\beta_{1-42}$-injected rat hippocampus (7 d injection). (A) Representative fluorescence imaging of NeuN (+)ve neurons in the hippocampal GCL after injection with PBS (upper left panel), reverse peptide (upper right panel) $A\beta_{1-42}$ (middle left panel), $A\beta_{1-42}$ with thalidomide (middle right panel) and thalidomide alone (lower panel). GCL, granular cell layer; ML, molecular layer; H, hilus. Scale bar: 80 μm. (B) Quantitative analysis for the number of NeuN (+)ve neurons in GCL at 7 d after peptide injection; Thalido, thalidomide. Data are mean ± SEM (n = 5 rats per group). $^{*}P < 0.05$ compared with PBS-injected group. $^{\#}P < 0.05$ compared with $A\beta_{1-42}$-injected group.

3.4 DISCUSSION

The overall results of this work suggest perturbations in vasculature as an integral component of inflammatory response following intra-hippocampal injection of $A\beta_{1-42}$ peptide. Acute injection of $A\beta_{1-42}$ elicits a marked activation and proliferation of microglia and our findings indicate that glial-mediated inflammatory processes are associated with perturbations in properties of vasculature including formation of new blood vessels and leakiness in BBB. Furthermore, the anti-inflammatory/angiogenic compound thalidomide was found to exhibit a broad spectrum of actions including inhibition of microgliosis and astrogliosis, blocking vascular remodeling and conferring neuroprotection in peptide-injected brain. As discussed below, our data are consistent with an effect of thalidomide to reduce microglial-derived levels of TNF-α.

The finding of altered vasculature in $A\beta_{1-42}$-injected hippocampus is particularly intriguing given the evidence for abnormalities in vascular properties in AD brain (de la Torre and Stefano, 2000; Zipser et al., 2007). The changes in vasculature induced by $A\beta_{1-42}$ peptide included an increased permeability of BBB and evidence for formation of new blood vessels. In the latter case, angiogenic activity was suggested by the proliferation of RECA-1 (+)ve endothelial cells and an altered structure of cells with blood vessels exhibiting large diameters and tubular shapes in peptide-injected brain. These patterns of RECA-1 ir were not observed with controls (injection of PBS or reverse peptide). Although RECA-1 does not differentiate between old and new vessels, the immunostaining data suggest induction of localized regions of neovascularization in peptide-injected brain. The findings with laminin (Fig. 3-2) support this conclusion since injection of $A\beta_{1-42}$, but not PBS or reverse peptide, led to a diffuse and marked increase in laminin ir. The enhanced laminin expression shows changes in extracellular matrix with patterns of immunostaining indicative of vascular remodeling and angiogenic activity in peptide-injected hippocampus (Casella et al., 2002; Zand et al., 2005).

Vascular remodeling and angiogenic activity could be correlated with regions of increased vascular permeability. This point was examined by measuring infiltration of the blood protein albumin as an indicator for leakiness in BBB (Fig. 3-3A). With PBS or reverse peptide injection, FITC-albumin-derived fluorescence was constrained to blood vessels with the latter exhibiting a similar morphology of thin structures to that observed with controls for RECA-1 immunostaining (Fig. 3-1A). A very different pattern was evident after peptide injection where intravascular FITC-albumin fluorescence demonstrated large tubular shaped vessels; in addition extravascular leakage of FITC-albumin was apparent with regions of diffuse fluorescence appearing outside of vessels.

As noted above, vascular changes could be secondary to, or part of, an inflammatory response. Thalidomide was employed as a pharmacological modulator since it has reported anti-inflammatory (Kumar and Anderson, 2005) and anti-angiogenic (D'Amato et al., 1994; Dredge et al., 2002) actions. Thalidomide treatment of $A\beta_{1-42}$-injected animals was highly effective in blocking perturbations and abnormalities in vascular processes. Staining patterns using RECA-1 (Fig. 3-1) showed cellular proliferation and size of individual blood vessels were diminished to similar extents by thalidomide. Laminin staining, absent in controls, was significantly reduced with thalidomide administration with $A\beta_{1-42}$ peptide (Fig. 3-2). Double immunostaining with RECA-1 and laminin (Fig. 3-2C) showed considerable regions of overlap for the two markers with thalidomide effective in decreasing the extent of merged areas of staining. Thalidomide treatment was also highly effective in blocking the areas of diffuse fluorescence of FITC-albumin and also restoring structure of vessels to the thin, spindly shapes observed with controls. Although immunogold electron microscopy staining was not carried out in this work, the use of the fluorescent markers RECA-1, laminin and albumin yielded consistent results for changes in properties of vasculature and BBB.

The results of our study are consistent with glia activity as cellular mediators to induce vascular remodeling. As demonstrated by double staining (Fig. 3-4), overlaps of Iba-1 (+)ve microglia with RECA-1 and albumin were evident. Marked microgliosis (Fig. 3-5) and astrogliosis (Fig. 3-6) were found with $A\beta_{1-42}$ injection with a low basal ir for both types of glia demonstrated in controls consistent with previous results (Ryu and Mclarnon, 2006). Thalidomide was effective in blocking the glial proliferative responses. Glial-derived TNF-α could mediate changes in vascular processes. In particular, double staining results showed a high extent of association of the pro-inflammatory/angiogenic cytokine TNF-α with microglia (Fig. 3-7). We speculate that TNF-α could act in an autocrine manner to amplify inflammatory responses in activated microglia and also as a paracrine signaling factor to induce neovascularization and perturbed BBB in $A\beta_{1-42}$-injected brain.

At 7 d post-peptide injection, a considerable extent of neuronal damage was evident in the granular cell layer of dentate gyrus (Fig. 3-8). Interestingly, thalidomide conferred a modest, but significant, degree of neuroprotection. At present, mechanisms underlying the increased neuronal viability are not known. One possibility, consistent with the hypothesis of interactions between activated microglia and perturbed BBB, is that neuroprotection is secondary to thalidomide inhibition of microglial inflammatory responses. Blocking microglial activation could reduce the output of inflammatory mediator, including TNF-α, which could damage

neurons. At present, however, our data are not conclusive as to the specific mechanism underlying thalidomide protection of hippocampal neurons in inflamed brain.

Our findings with thalidomide as a modulator of vasculature, gliosis, levels of TNF-α and neuronal viability in inflamed brain are novel. The compound has been reported to chelate metal ions (Cuajungco et al., 2000), inhibit histone deacetylase (Shinji et al., 2005) and block cyclooxygenase-2 activity (Fujita et al., 2001). Thalidomide was originally used as a sedative but subsequently banned due to adverse effects causing teratogenicity and dysmyelia (McBride, 1961; Lenz, 1962). However, the compound subsequently received approval for treatment of moderate to severe erythema nodosum leprosum (Calabrese and Fleischer, 2000) and multiple myeloma (Singhal et al., 1999; Richardson and Anderson, 2006). Recent work has reported thalidomide reduction of inflammatory factors leading to improved motor performance in transgenic amyotrophic lateral sclerosis (ALS) animals (Kiaei et al., 2006). Thalidomide analogues have recently been developed for anti-cancer therapy (Teo et al., 2005) and our results suggest possible utility of these compounds in inflamed AD brain.

The use of $A\beta_{1-42}$ injection in this and other work (El Khoury et al., 2003; Ryu et al., 2004; Dinamarca et al., 2006) emphasizes the induction of an inflammatory response with relevance to AD brain. However, pro-inflammatory responses in AD represent a manifestation in the sustained effects of multiple factors including amyloid plaques and neurofibrillary tangles and cannot be simulated by acute injection of peptide. In essence, the model of inflamed brain, using a short term amyloid-beta peptide insult, represents a simplified scheme incorporating reactive microglia, vascular modulatory factors, perturbed BBB, astrogliosis and neuronal damage. Nevertheless, the findings from this work provide a framework for future studies addressing neuroprotective efficacy in the pharmacological modulation of specific microglial-vasculature signaling pathways in other animal models of AD. These include transgenic animal models which can exhibit low levels of inflammation (Van Dam and De Deyn, 2006). Indeed, in certain circumstances enhanced inflammation can even be considered beneficial (Simard and Rivest, 2006; Wyss-Coray, 2006) and ongoing work is evaluating effects of Aβ immunization to reduce plaque burdens in AD (Schenk et al., 1999). Immunomodulatory agents acting to modify microglial-vasculature processes, including thalidomide or its analogues, are novel candidates for testing in inflamed brain.

3.5 REFERENCES

Akiyama, H., et al., 2000. Inflammation and Alzheimer's disease. Neurobiol. Aging 21, 383-421.

Banati, R.B., Gehrmann, J., Schubert, P., Kreutzberg, G.W., 1993. Cytotoxicity of microglia. Glia 7, 111-118.

Bartlett, J.B., Dredge, K., Dalgleish, A.G., 2004. The evolution of thalidomide and its IMiD derivatives as anticancer agents. Nat. Rev. Cancer 4, 314-322.

Breitner, J.C., Welsh, K.A., Helms, M.J., Gaskell, P.C., Gau, B.A., Roses, A.D., Pericak-Vance, M.A., Saunders, A.M., 1995. Delayed onset of Alzheimer's disease with nonsteroidal anti-inflammatory and histamine H2 blocking drugs. Neurobiol. Aging 16, 523-530.

Calabrese, L., Fleischer, A.B., 2000. Thalidomide: current and potential clinical applications. Am. J. Med. 108, 487-495.

Cao, L., Jiao, X., Zuzga, D.S., Liu, Y., Fong, D.M., Young, D., During, M.J., 2004. VEGF links hippocampal activity with neurogenesis, learning and memory. Nat. Genet. 36, 827-835.

Casella, G.T., Marcillo, A., Bunge, M.B., Wood, P.M., 2002. New vascular tissue rapidly replaces neural parenchyma and vessels destroyed by a contusion injury to the rat spinal cord. Exp. Neurol. 173, 63-76.

Cavaglia, M., Dombrowski, S.M., Drazba, J., Vasanji, A., Bokesch, P.M., Janigro, D., 2001. Regional variation in brain capillary density and vascular response to ischemia. Brain Res. 910, 81-93.

Combs, C.K., Johnson, D.E., Cannady, S.B., Lehman, T.M., Landreth, G.E., 1999. Identification of microglial signal transduction pathways mediating a neurotoxic response to amyloidogenic fragments of beta-amyloid and prion proteins. J. Neurosci. 19, 928-939.

Combs, C.K., Karlo, J.C., Kao, S.C., Landreth, G.E., 2001. beta-Amyloid stimulation of microglia and monocytes results in TNFalpha-dependent expression of inducible nitric oxide synthase and neuronal apoptosis. J. Neurosci. 21, 1179-1188.

Corral, L.G., Kaplan, G, 1999. Immunomodulation by thalidomide and thalidomide analogues. Ann. Rheum. Dis. Suppl. 1, I107-113.

Cuajungco, M.P., Fagét, K.Y., Huang, X., Tanzi, R.E., Bush, A.I., 2000. Metal chelation as a potential therapy for Alzheimer's disease. Ann. N. Y. Acad. Sci. 920, 292-304.

D'Amato, R.J., Loughnan, M.S., Flynn, E., Folkman, J., 1994. Thalidomide is an inhibitor of angiogenesis. Proc. Natl. Acad. Sci. U. S. A. 91, 4082-4085.

de la Torre, J.C., 2000. Cerebral hypoperfusion, capillary degeneration, and development of Alzheimer disease. Alzheimer Dis. Assoc. Disord. 14 Suppl 1, S72-81.

de la Torre, J.C., 2002. Vascular basis of Alzheimer's pathogenesis. Ann. N. Y. Acad. Sci. 977, 196-215.

de la Torre, J.C., Stefano, G.B., 2000. Evidence that Alzheimer's disease is a microvascular disorder: the role of constitutive nitric oxide. Brain Res. Brain Res. Rev. 34, 119-136.

Dinamarca, M.C., Cerpa, W., Garrido, J., Hancke, J.L., Inestrosa, N.C., 2006. Hyperforin prevents beta-amyloid neurotoxicity and spatial memory impairments by disaggregation of Alzheimer's amyloid-beta-deposits. Mol. Psychiatry 11, 1032-1048.

Dredge, K., Marriott, J.B., Macdonald, C.D., Man, H.W., Chen, R., Muller, G.W., Stirling, D., Dalgleish, A.G., 2002. Novel thalidomide analogues display anti-angiogenic activity independently of immunomodulatory effects. Br. J. Cancer 87, 1166-1172.

Duijvestijn, A.M., van Goor, H., Klatter, F., Majoor, G.D., van Bussel, E., van Breda Vriesman, P.J., 1992. Antibodies defining rat endothelial cells: RECA-1, a pan-endothelial cell-specific monoclonal antibody. Lab. Invest. 66, 459-466.

El Khoury, J.B., Moore, K.J., Means, T.K., Leung, J., Terada, K., Toft, M., Freeman, M.W., Luster, A.D., 2003. CD36 mediates the innate host response to beta-amyloid. J. Exp. Med. 197, 1657-1666.

Eikelenboom, P., van Gool, W.A., 2004. Neuroinflammatory perspectives on the two faces of Alzheimer's disease. J. Neural. Transm. 111, 281-294.

Franciosi, S., Choi, H.B., Kim, S.U., McLarnon, J.G., 2005. IL-8 enhancement of amyloid-beta (Abeta 1-42)-induced expression and production of pro-inflammatory cytokines and COX-2 in cultured human microglia. J. Neuroimmunol. 159, 66-74.

Franciosi, S., Ryu, J.K., Choi, H.B., Radov, L., Kim, S.U., McLarnon, J.G., 2006. Broad-spectrum effects of 4-aminopyridine to modulate amyloid beta1-42-induced cell signaling and functional responses in human microglia. J. Neurosci. 26, 11652-11664.

Fujita, J., Mestre, J.R., Zeldis, J.B., Subbaramaiah, K., Dannenberg, A.J., 2001. Thalidomide and its analogues inhibit lipopolysaccharide-mediated induction of cyclooxygenase-2. Clinical Cancer Research, 7, 3349-3355.

Ghabriel, M.N., Zhu, C., Hermanis, G., Allt, G., 2000. Immunological targeting of the endothelial barrier antigen (EBA) in vivo leads to opening of the blood-brain barrier. Brain Res. 878, 127-135.

Grammas, P., Samany, P.G., Thirumangalakudi, L., 2006. Thrombin and inflammatory proteins are elevated in Alzheimer's disease microvessels: implications for disease pathogenesis. J. Alzheimers Dis. 9, 51-58.

Gursoy-Ozdemir, Y., Qiu, J., Matsuoka, N., Bolay, H., Bermpohl, D., Jin, H., Wang, X., Rosenberg, G.A., Lo, E.H., Moskowitz, M.A., 2004. Cortical spreading depression activates and upregulates MMP-9. J. Clin. Invest. 113, 1447-1455.

Hardy, J., Selkoe, D.J., 2002. The amyloid hypothesis of Alzheimer's disease: progress and problems on the road to therapeutics. Science 297, 353-356.

Hellsten, J., West, M.J., Arvidsson, A., Ekstrand, J., Jansson, L., Wennström, M., Tingström, A., 2005. Electroconvulsive seizures induce angiogenesis in adult rat hippocampus. Biol. Psychiatry 58, 871-878.

Kaicker, S., McCrudden, K.W., Beck, L., New, T., Huang, J., Frischer, J.S., Serur, A., Kadenhe-Chiweshe, A., Yokoi, A., Kandel, J.J., Yamashiro, D.J., 2003. Thalidomide is anti-angiogenic in a xenograft model of neuroblastoma. Int. J. Oncol. 23, 1651-1655.

Kenyon, B.M., Browne, F., D'Amato, R.J., 1997. Effects of thalidomide and related metabolites in a mouse corneal model of neovascularization. Exp. Eye Res. 64, 971-978.

Kiaei, M., Petri, S., Kipiani, K., Gardian, G., Choi, D.K., Chen, J., Calingasan, N.Y., Schafer, P., Muller, G.W., Stewart, C., Hensley, K., Beal, M.F., 2006. Thalidomide and lenalidomide extend survival in a transgenic mouse model of amyotrophic lateral sclerosis. J. Neurosci. 26, 2467-2473.

Kumar, S., Anderson, K.C., 2005. Drug insight: thalidomide as a treatment for multiple myeloma. Nat. Clin. Pract. Oncol. 2, 262-270.

Lenz, W., 1962. Thalidomide and congenital abnormalities. Lancet 1, 45.

Lue, L.F., Rydel, R., Brigham, E.F., Yang, L.B., Hampel, H., Murphy, G.M. Jr., Brachova, L., Yan, S.D., Walker, D.G., Shen, Y., Rogers, J., 2001. Inflammatory repertoire of Alzheimer's disease and nondemented elderly microglia in vitro. Glia 35, 72-79.

McBride, W.G., 1961. Thalidomide and congenital abnormalities. Lancet 2, 1358.

McGeer, P.L., McGeer, E.G., 1999. Inflammation of the brain in Alzheimer's disease: implications for therapy. J. Leukoc. Biol. 65, 409-415.

McGeer, P.L., McGeer, E.G., 2006. NSAIDS and Alzheimer disease: Epidemiological, animal model and clinical studies. Neurobiol. Aging 28, 639-647.

McLarnon, J.G., Ryu, J.K., Walker, D.G., Choi, H.B., 2006. Upregulated expression of purinergic P2X(7) receptor in Alzheimer disease and amyloid-beta peptide-treated microglia and in peptide-injected rat hippocampus. J. Neuropathol. Exp. Neurol. 65, 1090-1097.

Moreira, A.L., Sampaio, E.P., Zmuidzinas, A., Frindt, P., Smith, K.A., Kaplan, G., 1993. Thalidomide exerts its inhibitory action on tumor necrosis factor alpha by enhancing mRNA degradation. J. Exp. Med. 177, 1675-1680.

Mrak, R.E., Griffin, W.S., 2005. Glia and their cytokines in progression of neurodegeneration. Neurobiol. Aging 26, 349-354.

Paxinos, G., Watson, C., 2005. The rat brain in stereotaxic coordinates. 5th edition. Elsevier Academic Press.

Pietra, G.G., Johns, L.W., 1996. Confocal- and electron-microscopic localization of FITC-albumin in H2O2-induced pulmonary edema. J. Appl. Physiol. 80, 182-190.

Pogue, A.I., Lukiw, W.J., 2004. Angiogenic signaling in Alzheimer's disease. Neuroreport 15, 1507-1510.

Prat, A., Biernacki, K., Wosik, K., Antel, J.P., 2001. Glial cell influence on the human blood-brain barrier. Glia 36, 145-155.

Richardson, P., Anderson, K., 2006. Thalidomide and dexamethasone: a new standard of care for initial therapy in multiple myeloma. J. Clin. Oncol. 24, 334-336.

Rogers, J., Strohmeyer, R., Kovelowski, C.J., Li, R., 2002. Microglia and inflammatory mechanisms in the clearance of amyloid beta peptide. Glia 40, 260-269.

Ryu, J.K., Franciosi, S., Sattayaprasert, P., Kim, S.U., McLarnon, J.G., 2004. Minocycline inhibits neuronal death and glial activation induced by beta-amyloid peptide in rat hippocampus. Glia 48, 85-90.

Ryu, J.K., McLarnon, J.G., 2006. Minocycline or iNOS inhibition block 3-nitrotyrosine increases and blood-brain barrier leakiness in amyloid beta-peptide-injected rat hippocampus. Exp. Neurol. 198, 552-557.

Ryu, J.K., Tran, K.C., McLarnon, J.G., 2007. Depletion of neutrophils reduces neuronal degeneration and inflammatory responses induced by quinolinic acid in vivo. Glia 55, 439-451.

Schenk, D., Barbour, R., Dunn, W., Gordon, G., Grajeda, H., Guido, T., Hu, K., Huang, J., Johnson-Wood, K., Khan, K., Kholodenko, D., Lee, M., Liao, Z., Lieberburg, I., Motter, R., Mutter, L., Soriano, F., Shopp, G., Vasquez, N., Vandevert, C., et al., 1999. Immunization with amyloid-beta attenuates Alzheimer-disease-like pathology in the PDAPP mouse. Nature 400, 173-177.

Shinji, C., Nakamura, T., Maeda, S., Yoshida, M., Hashimoto, Y., Miyachi, H., 2005. Design and synthesis of phthalimide-type histone deacetylase inhibitors. Bioorg. Med. Chem. Lett. 15, 4427-4431

Simard, A.R., Rivest, S., 2006. Neuroprotective properties of the innate immune system and bone marrow stem cells in Alzheimer's disease. Mol. Psychiatry 11, 327-335.

Singhal, S., Mehta, J., Desikan, R., Ayers, D., Roberson, P., Eddlemon, P., Munshi, N., Anaissie, E., Wilson, C., Dhodapkar, M., Zeddis, J., Barlogie, B., 1999. Antitumor activity of thalidomide in refractory multiple myeloma. N. Engl. J. Med. 341, 1565-1571.

Sobel, R.A., Hinojoza, J.R., Maeda, A., Chen, M., 1998. Endothelial cell integrin laminin receptor expression in multiple sclerosis lesions. Am. J. Pathol. 153, 405-415.

Sunderkotter, C., Steinbrink, K., Goebeler, M., Bhardwaj, R., Sorg, C., 1994. Macrophages and angiogenesis. J. Leukoc. Biol. 55, 410-422.

Tarkowski, E., Issa, R., Sjogren, M., Wallin, A., Blennow, K., Tarkowski, A., Kumar, P., 2002. Increased intrathecal levels of the angiogenic factors VEGF and TGF-beta in Alzheimer's disease and vascular dementia. Neurobiol. Aging 23, 237-243.

Teo, S.K., Stirling, D.I., Zeldis, J.B., 2005. Thalidomide as a novel therapeutic agent: new uses for an old product. Drug Discov. Today 10, 107-114.

Ujiie, M., Dickstein, D.L., Carlow, D.A., Jefferies, W.A., 2003. Blood-brain barrier permeability precedes senile plaque formation in an Alzheimer disease model. Microcirculation 10, 463-470.

Vagnucci, A.H. Jr., Li, W.W., 2003. Alzheimer's disease and angiogenesis. Lancet 361, 605-608.

Van Dam, D., De Deyn, P.P., 2006. Drug discovery in dementia: the role of rodent models. Nat. Rev. Drug Discov. 5, 956-970.

Walker, D.G., Link, J., Lue, L.F., Dalsing-Hernandez, J.E., Boyes, B.E., 2006. Gene expression changes by amyloid beta peptide-stimulated human postmortem brain microglia identify activation of multiple inflammatory processes. J. Leukoc. Biol. 79, 596-610.

Wyss-Coray, T., 2006. Inflammation in Alzheimer disease: driving force, bystander or beneficial response? Nat. Med. 12, 1005-1015.

Zand, L., Ryu, J.K., McLarnon, J.G., 2005. Induction of angiogenesis in the beta-amyloid peptide-injected rat hippocampus. Neuroreport 16, 129-132.

Zipser, B.D., Johanson, C.E., Gonzalez, L., Berzin, T.M., Tavares, R., Hulette, C.M., Vitek, M.P., Hovanesian, V., Stopa, E.G., 2007. Microvascular injury and blood-brain barrier leakage in Alzheimer's disease. Neurobiol. Aging 28, 977-986.

Zlokovic, B.V., 2005. Neurovascular mechanisms of Alzheimer's neurodegeneration. Trends Neurosci. 28, 202-208.

CHAPTER 4: A LEAKY BLOOD-BRAIN BARRIER AND FIBRINOGEN INFILTRATION IN INFLAMED ALZHEIMER'S DISEASE BRAIN [3]

4.1 INTRODUCTION

Blood proteins such as fibrinogen, plasminogen and thrombin have essential functions in the maintenance of integral vasculature homeostatic processes involved in blood clotting. However, under pathological conditions a weakened blood-brain barrier (BBB) could allow extravasation of plasma proteins into parenchymal regions of the brain. A likely consequence of increased infiltration of proteins is the exacerbation of inflammatory responses mediated by the resident immune responding cells, microglia. At present, limited experimental evidence is available to characterize the links between abnormalities in properties of BBB, increased levels of plasma proteins in parenchyma, microglial inflammatory reactivity and neuronal degeneration and their contributions to chronic brain inflammation.

Elevated levels of fibrinogen are reported in neurodegenerative diseases. Inflammatory lesions in multiple sclerosis (MS) indicated fibrin deposits in association with regions of active demyelination (Kwon and Prineas, 1994) and in experimental encephalomyelitis (EAE), an animal model of MS, infiltration of fibrinogen was found as an early response preceding inflammatory damage (Floris et al., 2004). Subsequent work, using a transgenic mouse model of MS, has shown fibrin depletion as an effective strategy to inhibit inflammation and the onset of demyelinating lesions (Akassoglou et al., 2004). Recent work has demonstrated fibrin deposition and damaged vasculature in three different transgenic animal models of AD (Paul et al., 2007). In this work enhanced levels of fibrinogen exacerbated vascular damage whereas inhibition of fibrinogen attenuated neurovascular pathology.

We have previously reported intrahippocampal injection of $A\beta_{1-42}$ peptide induces considerable vascular remodeling including evidence for angiogenic activity and increased permeability of BBB (Ryu and Mclarnon, 2006, 2007). Microgliosis, both proliferation and activation of cells, accompanied the vascular changes suggesting that microglial inflammatory responses could be involved, or even causative, for the perturbations in vascular processes and also for the neurodegeneration evident in peptide-injected brain. Treatment of animals with the anti-angiogenic and anti-inflammatory compound thalidomide was effective in reducing

---

[3] A version of this chapter has been submitted for publication. Ryu, J.K. and McLarnon, J.G. A leaky blood-brain barrier and fibrinogen infiltration in inflamed Alzheimer's disease brain.

microgliosis, inhibiting vascular remodeling, diminishing expression of the pro-inflammatory cytokine TNF-α and conferring neuroprotection.

In the present study we have used immunohistochemical analysis to investigate inflammatory reactivity and permeability of BBB to the glycoprotein fibrinogen in tissue obtained from AD patients and in $A\beta_{1-42}$-injected rat brain. The strategy was to initially examine entorhinal cortical tissue obtained from AD and ND (nondemented) brains for leakiness of BBB, as measured from extents of fibrinogen and IgG immunoreactive (ir) regions, for abnormalities in blood vessels as indicated by staining for the endothelial cell glycoprotein, von Willebrand factor (vWF), and for association of vascular factors with activated microglia and astrocytes. Subsequently, peptide-and peptide plus fibrinogen-injected rat brain was studied for similar vascular remodeling, gliosis and neuronal viability with two different pharmacological interventions; using the defibrinogenating compound ancrod or using the monoclonal antibody, anti-Mac-1, to inhibit microglial activation. Overall, our results suggest the novel possibility that Aβ deposits could initially induce microglial immunoreactivity which subsequently initiates vascular remodeling, including angiogenic activity and extravasation of fibrinogen through a leaky BBB, which then amplifies and sustains a chronic inflammatory environment toxic to bystander neurons.

4.2 MATERIALS AND METHODS

4.2.1 Human brain tissue and immunohistochemistry

Postmortem brain tissues containing the entorhinal cortex from seven ND cases (60-80 years of age; postmortem intervals, 4-24 hr) and eight AD cases (67-78 years of age; postmortem intervals, 4-10 hr) were obtained from the Kinsmen Laboratory brain bank at the University of British Columbia (UBC, Vancouver, BC). All cases of AD were confirmed by the clinical criteria for AD, as defined by the National Institute of Neurological and Communicative Disorders, and the Stroke/Alzheimer's Disease and Related Disorders Association. ND cases had no clinical or pathological history of AD.

In this study, single/double immunohistochemical methods (visualized using 3,3'-diaminobenzidine (DAB) and nickel-ammonium sulfate as the chromogen) and double immunofluorescent staining (visualized by fluorescent secondary antibody) were applied for human tissue section staining as described below. Single immunohistochemistry was performed as described previously (Arai et al., 2006). Free-floating sections (30 μm) from ND and AD tissues were treated for 30 min with 0.3% hydrogen peroxide (H_2O_2) solution in phosphate buffered saline with Triton X-100 (PBST; 0.01 M phosphate-buffered saline, pH 7.4, containing 0.3% Triton X-100) and transferred into 5% skim milk in PBST for 1 hr. Sections were then incubated for 48 hr at 4°C with the following primary antibodies: anti-fibrinogen (1:800; DakoCytomation, Carpinteria, CA) or anti-human IgG (1:100; Serotec, Oxford, UK). Sections were washed and incubated with the appropriate biotinylated secondary antibody (1:1000; DakoCytomation) followed by incubation with avidin-biotinylated horseradish peroxidase complex (ABC Elite, Vector Labs, Burlingame, CA) for 1 hr. Peroxidase labeling was visualized by incubation of the sections in 0.01% 3,3'-diaminobenzidine (Sigma-Aldrich, St Louis, MO) containing 0.6% nickel ammonium sulfate, 50 mM imidazole and 0.001% H_2O_2 in 0.05 M Tris-HCl buffer, pH 7.6. When a dark purple color developed, sections were washed, mounted on glass slides, and coverslipped with Entellan (E Merck, Darmstadt, Germany).

For double immunohistochemical staining for CR3/43 (HLA-DR, a marker for microglia; DakoCytomation) and β-amyloid (Aβ, clone 6F/3D; DakoCytomation) in ND and AD tissues, pretreatment of tissue sections with 100% formic acid (Sigma) was performed for 15 min, prior to primary antibody incubation (Guo et al., 2006). Sections were incubated for 24 hr at 4°C with anti-HLA-DR polyclonal antibody (1:1000, DakoCytomation) followed by incubation with a biotinylated secondary antibody and ABC solution. After the DAB/nickel ammonium sulfate reaction, sections were washed in PBST and incubated in blocking solution (5% skim milk) for

1 hr. Sections were then incubated for 24 hr at 4°C with the anti-Aβ monoclonal antibody (1:200; DakoCytomation), followed by incubation with a biotinylated secondary antibody and ABC solution. The developing reaction was done in DAB solution.

For double immunofluorescent staining of ND and AD brains (Guo et al., 2006), free-floating sections were incubated with a mixture of two primary antibodies: Fibrinogen (1:500; DakoCytomation) in combination with beta-amyloid (Aβ, 1:100; DakoCytomation), vWF (1:500; Santa Cruz Biotechnology, Santa Cruz, CA), HLA-DR (1:500, DakoCytomation) or GFAP (1:1000, DakoCytomation). After a rinse in PBST, the sections were then incubated with appropriate fluorescence secondary antibodies (Molecular Probes, Eugene, OR) for 2 hr.

To test the specificity of the primary antibodies (anti-fibrinogen and anti-IgG), preincubation of the primary antibody with the epitope specific peptide was performed prior to ND and AD tissue staining. For all immunohistochemical staining, control sections were prepared by following the same procedure except that the primary antibody was omitted.

4.2.2 Immunohistochemical analysis of human ND/AD tissue

Tissue sections from ND and AD cases were used for the quantification analysis. The boundaries of entorhinal cortex were defined as described by Insausti et al. (1995). Images from five nonoverlapping random fields of superficial layers (layer II and III) in the entorhinal cortex were collected using a Zeiss Axioplan-2 light microscope equipped with a DVC camera (Diagnostic Instruments, Sterling Heights, MI) at 400× magnification under a constant predefined light setting. The digitized images were then analyzed using Northern Eclipse software (Empix Imaging, Mississauga, ON). The areas occupied by blood proteins fibrinogen and IgG in cases of ND (n = 7) and AD (n = 8) were quantified by measuring the number of pixels per image above a predetermined threshold level of intensity. The measurement of pixel intensity is represented as percent area density defined as the number of pixels (positively stained area) divided by the total number of pixels (sum of positively and negatively stained area) in the imaged field.

4.2.3 *In Vivo* studies: animals and surgical procedures

All animal procedures were carried out according to protocols approved by the UBC Animal Care Ethics Committee, adhering to guidelines of the Canadian Council on Animal Care. Male Sprague-Dawley rats (250-300 g; Charles River Laboratories, St. Constant, PQ) were anesthetized with intraperitoneal (i.p.) injection of ketamine hydrochloride (72 mg/kg; Bimeda-

MTC, Cambridge, ON) and xylazine hydrochloride (9 mg/kg; Bayer Inc., Etobicoke, ON) and placed in a stereotaxic apparatus (David Kopf Instruments, Tujunga, CA). A midline skin incision was made in the scalp to expose the skull and stereotaxic unilateral injection of beta-amyloid (Aβ) peptide was performed as previously described (Ryu et al., 2004; Franciosi et al., 2006). Injection coordinates for the hippocampus were as follows: anteriorposterior (AP): -3.3 mm; mediallateral (ML): -1.6 mm; dorsoventral (DV): -3.2 mm, from bregma. Peptides (2 nmol in 1 μl) were slowly injected (0.2 μl/min) into the superior blade of the dentate gyrus of hippocampus.

4.2.4 Preparation and administration of amyloid-beta peptide and fibrinogen

Amyloid-beta peptide ($A\beta_{1-42}$): Peptides (full length $A\beta_{1-42}$ or reverse peptide $A\beta_{42-1}$; California Peptide, Napa, CA) were prepared as previously described (Lue et al., 2001; Franciosi et al., 2006). The compounds were first dissolved in 35% acetonitrile (Sigma, St. Louis, MO) and further diluted to 500 μM with incremental additions of PBS with vortexing. The peptide solution was subsequently incubated at 37°C for 18 hr to promote fibrilization and aggregation and stored at -20°C.

Fibrinogen: In some experiments fibrinogen was injected, in addition to $A\beta_{1-42}$, as an inflammatory stimulus. These studies used fibrinogen at a concentration of 4 mg/ml (dissolved in PBS; Sigma). This concentration of fibrinogen employed for stereotaxic *in vivo* injection was selected based on a previous analysis of normal fibrinogen concentration in the blood, which ranged from 1.5-4 mg/ml (Lip, 1995; Adams et al., 2004).

4.2.5 Administration of pharmacological modulators

In this study we have employed two different pharmacological strategies to modulate inflammatory responses using the defibrinogenating compound ancrod and a monoclonal antibody for CD11b (anti-Mac-1) expressed in monocyte-macrophage cells. In this work we refer specifically to microglia as the cells expressing CD11b.

Ancrod: This compound is derived from the venom of the Malayan pit viper. Ancrod cleaves the A-chains of fibrinogen resulting in generation of soluble fibrin degradation products that are removed from the circulation (Dempfle et al., 2000). Ancrod was obtained from the National Institute for Biological Standards and Control (NIBSC, Potters Bar, UK) and dissolved in distilled water at a concentration of 55 I.U. Animals were injected i.p. with ancrod at 10 I.U.

(ml/kg) one day before the $A\beta_{1-42}$ peptide injection, followed by twice daily injections for 7 d. This administration regimen for ancrod has previously been reported effective in defibrination (Chowdhury and Hubbell, 1996; Sun et al., 2004).

Anti-Mac-1 antibody: This neutralizing monoclonal antibody against rat adhesive receptor Mac-1 was obtained from BD Pharmingen (San Diego, CA). It reacts with the α-chain of rat Mac-1 (CD11b/CD18, α[M]β2 integrin) and is reported to block the binding of fibrinogen to Mac-1 on microglia (Flick et al., 2004). Anti-Mac-1 (10 μg) was injected into the intracerebroventricle at 30 min prior to peptide treatment. Rat IgG2b was used as the isotype control antibody for $A\beta_{1-42}$ peptide-injected animals.

4.2.6 Immunohistochemistry of rat brain

The procedure followed here used previously published protocols (Ryu et al., 2004, 2007). Animals were transcardially perfused with heparinized cold saline followed by 4% paraformaldehyde in 0.1 M phosphate buffer (0.1 M PB, pH 7.4) under ketamine/xylazine anesthesia. Brains were removed from the skull, postfixed in the same fixative overnight and then placed in 30% sucrose for cryoprotection. The brains were then rapidly frozen in powdered dry ice and stored at -70°C. Coronal sections (40 μm) were cut on a cryostat throughout the hippocampus and stored in cryoprotectant solution. Free-floating sections were processed for single immunohistochemistry. Briefly, sections were permeabilized by incubation in PBS containing 1% bovine serum albumin (BSA; Sigma-Aldrich), 10% normal goat serum (NGS) and 0.2% Triton X-100 for 1 hr. Sections were then incubated overnight at 4°C with the following primary antibodies: anti-fibrinogen (a marker for BBB damage, 1:1000; DakoCytomation), anti-CR3R (OX-42, a marker for microglia/macrophages, 1:500; Serotec), anti-glial fibrillary acidic protein (GFAP, a marker for astrocytes, 1:1000; Sigma-Aldrich), anti-ionized calcium binding adapter molecule 1 (Iba-1, a marker for microglia, 1:500; Wako Chemicals, Richmond, VA), or anti-neuronal nuclei (NeuN, a marker for neurons, 1:1000; Chemicon, Temecula, CA). Sections were rinsed in PBS with 0.5% BSA and incubated with Alexa Fluor 488- or 594-conjugated secondary antibody (1:200; Molecular Probes, Eugene, OR) for 2 hr. To determine the integrity of the BBB, immunoglobulin G (IgG) immunostaining was performed according to the method described previously (Ryu et al., 2006). For the immunostaining control, primary antibody was omitted from the staining procedures.

Double immunofluorescence staining was performed as described previously (Choi et al., 2007). Free-floating sections were incubated overnight at 4°C with a mixture of two primary

antibodies: Fibrinogen (1:1000; DakoCytomation) in combination with OX-42 (1:500; Serotec) or GFAP (1:1000; Sigma-Aldrich); and NeuN (1:500; Chemicon) in combination with Iba-1 (1:500; Wako Chemicals). Sections were then incubated in a mixture of Alexa Fluor 488- and 594-conjugated secondary antibodies (1:100; Molecular Probes) for 2 hr.

4.2.7 Immunohistochemical analysis of rat brain

Quantitative image analysis for the immunostained rat hippocampal sections was performed on three equally spaced sections. In each stained section, the hippocampal subregion boundaries were outlined as previously described (Ryu and McLarnon, 2007) with immunohistochemical analysis carried out in the superior blade of the granule cell layer (GCL) of the dentate gyrus. The molecular layer (ML) region refers to the area between the GCL border and the hippocampal fissure. Four fields within the GCL and ML regions were then selected in each section at a magnification of ×400. For measurement of vascular permeability (fibrinogen and IgG markers) and astrogliosis (GFAP marker), the area of positive staining above a threshold intensity was quantified (n = 6 rats/group) in GCL and ML regions, which was represented as the percent area density. The measurements of microglial activation (Iba-1 marker) and neuronal survival (NeuN marker) were made on immunostained sections by counting the number of immunoreactive cells (n = 6 rats/group) in GCL. All quantitative analyses were performed in a blind manner.

4.2.8 Statistical Analysis

Values are expressed as means ± SEM. Statistical significance was assessed by Student's *t*-tests or ANOVA, followed by Newman-Keuls multiple comparison test (GraphPad Prism 3.0). Significance was set at $p < 0.05$.

4.3 RESULTS

4.3.1 Patterns of fibrinogen staining in AD and ND brain sections

An impetus for this study was the finding of a marked enhancement in expression of fibrinogen immunoreactivity (ir) in AD, compared to ND, brains. Representative staining for fibrinogen in entorhinal cortical regions is presented for AD/ND brain tissue in Fig. 4-1A with the left and middle panels showing respective, low (4X) and high (40X), magnifications. AD tissue was characterized by a diffuse pattern of fibrinogen ir, which was generally absent in ND tissue. In ND brain, fibrinogen ir appeared restricted to the lumens of blood vessels, whereas, in AD brain tissue, the glycoprotein showed intense staining both within and external to vessels. The inset in Fig. 4-1A (right panel) shows a typical pattern of fibrinogen ir in AD tissue with most staining localized to regions in proximity to blood vessels (arrow indicates one example). In this work, the specificity of fibrinogen antibody staining was demonstrated by the findings of negligible staining with either omission of the primary antibody or with pre-incubation of antibody with fibrinogen prior to tissue incubation with antibody (data not shown; see Methods). The quantification of fibrinogen immunoreactivity (ir) is presented as area density in Fig. 4-1B with data collated from a total of 8 AD and 7 ND brain entorhinal cortical samples. Overall, fibrinogen positive ir areas were increased 4.5-fold in AD, compared to ND, tissue.

We also examined for fibrinogen association with deposits of Aβ. ND brain sections showed very low levels of Aβ (upper left panel, Fig. 4-1C) and no evidence for any double staining of fibrinogen with Aβ (upper right panel, Fig. 4-1C). However, AD brain tissue demonstrated considerable areas of both Aβ deposition and fibrinogen ir (lower left and middle panels, Fig. 4-1C). The patterns of fibrinogen ir indicated regions where the serum protein was in proximity to amyloid plaque deposits (see magnified inset in lower right panel) and regions with no evident colocalization of markers (lower right panel).

4.3.2 Patterns of vascular staining (vWF ir) and BBB leakiness (IgG permeability) in AD and ND brain sections

To provide a more detailed investigation of changes in vasculature, we also employed immunohistochemical staining for von Willebrand factor (vWF), a glycoprotein produced by endothelial cells, in the same tissue sections used for fibrinogen expression. Additionally, integrity of BBB was examined by measuring permeability of IgG through the barrier. Representative double staining for vWF and fibrinogen in AD and ND sections are presented in Fig. 4-2A. The vWF staining in ND tissue was characterized by clearly delineated blood vessels

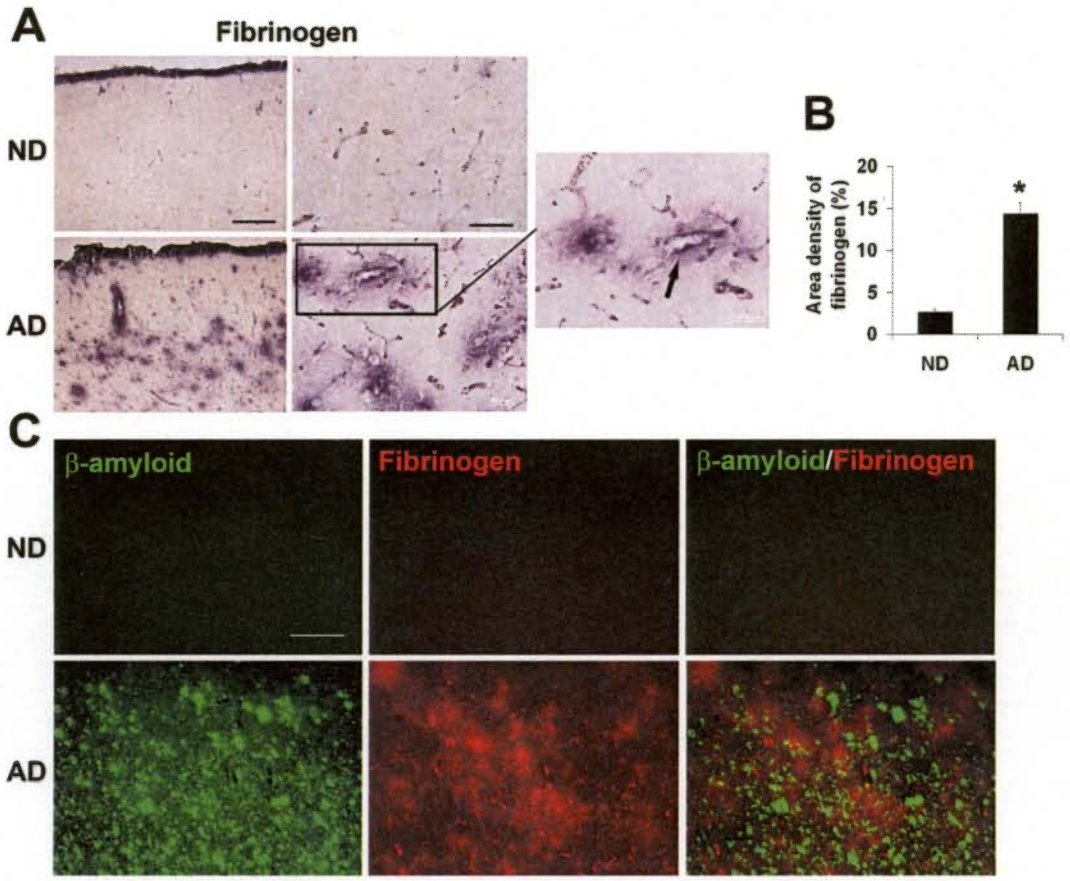

Figure 4-1. Fibrinogen immunostaining of tissues from the entorhinal cortex of ND and AD brain. (**A**) Low (left panels, scale bar = 500 μm) and high (right panels, scale bar = 100 μm) magnifications of fibrinogen immunoreactivity (ir). ND brain was characterized by low levels of fibrinogen ir localized to blood vessels (top panels) whereas AD sections showed intense and diffuse patterns of fibrinogen staining. The single panel (right) shows a detailed view of an AD section with arrow indicating fibrinogen ir in proximity to a blood vessel. (**B**) Quantification of fibrinogen ir in ND (n = 7 cases) and AD (n = 8 cases) brain tissue; * indicates $p < 0.05$ difference. (**C**) Representative double staining of fibrinogen with Aβ peptide deposits. Scale bar represent 200 μm. The magnified inset in the lower right panel (scale bar: 30 μm) shows a detailed view of an AD section indicating fibrinogen ir in proximity to peptide.

(upper left panel) whereas in AD sections vWF ir showed a pattern of discontinuous and distorted vessel staining with accumulation of vWF particles outside the vessel (lower left panel). The appearance of small clusters of vWF has been interpreted as indicative of abnormalities and dysfunction of endothelium (Lip and Blann, 1997). In ND brain, fibrinogen ir showed considerable areas of overlap with vWF (upper right panel) indicating well-defined blood vessels. AD tissue demonstrated diffuse regions of fibrinogen ir with considerable extents of staining located external to blood vessels and separate from vWF ir (lower right panel). The overall results point to a generalized pattern of vascular abnormalities in AD tissue including evidence for leakiness of BBB to endogenous blood proteins.

The pattern of fibrinogen staining in parenchymal entorhinal cortical regions of AD brain tissue indicated leakiness and increased permeability of BBB. This point was further investigated by staining for IgG as a marker for integrity of the barrier (Ryu and McLarnon, 2006). A low magnification photomicrograph of entorhinal cortical IgG ir is presented for ND and AD sections (Fig. 4-2B). A considerably increased intensity of IgG staining was evident in AD, relative to ND, brain. The overall density of IgG, from analysis of 8 AD and 7 ND samples, is presented in Fig. 4-2C. AD tissue demonstrated a 2.4-fold increase in IgG ir compared with ND tissue.

4.3.3 Association of fibrinogen expression with microgliosis and astrogliosis

We have recently demonstrated activated microglia are associated with vascular remodeling and leaky BBB in peptide-injected rodent brain (Ryu and McLarnon, 2007). We used double immunostaining to qualitatively examine association of fibrinogen ir with expression of HLA-DR (+)ve microglia and GFAP (+)ve astrocytes. For microglia, relatively low levels of fibrinogen and HLA-DR ir were evident in ND tissue (top panels, Fig. 4-3A) whereas AD tissue exhibited considerably elevated levels of both markers (lower panels, Fig. 4-3A). Areas of overlap between cellular and glycoprotein ir were evident in AD tissue (merged staining in lower right panel) and which were absent from ND entorhinal cortical sections (upper right panel).

A low level of astrocyte ir was observed in ND tissue sections (upper panels, Fig. 4-3B) with enhanced reactivity demonstrated in AD tissue (lower panels, Fig. 4-3B). In the latter case regions of overlap of fibrinogen with GFAP (+)ve astrocytes was demonstrated. Overall, however, microglia exhibited a considerably larger extent of co-association with fibrinogen, compared with astrocytes, in AD brain tissue.

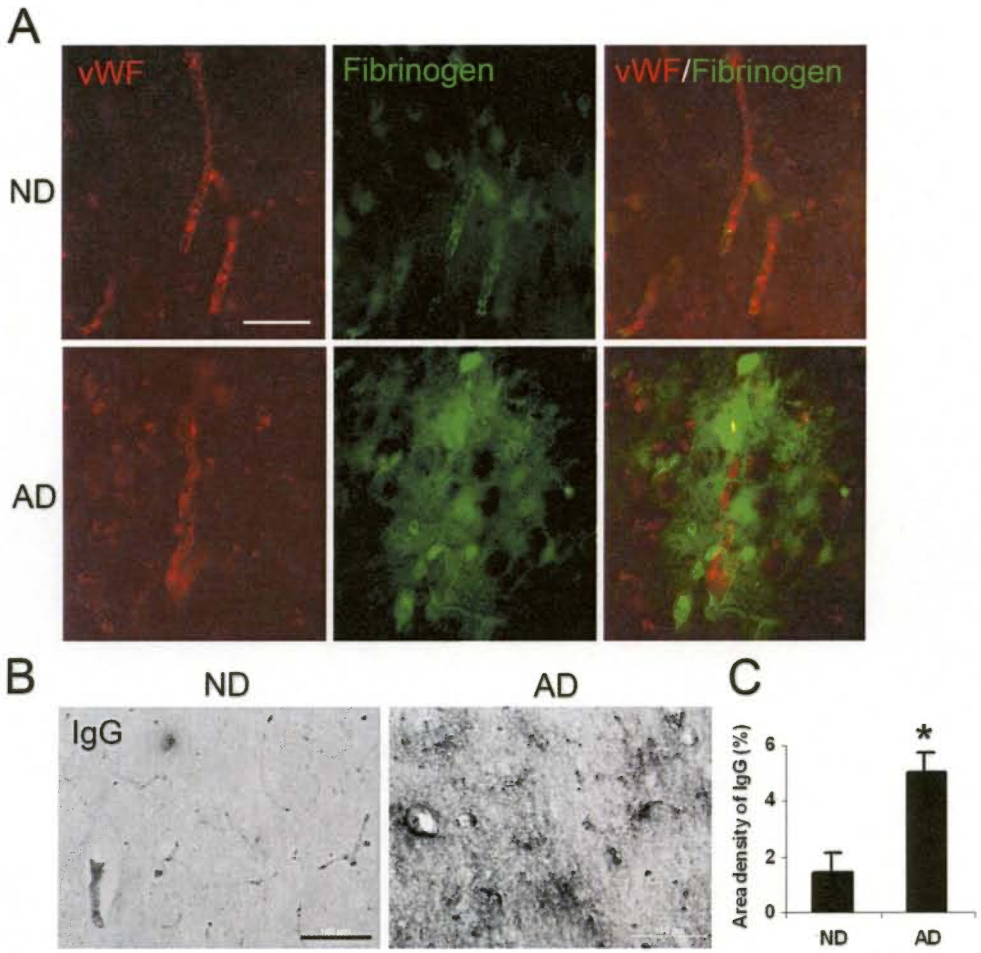

Figure 4-2. Representative fluorescent double staining for fibrinogen, vWF and IgG. (**A**) Double immunofluorescent staining for vWF (red, left panels) and fibrinogen (green, middle panels) in the entorhinal cortex of ND and AD sections; the merged image is presented in right panels. Scale bar shown is 60 μm. (**B**) IgG ir for ND/AD tissue with low magnification._scale bar = 100 μm. (**C**) Quantification of IgG ir in ND (n = 7 cases) and AD (n = 8 cases) sections. * indicates $p < 0.05$ difference.

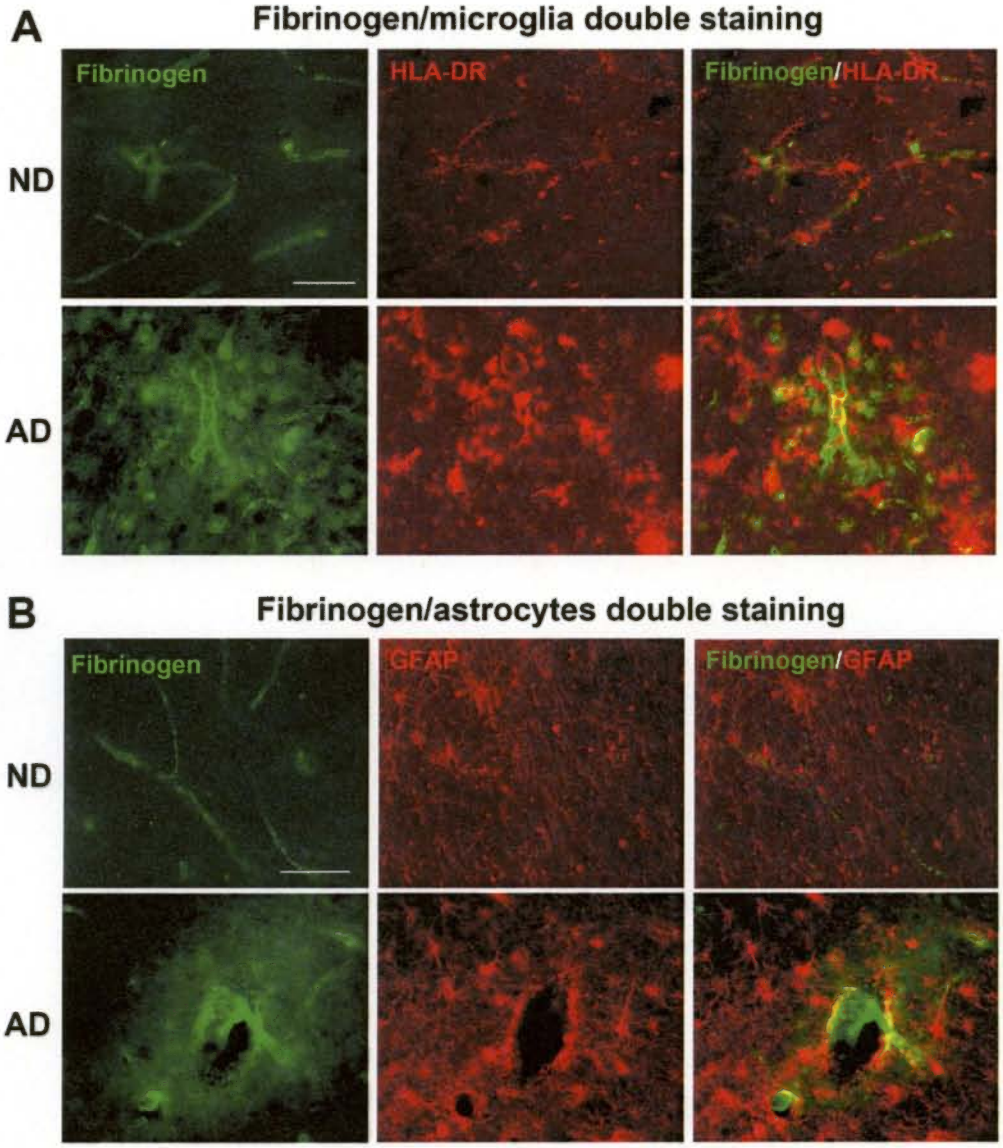

Figure 4-3. Representative double immunofluorescence staining of fibrinogen with microglia (HLA-DR marker) and astrocytes (GFAP marker) in the entorhinal cortex of ND and AD brain. (**A**) ND tissue (upper panels) showed low levels of fibrinogen ir with microglia whereas AD tissue (lower panels) was characterized by extensive areas of diffuse fibrinogen deposition in association with microglia. Scale bar = 100 μm. (**B**) Representative staining for astrocytes in ND (upper panels) and AD (lower panels) sections. Double staining shows merged areas of markers. Scale bar = 100 μm.

4.3.4 Patterns of staining for vessels, microglia and Aβ

We were interested in the question as to whether AD sections would show a composite of association between vessels, Aβ and microglia. Additionally, we examined if microglia in AD brain exhibited a morphology that was consistent with their activation. Representative high magnifications of ND and AD entorhinal cortical sections are presented in Fig. 4-4. The blood vessel (V) in ND brain shows only a low level of associated Aβ ir, with no evident interactions with HLA-DR (+)ve microglia. Moreover the few microglia evident in the panel exhibit a ramified morphology with extensive processes (Fig. 4-4, upper panel). Ramified shapes have been suggested as indicative of quiescent microglia (Conde and Streit, 2006). A very different profile was observed in AD sections where deposits of Aβ were localized in close apposition to vessels. Furthermore, microglia were characterized by a predominant ameboid morphology, distinguished by retracted processes and swollen cell bodies, indicating reactive cells (Fig. 4-4, lower panel). These patterns of immunostaining were consistent throughout entorhinal cortical regions.

4.3.5 Effects of $A\beta_{1-42}$ intrahippocampal injection on microgliosis, astrogliosis and vasculature

The results described above indicate AD brain tissue is characterized by an inflammatory microenvironment including evidence for an increased vascular permeability to the blood protein fibrinogen and also infiltration of IgG, abnormalities in vessels indicated by patterns of vWF staining and the presence of activated and proliferating microglia. These findings prompted a detailed analysis of these factors and neuronal viability using an *in vivo* animal model of inflamed brain with hippocampal injection of $A\beta_{1-42}$ peptide. A particular focus of these experiments was the investigation of effects of pharmacological modulations targeting reduction of levels of fibrinogen or inhibition of microglial activation.

We initially examined fibrinogen ir and microglial responses at time points of 1, 3 and 7 d post-peptide injection. Two controls were employed in the experiments; injection of PBS or reverse peptide $A\beta_{42-1}$ (for 7 d). Representative double staining for fibrinogen and OX-42 (+)ve microglia for the two controls are presented in Fig. 4-5A (upper two panels). A low level of ir was demonstrated for fibrinogen or microglia with either PBS or $A\beta_{42-1}$ injection. Intra-hippocampal $A\beta_{1-42}$ injection caused time-dependent (3-7 d post-injection) increases in fibrinogen ir and numbers of microglia (lower 3 panels). At 7 d of peptide injection, double staining showed considerable overlaps between areas of fibrinogen and microglial staining

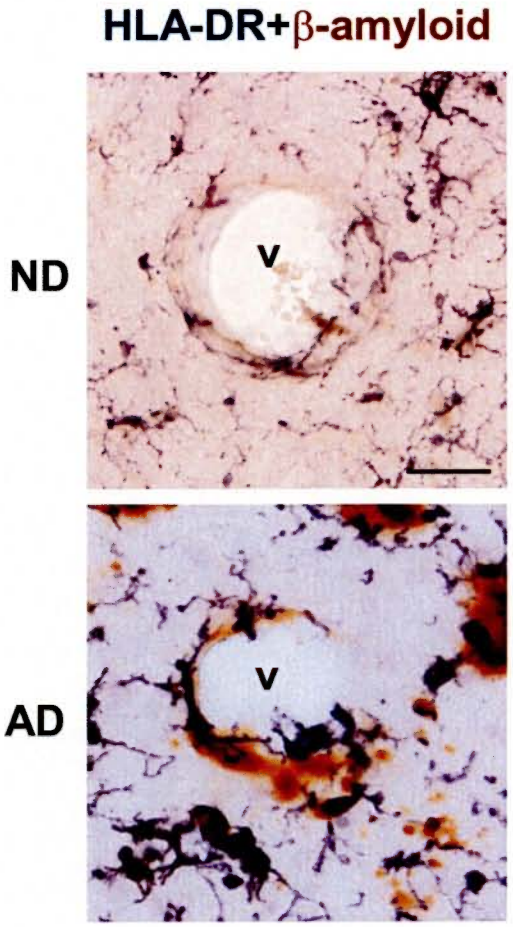

Figure 4-4. Representative double immunohistochemical staining for microglia (HLA-DR marker) and Aβ (6F/3D marker) in the entorhinal cortex of ND and AD tissue. Sections were incubated with HLA-DR and Aβ followed by visualization using DAB/nickel ammonium sulfate (anti-HLA-DR, dark purple color) or DAB (anti-Aβ, brown color). Staining shows blood vessels (v) with AD tissue demonstrating close association between Aβ, microglia and vessel. Scale bar represents 50 μm. Note the predominant ramified and ameboid morphologies of microglia in ND and AD tissue, respectively.

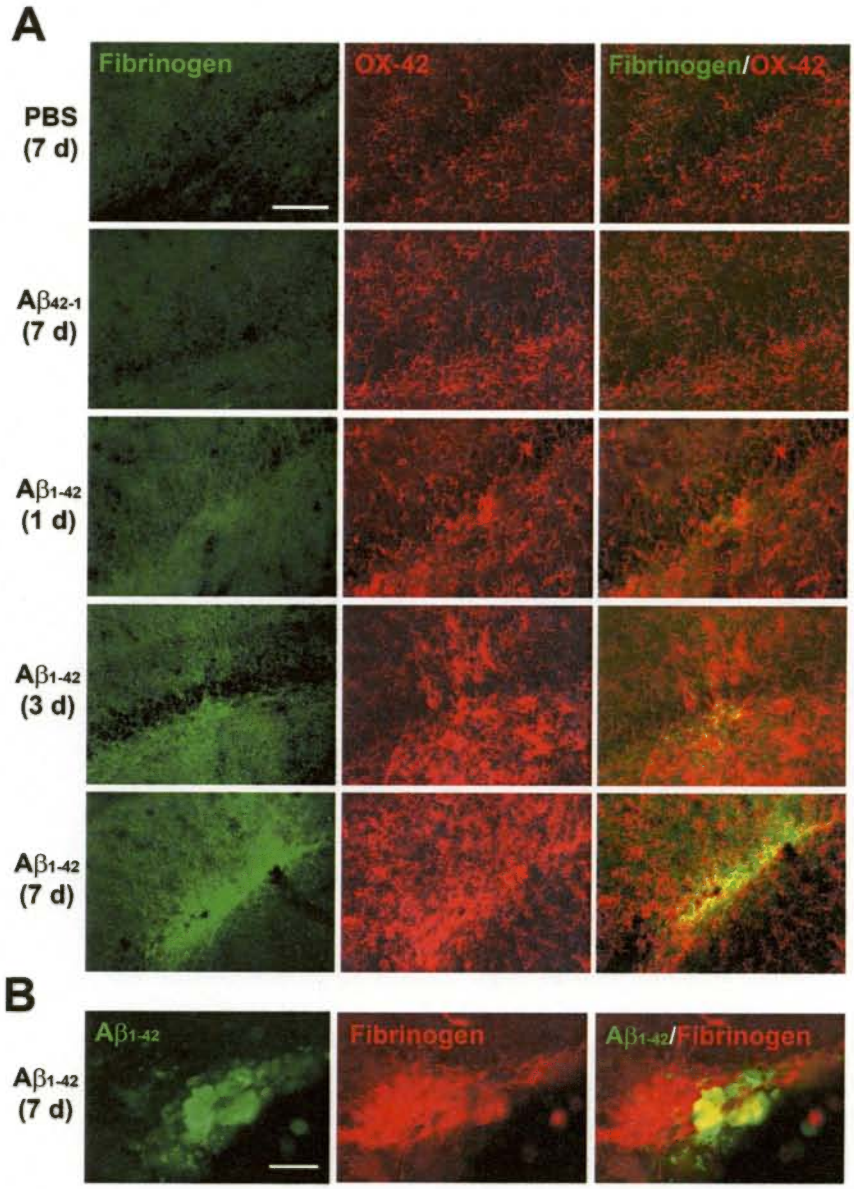

Figure 4-5. Fibrinogen and microglia (OX-42) double immunofluorescent staining in $A\beta_{1-42}$-injected rat hippocampus. **(A)** In controls (7 d injection of PBS, upper panel or reverse peptide $A\beta_{42-1}$, 2nd panel) low levels of fibrinogen (left column) and numbers of microglia (middle column) are evident. The right column shows merged staining. Subsequent vertical panels show progressive time-dependent changes in fibrinogen/OX-42/merged ir for 1, 3 and 7 d durations of $A\beta_{1-42}$ peptide injection. Scale bar represents 200 μm. **(B)** Double staining for $A\beta_{1-42}$ and fibrinogen (7 d post-peptide injection). Scale bar = 80 μm.

(lower right panel, Fig. 4-5A). Areas of fibrinogen ir appeared associated with Aβ as indicated in the double staining photomicrograph (Fig. 4-5B). Previous work from this laboratory has demonstrated colocalization of microglia with Aβ-immunoreactive plaques (McLarnon et al., 2006).

Astrocytic responses were also examined with fibrinogen at the single time point of 7 d post-peptide injection. Double staining for controls (PBS or reverse peptide injection) indicated little or no association of fibrinogen ir with GFAP (+)ve astrocytes (right panels, Fig. 4-6). Representative staining following peptide injection (lower panels, Fig. 4-6) indicated astrocyte proliferative responses with some evidence for areas of overlap with fibrinogen staining. Overall, regions of coincident fibrinogen staining with astrocytes were considerably less than observed with microglial-fibrinogen association.

4.3.6 Effects of the defibrinogenating compound, ancrod on vascular integrity, gliosis and neuronal integrity in peptide-injected hippocampus

Ancrod and vascular integrity: The results presented above point to vascular remodeling allowing glycoprotein extravasation in AD tissue and as a component of inflammatory response in peptide-injected rat hippocampus. Evidence also suggested microgliosis was correlated with perturbations in vasculature including leakiness in BBB. We next investigated effects of pharmacological intervention on the components of inflammation. Two different approaches were employed in these experiments; use of the specific defibrinogenating compound, ancrod, to inhibit systemic circulating levels of the glycoprotein (see Methods) and anti-Mac-1 to inhibit microglial activation (see below).

Representative staining for fibrinogen and IgG, in the absence and presence of ancrod treatment with 7 d injection of $A\beta_{1-42}$, are presented in Fig. 4-7A. Both vascular markers exhibited intense staining following peptide injection with considerable extents of ir colocalized with vessels. Ancrod treatment reduced ir levels for both markers. Quantification for the effects of ancrod intervention on the vascular proteins are presented in Fig. 4-7B (overall results from n=6 animals). Ancrod was highly effective in reduction of fibrinogen ir with a decrease of 80% compared with no drug treatment of peptide-injected hippocampus. The corresponding reduction in IgG levels with ancrod was 52% also representing a significant decrease.

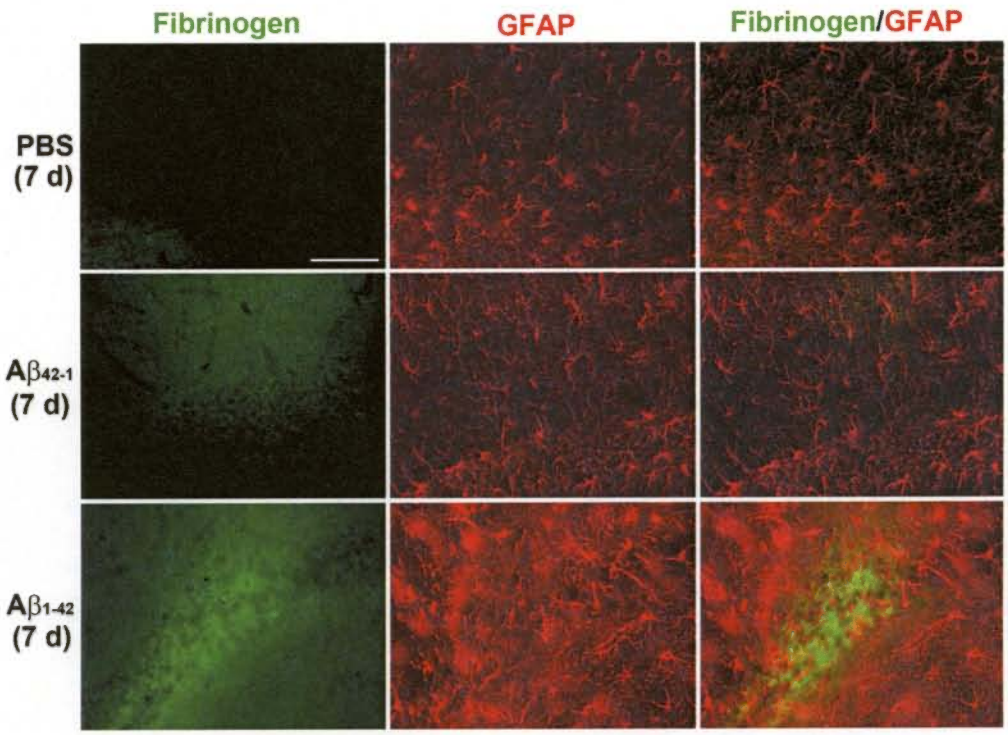

Figure 4-6. Fibrinogen and astrocyte (GFAP) double immunofluorescent staining in peptide-injected (7 d) hippocampus. GFAP ir (middle panels) was increased with $A\beta_{1-42}$ compared to controls (PBS and $A\beta_{42-1}$). Typical merged staining is shown in the right panels. Scale bar = 200 µm.

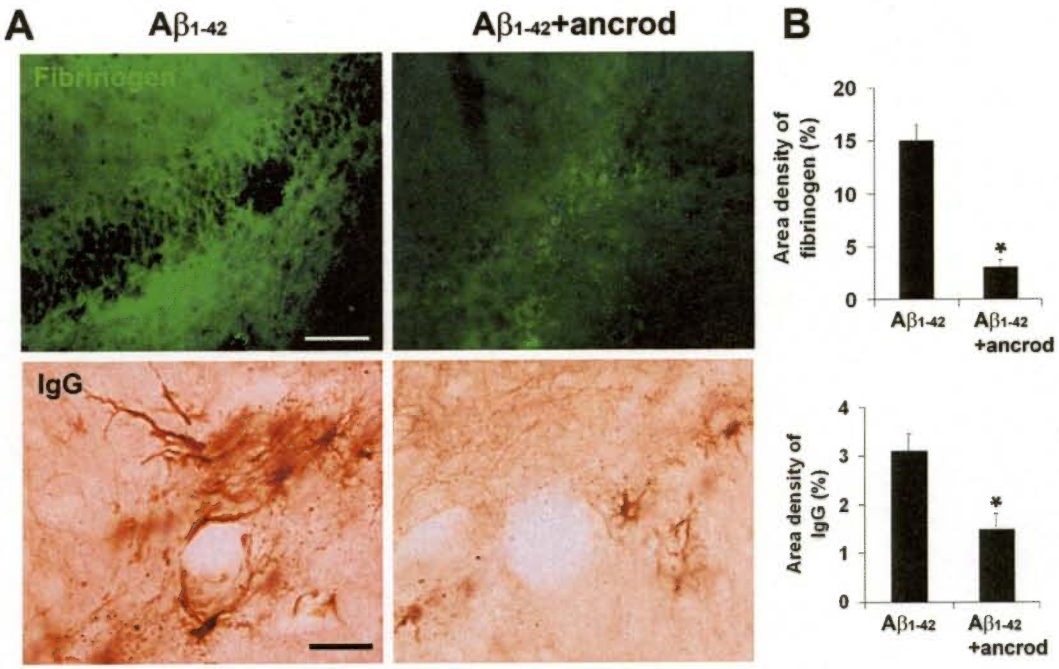

Figure 4-7. Effects of the defibrinogenating compound, ancrod, on parenchymal fibrinogen and IgG in $A\beta_{1-42}$–injected hippocampus. (A) Representative ir for fibrinogen (upper left panel) and IgG (lower left panel) in 7 d peptide-injected hippocampus. Effects of ancrod treatment with peptide are presented in the right panels. The IgG staining includes examples showing blood vessels. Scale bars are 100 μm (for fibrinogen) and 50 μm (for IgG). (**B**) Quantification of ancrod effects on fibrinogen ir (upper bar graph) and IgG ir (lower bar graph). Data are means ± SEM from 6 animals. * denotes significant difference for $p < 0.05$.

Ancrod effects on gliosis and neuronal integrity: Typical patterns of microglial (Iba-1), astrocyte (GFAP) and neuronal (NeuN) staining are shown in Fig. 4-8A with PBS (left panels), $A\beta_{1-42}$ alone (middle panels) and peptide with ancrod treatment (right panels). Markers for microgliosis (Iba-1) and astrogliosis (GFAP) showed high intensity staining in $A\beta_{1-42}$, but not PBS, injected brain. Ancrod treatment of peptide-injected animals reduced both gliotic markers. Quantification of data (n=6 animals) showed microgliosis significantly diminished (by 44%) in the presence of ancrod (Fig. 4-8B). Although astrogliosis was lower in ancrod-injected animals (by 17%), this effect did not reach significance.

Neuronal viability in the granule cell layer was determined by measuring NeuN ir for the three different animal groups. Representative data (lower panels, Fig 4-8A) show a considerable decrease in numbers of neurons in $A\beta_{1-42}$-injected hippocampus compared to control PBS injection. Treatment of peptide-injected animals with ancrod was effective in increasing viability of neurons. Quantitative analysis (n = 6 animals) demonstrated the efficacy of ancrod treatment in providing a significant degree of neuroprotection with the numbers of dentate gyrus neurons increased by 26% compared with PBS-injected animals (Fig. 4-8B).

4.3.7 Effects of enhanced *in vivo* stimulation with $A\beta_{1-42}$ combined with fibrinogen and inhibition of microglial activation using anti-Mac-1

The presence of fibrinogen ir in parenchymal regions for both AD brain and *in vivo* following injection of $A\beta_{1-42}$ into the rat hippocampus, suggested the relevance in testing for the effects of combining peptide plus fibrinogen as an enhanced stimulus for microgliosis, vascular remodeling and intactness of BBB and neuronal damage. We further hypothesized that inflammatory responses mediated by activated microglia could be involved in perturbations in vascular processes. Thus, we also investigated for effects of reducing microglial activation using anti-Mac-1 antibody (Flick et al., 2004), in the presence of peptide plus fibrinogen stimulation.

Initial experiments examined the effects of combined stimulation ($A\beta_{1-42}$ + fibrinogen for 7 d) and use of anti-Mac-1 on microgliosis (Iba-1 marker). Representative staining shows relatively low expression of Iba-1 in controls (PBS and reverse peptide, left panels of Fig. 4-9A). Microgliosis was increased with peptide injection (upper middle panel) and further amplified in the presence of the combined stimuli (upper right panel). Anti-Mac-1 administration was effective in inhibiting Iba-1 ir for both $A\beta_{1-42}$ (lower middle panel) and for $A\beta_{1-42}$ + fibrinogen (lower right panel), injections.

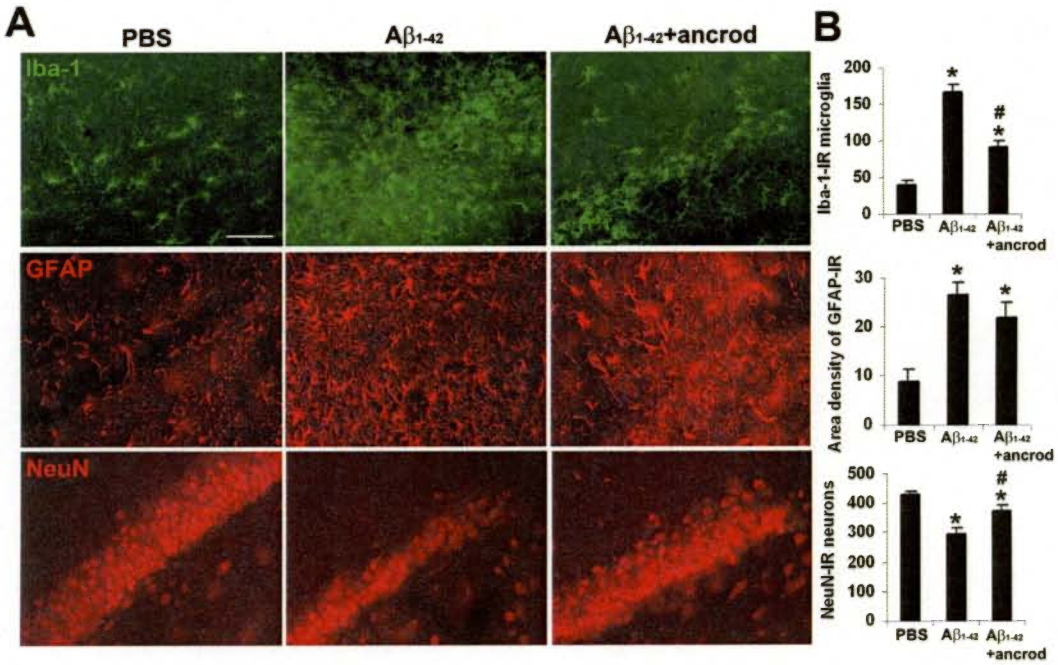

Figure 4-8. Effects of ancrod on gliosis and neuronal viability in $A\beta_{1-42}$-injected hippocampus. (**A**) Representative microglial (Iba-1 marker, upper panels), astrocyte (GFAP marker, middle panels) and neuronal (NeuN marker, lower panels) staining at 7 d with PBS, $A\beta_{1-42}$ and $A\beta_{1-42}$ plus ancrod treatment. Scale bars represent 100 μm. (**B**) Quantification of ancrod effects on microgliosis (upper bar graph), astrogliosis (middle bar graph) and neuronal viability (lower bar graph). Data are means ± SEM from 6 animals. * denotes significant difference for $p < 0.05$.

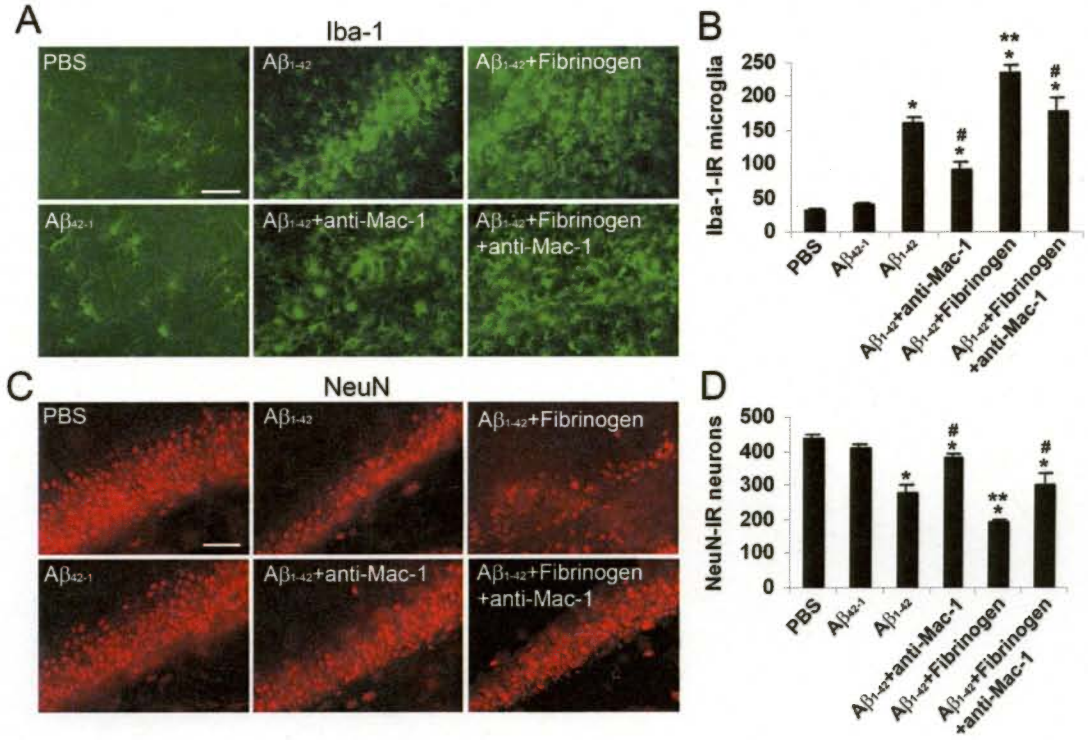

Figure 4-9. Microglial (Iba-1 marker) and neuronal (NeuN marker) staining following 7 d intra-hippocampal injection of $A\beta_{1-42}$ and $A\beta_{1-42}$ plus fibrinogen in the absence/presence of anti-Mac-1 treatment. (**A**) Controls (left panels) show that PBS and $A\beta_{42-1}$ injections are associated with low numbers of microglia. Injection of $A\beta_{1-42}$ (upper middle panel) or $A\beta_{1-42}$ plus fibrinogen (upper right panel) progressively increases microgliosis. Effects of anti-Mac-1 on microgliosis with peptide (lower middle panel) and peptide plus fibrinogen (lower right panel) injections. Scale bar represents 100 μm. (**B**) Quantification (n = 6 animals) of Iba-1 ir for the different treatments. $*p < 0.05$ vs. PBS; $\#p < 0.05$ vs. $A\beta_{1-42}$ or $A\beta_{1-42}$ plus fibrinogen; $**p < 0.05$ vs. $A\beta_{1-42}$. (**C**) Representative NeuN ir for controls (left panels), $A\beta_{1-42}$ and $A\beta_{1-42}$ plus fibrinogen (middle and right upper panels, respectively) and $A\beta_{1-42}$ and $A\beta_{1-42}$ plus fibrinogen with anti-Mac-1 treatment (middle and right lower panels, respectively). Scale bar represents 100 μm. (**D**) Quantification (n = 6 animals) of NeuN ir for the different treatments. $*p < 0.05$ vs. PBS; $\#p < 0.05$ vs. $A\beta_{1-42}$ or $A\beta_{1-42}$ plus fibrinogen; $**p < 0.05$ vs. $A\beta_{1-42}$.

Quantification of data (n = 6 animals) is presented in Fig. 4-9B. Expression of Iba-1 was increased 45% with the combined stimulation compared with peptide alone with anti-Mac-1 effective in reducing this expression (by 24%). Administration of anti-Mac-1 also significantly inhibited Iba-1 ir with peptide injection alone (by 44%). Control injections with PBS or reverse peptide demonstrated regions of intact dentate gryrus neurons (left panels, Fig. 4-9C). Considerable neuronal loss accompanied peptide injection, which was further exacerbated with inclusion of fibrinogen with peptide (upper middle and right panels, Fig. 4-9C). Administration of anti-Mac-1 protected against neuronal loss for both combined stimuli (lower right panel, Fig. 9C) and $A\beta_{1-42}$ alone (lower middle pane, Fig. 4-9C).

Quantification of data (Fig. 4-9D) showed $A\beta_{1-42}$ + fibrinogen injection increased neuronal loss by 45% compared to peptide alone. Treatment with anti-Mac-1 increased numbers of neurons by 35% with stimuli combined and by 26% with peptide injection; these values represented significant degrees of neuroprotection with anti-Mac-1.

Intactness of BBB was also determined in these experiments using staining for IgG. Low levels of IgG activity were measured in PBS and reverse peptide controls (left panels of Fig. 4-10A) with $A\beta_{1-42}$ + fibrinogen exhibiting an enhanced IgG ir (upper right panel) compared with peptide injection alone (upper middle panel). Anti-Mac-1 treatment reduced expression of IgG with both combined stimulation and with peptide injected alone (right and middle lower panels).

Overall (n = 6 animals), the area density of IgG was increased by 98% with $A\beta_{1-42}$+ fibrinogen compared with $A\beta_{1-42}$ alone (Fig. 4-10B). IgG expression was attenuated by 38% by anti-Mac-1 in the presence of the combined stimuli. The corresponding value for anti-Mac-1 inhibition of IgG with peptide injection alone was 65%. These reductions in IgG levels, induced by the inhibition of microglial activation, were significant.

Data were also obtained with fibrinogen injected alone, in both the absence and presence, of anti-Mac-1 treatment. The results (data not shown) showed modest, but significant, increases in vascular and inflammatory processes relative to control values. These increases were attenuated with application of anti-Mac-1 treatment (data not shown).

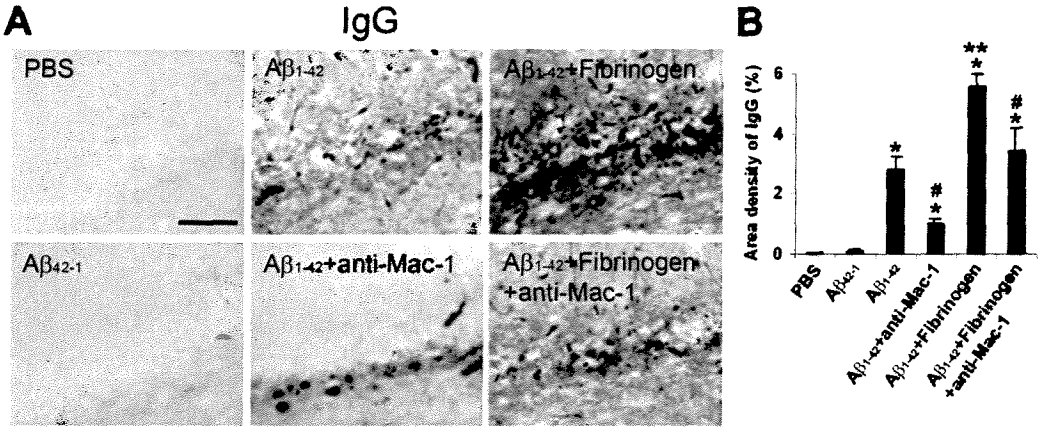

Figure 4-10. Effects of anti-Mac-1 on IgG staining in $A\beta_{1-42}$ and $A\beta_{1-42}$ plus fibrinogen-injected hippocampus. (**A**) Typical patterns of IgG ir in controls (left panels) and with peptide (upper middle panel) and peptide plus fibrinogen (upper right panel). Effects of anti-Mac-1 are shown in lower middle and right panels. Scale bar represents 100 μm. (**B**) Quantification (n = 6 animals) of IgG ir for the different treatments. $*p < 0.05$ vs. PBS; $\#p < 0.05$ vs. $A\beta_{1-42}$ or $A\beta_{1-42}$ plus fibrinogen; $**p < 0.05$ vs. $A\beta_{1-42}$.

4.4 DISCUSSION

Our results provide novel evidence for correlations between microglial immunoreactivity, vascular remodeling, fibrinogen extravasation and neuronal viability in AD brain tissue and in $A\beta_{1-42}$-injected hippocampus. Overall, the data support the premise that perturbations in vasculature and elevated parenchymal plasma glycoproteins are integral components of inflammatory reactivity in AD brain. We employed a strategy whereby findings of altered gliosis and vasculature in AD brain tissue provided a framework in testing for similar processes, and for measuring their modulations and extents of neuronal damage with pharmacological interventions, in vivo. The results suggest that intrahippocampal injection of peptide induces an inflammatory microenvironment in brain which is attenuated by increasing BBB integrity and reducing microglial reactivity.

Immunohistochemical analysis demonstrated AD, but not ND, brain tissue expressed considerable levels of fibrinogen ir. The expression of this plasma protein appeared diffusely in parenchymal regions in proximity to blood vessels. Fibrinogen ir within vessels was co-localized with vWF, an endothelial glycoprotein, as shown by the representative staining in Fig. 4-2A. However, the patterns of vWF staining also showed irregularities in vessel walls with small fragments of extraneous particles suggesting abnormalities in vasculature in AD tissue. Increased levels of extravascular vWF in brain have been suggested as indicating damaged endothelium (Lip and Blann, 1997). Considerable extents of fibrinogen ir appeared in association with deposits of Aβ in AD brain (Fig. 4-1C) indicating that Aβ deposits may serve as a locus for inflammatory reactivity. Elevated levels of fibrinogen have been reported in AD, relative to ND, brain (Fiala et al., 2002) with increased plasma fibrinogen reported to increase the risk of AD and vascular dementia (van Oijen et al., 2005). Recently, fibrin brain deposition has been documented in several animal models of AD (Paul et al, 2007), a result considered in detail below.

The patterns of staining for both fibrinogen and vWF suggested an increased permeability of BBB in AD, compared to ND, tissue. Infiltration of IgG was used as an independent marker to indirectly measure leakiness of BBB. AD, but not ND, brain tissue exhibited patterns of intense IgG ir in parenchyma with prominent staining near vessels (Fig. 4-2B). Previous work has reported elevated levels of IgG in AD brain tissue (D'Andrea, 2003, 2005) and in peptide-injected rat hippocampus (Ryu and Mclarnon, 2006). Overall, our data implicate perturbed and abnormal blood vessels as a component of inflammatory response in AD brain (Rogers and Lue, 2001).

Gliosis, both micro-(Fig. 4-3A) and astro-(Fig. 4-3B) were considerably higher in AD, compared with ND, brain tissue. Double staining analysis indicated areas of overlap of microgliosis with fibrinogen ir in AD brain (Fig. 4-3A). Interestingly, representative patterns of staining showed numerous examples where microglial-fibrinogen ir was in apparent association with blood vessels. Instances of colocalization of microglia with Aβ were also documented in AD tissue and representative double staining included examples where microglia-Aβ ir was in apposition to blood vessels (Fig 4-4). Although microglial ir with fibrinogen, Aβ or vessels was not quantified in AD brain tissue, such associations were relatively common. The predominant ameboid morphology of AD microglia suggested cells were activated (Walker et al., 2001; Conde and Streit, 2006).

The findings from analysis of AD and ND tissue prompted detailed in vivo experiments using intrahippocampal injection of $A\beta_{1-42}$, alone or combined with fibrinogen and pharmacological modifications of fibrinogen levels and microglial activation. Injection of peptide caused time-dependent (3-7 d) increases in expression of fibrinogen and microgliosis whereas controls (7 d injection of PBS or $A\beta_{42-1}$) exhibited low levels of both (Fig. 5A). Double staining showed areas of association of fibrinogen with proliferating microglia which increased with duration of peptide injection. Merged staining also indicated evidence for fibrinogen expression coincident with $A\beta_{1-42}$ ir (Fig. 4-5B). Overall, the in vivo patterns of gliosis were similar to those observed in AD brain tissue.

The administration of ancrod, a protease acting to reduce vascular fibrinogen, was investigated for effects on parenchymal levels of fibrinogen and IgG, numbers of microglia and astrocytes and for neuroprotection in peptide-injected (7 d) brain (Fig. 4-7). Ancrod treatment significantly attenuated fibrinogen and IgG ir, which is consistent with a common effect of the compound to diminish permeability of BBB to these proteins. Ancrod was also highly effective in reducing microgliosis, but not astrogliosis, in peptide-injected hippocampus (Fig. 4-8). Importantly, ancrod also demonstrated an efficacy for protection of hippocampal neurons. One possibility consistent with these data, is that reduced levels of fibrinogen diminished microglial inflammatory responses resulting in an increased viability for bystander neurons. Although plasma fibrinogen levels were not measured after ancrod application, similar treatments have been reported to reduce plasma fibrinogen levels or fibrinogen-dependent processes by 60-70% (Chowdhury and Hubbell, 1996; Sun et al., 2004).

A number of studies have suggested a damaged BBB could contribute to lesions in CNS pathology including MS (Akassoglou et al., 2004; Vos et al., 2005; Adams et al., 2007) and AD

(Dickstein et al., 2006; Zipser et al, 2007). As noted, the analysis of several mouse models of AD (Paul et al, 2007) has demonstrated fibrin deposition as a mediator of neurovascular pathology with increased levels of Aβ peptide and microgliosis implicated in vascular damage. Increased fibrin was associated with enhanced vascular damage in cortical and hippocampal regions with inhibition of plasma fibrinogen, using ancrod treatment, diminishing neurovascular pathology. Neuroinflammatory responses to the accumulation of parenchymal fibrin were indicated as primary contributors to the abnormalities in BBB; interestingly, no evidence for neurodegeneration was found in the transgenic animals. Our present study suggests the critical nature of fibrinogen extravasation in AD brain and in peptide-injected rat hippocampus in mediating chronic inflammation. It is noteworthy that we measured significant loss of granule cell neurons in rat brain.

It was hypothesized that if microglial responses to $A\beta_{1-42}$ contributed to vascular remodeling and neuronal damage, then pharmacological inhibition of microglial activation could confer neuroprotection and also reduce vascular abnormalities. Furthermore, we postulated that injection of fibrinogen with $A\beta_{1-42}$ could enhance inflammatory reactivity and neuronal damage relative to that measured with peptide injection alone. Both premises were examined using anti-Mac-1 antibody, which binds to the same microglial CD11b/CD18 integrin as does fibrinogen (Flick et al., 2004). Microgliosis was markedly increased with $A\beta_{1-42}$, compared with PBS, injection (Fig. 4-9B) and increased further with the combination of fibrinogen plus peptide. Anti-Mac-1 was effective in reducing microglial activity for both stimuli combined and for peptide-injection alone. Neuronal viability was significantly lower, relative to controls, with peptide injection alone and further diminished with fibrinogen plus peptide (Fig. 4-9D). In both cases anti-Mac-1 was effective in providing a significant degree of neuroprotection. Although these data are necessarily correlative, the results could implicate microglial inflammatory responses as a putative contributing factor for neuronal degeneration.

We considered that if microglial reactivity underlied the changes in neuronal damage, then decreasing the severity of brain insult using peptide alone (compared with peptide plus fibrinogen) and inhibiting cell activation (with anti-Mac-1) could have effects to increase the integrity of BBB. In these experiments permeability of BBB was determined by extents of IgG infiltration. IgG ir was minimal in controls but markedly increased following $A\beta_{1-42}$ injection and enhanced further in the presence of both stimuli (Fig. 4-10). Inclusion of anti-Mac-1 was highly effective in diminishing IgG for both combined stimuli and peptide alone. These results are consistent with a reduced microglial reactivity linked to an increased intactness of BBB.

Our data provide evidence that microglial responses to peptide can lead to extensive vascular remodeling which induces BBB leakage and subsequent plasma protein infiltration. Thus, microglia may not only initiate an inflammatory response to peptide but also amplify and sustain inflammation in response to fibrinogen extravasation. In this case a chronic inflammatory environment could be maintained by reciprocal signaling between activated microglia and perturbed vasculature. It is noteworthy that our study showed considerable consistency between results obtained in vivo and from analysis of AD brain tissue. Clearly, injection of $A\beta_{1-42}$ combined with fibrinogen, or for that matter peptide alone, represents only an approximate model of AD brain. Nevertheless, the model could have particular utility in emphasizing a localized inflammatory microenvironment in AD brain (Akiyama et al., 2000; Combs et al., 2001). This point is demonstrated by the utility of anti-Mac-1 to not only inhibit microglial reactivity but also to decrease BBB permeability and provide neuroprotection.

Overall, our results suggest reciprocal interactions between activated microglia and a leaky BBB help sustain a chronic inflammatory environment in peptide-injected brain. At present, our data are best interpreted as providing correlations between inflammatory responses, intactness of BBB, infiltration of glycoproteins such as fibrinogen and neuronal viability. However, correlative relationships between these processes compose an integral framework for future investigation into the underlying mechanisms and factors, which link microglial inflammatory responses to perturbations in vasculature and neuronal damage and loss of cognitive function in AD brain.

4.5 REFERENCES

Adams RA, Bauer J, Flick MJ, Sikorski SL, Nuriel T, Lassmann H, et al. The fibrin-derived gamma377-395 peptide inhibits microglia activation and suppresses relapsing paralysis in central nervous system autoimmune disease. J Exp Med 2007; 204: 571-582.

Adams RA, Passino M, Sachs BD, Nuriel T, Akassoglou K. Fibrin mechanisms and functions in nervous system pathology. Mol Interv 2004; 4: 163-176.

Akassoglou K, Adams RA, Bauer J, Mercado P, Tseveleki V, Lassmann H, et al. Fibrin depletion decreases inflammation and delays the onset of demyelination in a tumor necrosis factor transgenic mouse model for multiple sclerosis. Proc Natl Acad Sci U S A 2004; 101: 6698-6703.

Akiyama H, Barger S, Barnum S, Bradt B, Bauer J, Cole GM, et al.. Inflammation and Alzheimer's disease. Neurobiol Aging 2000; 21: 383-421.

Arai T, Miklossy J, Klegeris A, Guo JP, McGeer PL. Thrombin and prothrombin are expressed by neurons and glial cells and accumulate in neurofibrillary tangles in Alzheimer disease brain. J Neuropathol Exp Neurol 2006; 65: 19-25.

Choi HB, Ryu JK, Kim SU, McLarnon JG. Modulation of the purinergic P2X7 receptor attenuates lipopolysaccharide-mediated microglial activation and neuronal damage in inflamed brain. J Neurosci 2007; 27: 4957-4968.

Chowdhury SM, Hubbell JA. Adhesion prevention with ancrod released via a tissue-adherent hydrogel. J Surg Res 1996; 61: 58-64.

Combs CK, Karlo JC, Kao SC, Landreth GE. beta-Amyloid stimulation of microglia and monocytes results in TNFalpha-dependent expression of inducible nitric oxide synthase and neuronal apoptosis. J Neurosci 2001; 21: 1179-1188.

Conde JR, Streit WJ. Microglia in the aging brain. J Neuropathol Exp Neurol 2006; 65: 199-203.

D'Andrea MR. Evidence linking neuronal cell death to autoimmunity in Alzheimer's disease. Brain Res 2003; 982: 19-30.

D'Andrea MR. Evidence that immunoglobulin-positive neurons in Alzheimer's disease are dying via the classical antibody-dependent complement pathway. Am J Alzheimers Dis Other Demen 2005; 20: 144-150.

Dempfle CE, Argiriou S, Kucher K, Müller-Peltzer H, Rübsamen K, Heene DL. Analysis of fibrin formation and proteolysis during intravenous administration of ancrod. Blood 2000; 96: 2793-2802.

Dickstein DL, Biron KE, Ujiie M, Pfeifer CG, Jeffries AR, Jefferies WA. Abeta peptide immunization restores blood-brain barrier integrity in Alzheimer disease. FASEB J 2006; 20: 426-433.

Fiala M, Liu QN, Sayre J, Pop V, Brahmandam V, Graves MC, et al. Cyclooxygenase-2-positive macrophages infiltrate the Alzheimer's disease brain and damage the blood-brain barrier. Eur J Clin Invest 2002; 32: 360-371.

Flick MJ, Du X, Witte DP, Jirousková M, Soloviev DA, Busuttil SJ, et al. Leukocyte engagement of fibrin(ogen) via the integrin receptor alphaMbeta2/Mac-1 is critical for host inflammatory response in vivo. J Clin Invest 2004; 113: 1596-1606.

Floris S, Blezer EL, Schreibelt G, Dopp E, van der Pol SM, Schadee-Eestermans IL, et al. Blood-brain barrier permeability and monocyte infiltration in experimental allergic encephalomyelitis: a quantitative MRI study. Brain 2004; 127: 616-627.

Franciosi S, Ryu JK, Choi HB, Radov L, Kim SU, McLarnon JG. Broad-spectrum effects of 4-aminopyridine to modulate amyloid beta1-42-induced cell signaling and functional responses in human microglia. J Neurosci 2006; 26: 11652-11664.

Guo JP, Arai T, Miklossy J, McGeer PL. Abeta and tau form soluble complexes that may promote self aggregation of both into the insoluble forms observed in Alzheimer's disease. Proc Natl Acad Sci U S A 2006; 103: 1953-1958.

Insausti R, Tuñón T, Sobreviela T, Insausti AM, Gonzalo LM. The human entorhinal cortex: a cytoarchitectonic analysis. J Comp Neurol 1995; 355: 171-198.

Kwon EE, Prineas JW. Blood-brain barrier abnormalities in longstanding multiple sclerosis lesions. An immunohistochemical study. J Neuropathol Exp Neurol 1994; 53: 625-636.

Lip GY. Fibrinogen and cardiovascular disorders. QJM 1995; 88: 155-165.

Lip GY, Blann A. von Willebrand factor: a marker of endothelial dysfunction in vascular disorders? Cardiovasc Res 1997; 34: 255-265.

Lue LF, Rydel R, Brigham EF, Yang LB, Hampel H, Murphy GM Jr, et al. Inflammatory repertoire of Alzheimer's disease and nondemented elderly microglia in vitro. Glia 2001; 35: 72-79.

McLarnon JG, Ryu JK, Walker DG, Choi HB. Upregulated expression of purinergic P2X(7) receptor in Alzheimer disease and amyloid-beta peptide-treated microglia and in peptide-injected rat hippocampus. J Neuropathol Exp Neurol 2006; 65: 1090-1097.

Paul J, Strickland S, Melchor JP. Fibrin deposition accelerates neurovascular damage and neuroinflammation in mouse models of Alzheimer's disease. J Exp Med 2007; 204: 1999-2008.

Rogers J, Lue LF. Microglial chemotaxis, activation, and phagocytosis of amyloid beta-peptide as linked phenomena in Alzheimer's disease. Neurochem Int 2001; 39: 333-340.

Ryu JK, Franciosi S, Sattayaprasert P, Kim SU, McLarnon JG. Minocycline inhibits neuronal death and glial activation induced by beta-amyloid peptide in rat hippocampus. Glia 2004; 48: 85-90.

Ryu JK, McLarnon JG. Minocycline or iNOS inhibition block 3-nitrotyrosine increases and blood-brain barrier leakiness in amyloid beta-peptide-injected rat hippocampus. Exp Neurol 2006; 198: 552-557.

Ryu JK, McLarnon JG. Thalidomide inhibition of perturbed vasculature and glial-derived tumor necrosis factor-α in an animal model of inflamed Alzheimer's disease brain. Neurobiol Dis 2007; doi:10.1016/j.nbd.2007.08.019.

Ryu JK, Tran KC, McLarnon JG. Depletion of neutrophils reduces neuronal degeneration and inflammatory responses induced by quinolinic acid in vivo. Glia 2007; 55: 439-451.

Sun H, Ringdahl U, Homeister JW, Fay WP, Engleberg NC, Yang AY, et al. Plasminogen is a critical host pathogenicity factor for group A streptococcal infection. Science 2004; 305: 1283-1286.

Van Oijen M, Witteman JC, Hofman A, Koudstaal PJ, Breteler MB. Fibrinogen is associated with an increased risk of Alzheimer disease and vascular dementia. Stroke 2005; 36: 2637-2641.

Vos CM, Geurts JJ, Montagne L, van Haastert ES, Bö L, van der Valk P, et al. Blood-brain barrier alterations in both focal and diffuse abnormalities on postmortem MRI in multiple sclerosis. Neurobiol Dis 2005; 20: 953-960.

Walker DG, Lue LF, Beach TG. Gene expression profiling of amyloid beta peptide-stimulated human post-mortem brain microglia. Neurobiol Aging 2001; 22: 957-966.

Zipser BD, Johanson CE, Gonzalez L, Berzin TM, Tavares R, Hulette CM, et al. Microvascular injury and blood-brain barrier leakage in Alzheimer's disease. Neurobiol Aging 2007; 28: 977-986.

CHAPTER 5: MICROGLIAL VEGF RECEPTOR RESPONSE IS AN INTEGRAL CHEMOTACTIC COMPONENT IN ALZHEIMER'S DISEASE PATHOLOGY[4]

5.1 INTRODUCTION

Vascular endothelial growth factor (VEGF) is a potent stimulator for the development of new blood vessels (angiogenesis) (Leung et al., 1989) and concomitantly can increase vascular permeability in tissue (Ferrara et al., 1998; Bates et al., 1999). Three receptors have been found to transduce VEGF actions and have been designated, VEGF receptor-1 (Flt-1), VEGF receptor-2 (KDR/Flk-1) and VEGF receptor-3 (Flt-4) (Ferrara et al., 2003). Both the Flt-1 and KDR/Flk-1-type receptors are highly expressed by endothelial cells. In particular, a prominent role for KDR/Flk-1 as a mediator of endothelial proliferative responses and for formation of new blood vessels has been reported (Millauer et al., 1993). Some evidence has suggested that the Flt-1 subtype of VEGF receptor may serve a function in mediating chemotactic responses of immune responding cells. These studies have associated activation of Flt-1 with increased migration of monocyte/macrophage-type cells (Barleon et al., 1996; Forstreuter et al., 2002).

In addition to physiological roles in chemotaxis, the results from several studies have indicated that Flt-1-mediated signaling could contribute to pathological conditions in disease (Skold et al., 2005). Elevated VEGF expression has been documented in asthma (Hoshino et al., 2001) and sepsis (Yano et al., 2006) and eosinophil inflammatory responses are dependent on activation of Flt-1 (Feistritzer et al., 2004). In a model of rheumatoid arthritis (RA), blockade of Flt-1 was effective in reducing symptoms of disease whereas inhibition of the Flk-1 subtype of VEGF receptor was without effect (De Bandt, 2003). Recently, a number of pathological inflammatory responses have been found to be attenuated in Flt-1-deficient mice compared to their wild type cohorts in a murine model of RA (Murakami, 2006). It was concluded that enhanced inflammation in this disease was mediated by Flt-1-dependent signaling in activated monocytes/macrophages.

At present, functional roles for Flt-1 in neurodegenerative brain disease have not been addressed. Deposition of amyloid-beta peptide (Aβ) is considered a critical aspect in the induction of inflammatory responses and neuronal damage in AD brain (Combs et al., 2001;

---

[4]A version of this chapter has been submitted for publication. Ryu, J.K., Choi, H.B., Cho, T., Wang, Y.T. and McLarnon, J.G. Microglial VEGF receptor response is an integral chemotactic component in Alzheimer's disease pathology.

Hardy and Selkoe, 2002; Spires et al., 2005). An impetus for our study was the finding in this laboratory that intra-hippocampal injection of full-length peptide ($A\beta_{1-42}$) increased inflammatory reactivity and vascular remodeling with the latter indicating evidence for the formation of new blood vessels (angiogenesis) (Zand et al., 2004) and leakiness of blood-brain barrier (BBB) (Ryu et al., 2006). Furthermore, separate *in vivo* experiments have shown increased expression of VEGF, neovascularization and neurodegeneration in inflamed rat brain (Tran et al., 2005). Double staining analysis showed VEGF expression was primarily associated with microglia, the resident immune-responding cells of brain. Thus, our data indicate that activated microglia could act both as a source (paracrine signal) and as a responder (autocrine signal via Flt-1) to VEGF.

Overall, our findings suggested the possibility that Flt-1 and VEGF-dependent mobilization of microglia and cellular chemotactic responses could serve specific functions as a component of inflammatory reactivity. To test this premise we have used intra-hippocampal injection of $A\beta_{1-42}$ in rat brain and peptide stimulation of cultured human microglia and analyzed postmortem brain tissue and microglia obtained from Alzheimer's disease (AD) and non-demented (ND) individuals, to investigate expression and function of microglial Flt-1 in inflammatory conditions relevant to AD brain.

5.2 MATERIALS AND METHODS

5.2.1 Preparation of human ND and AD sections

Entorhinal cortical sections from six ND cases (ages from 40 to 85 years, postmortem intervals, 4-24 hr) and seven AD cases (ages from 67 to 87 years, postmortem intervals, 5-10 hr) were obtained from the Kinsmen Laboratory brain bank at the University of British Columbia (UBC, Vancouver, BC). All cases of AD met the clinical criteria and postmortem confirmation for AD.

5.2.2 Reverse transcription-PCR in microglia from human ND and AD brains

Adult human microglia from frontal neocortex of ND and AD brains were provided by Dr. Douglas G. Walker (Laboratory of Neuroinflammation, Sun Health Research Institute). In one set of experiments, expressions of Flt-1 and VEGF mRNA in microglia from ND (n = 8 cases) and AD brains (n = 6 cases) were examined. In another set of experiments, human microglia from ND samples (n = 4 individuals) were plated on 12 well multiplates and incubated in serum free medium for 48 hr (McLarnon et al., 2006; Ryu and McLarnon, 2007) prior to treatment with PBS or $A\beta_{1-42}$ (8 hr exposure to 5 μM peptide). Reverse transcription (RT)-PCR analysis was performed as described previously (McLarnon et al., 2006) using specific human primers for Flt-1, VEGF and GAPDH: human Flt-1 (sense primer, 5'-TGCCACCTCCATGTTTGATG-3' and antisense primer 5'- CAGCTGGAATGGCAGAAACTG-3'; 188 bp), human VEGF (sense primer, 5′-GCACCCATGGCAGAAGGAGG-3′ and antisense primer, 5′-CCTTGGTGAGGTTTGATCCGCATA-3′; 263 bp), and GAPDH (sense primer, 5'-CCATGTTCGTCATGGGTGTGAACCA-3' and antisense primer, 5'-GCCAGTAGAGGCAGGGATGATGTTC-3'; 251 bp).

5.2.3 Immunohistochemical staining and analysis in human ND and AD sections

For single immunofluorescent staining (Arai et al., 2006), free-floating sections (30 μm) from ND and AD tissues were incubated for 48 hr at 4°C with anti-human vascular endothelial growth factor receptor-1 (Flt-1, 1:200; R&D systems) or anti-VEGF (1:200; Santa Cruz Biotechnology) antibody. Sections were then incubated with Alexa Fluor 488-conjugated secondary antibody (1:200; Invitrogen Canada Inc) for 1 hr at room temperature. For double immunofluorescent staining (Guo et al., 2006), free-floating sections were incubated for 48 hr at 4°C with a mixture of two primary antibodies: anti-Flt-1 (1:100; R&D systems) in combination

with anti-HLA-DR (1:500; DakoCytomation) or anti-β-amyloid (Aβ, clone 6F/3D, 1:100; DakoCytomation) and anti-VEGF (1:100; Santa Cruz Biotechnology) in combination with anti-HLA-DR or anti-β-amyloid. For Aβ staining, 100% formic acid (Sigma) pre-treatment for 15 min at room temperature (RT) was performed before primary antibody incubation. After incubation with the indicated primary antibodies, sections were incubated for 1 hr at room temperature with a mixture of Alexa Fluor 488/594-conjugated secondary antibody (1:200; Invitrogen) For immunostaining control, sections were stained following the same procedure, but with omission of the primary antibody.

Images from five nonoverlapping random fields of superficial layers (layer II and III) in the entorhinal cortex (defined by Insausti et al., 1995) were then collected using a Zeiss Axioplan-2 fluorescence microscope equipped with a DVC camera (Diagnostic Instruments) at 200× magnification under a constant predefined exposure setting. The digitized images were then analyzed using Northern Eclipse software (Empix Imaging). The number of pixels per image with an intensity above a pre-determined threshold level was quantified to measure the areas occupied by Flt-1 and VEGF. To analyze HLA-DR (+)ve microglia expressing Flt-1 and VEGF in ND/AD brains, double immunostained images were used for measuring the number of merged cells. All quantitative analyses were performed in a blind manner.

5.2.4 Surgical procedures

All animal procedures were approved by the University of British Columbia Animal Care Ethics Committee, with adherence to guidelines of the Canadian Council on Animal Care. Male Sprague-Dawley rats weighing 280-300 g (Charles River Laboratories) were used for stereotaxic injection of $A\beta_{1-42}$, or controls (PBS and reverse peptide $A\beta_{42-1}$) as previously described (Franciosi et al., 2006; Ryu and McLarnon, 2006, 2007). In brief, animals received intraperitoneal (i.p.) injection of an anesthetic mixture (ketamine hydrochloride 100 mg/kg and xylazine hydrochloride 10 mg/kg) and were placed in a stereotaxic apparatus (David Kopf Instruments). Beta-amyloid (Aβ) peptide (2 nmol; California Peptides, Napa, CA) was stereotaxically injected into the dentate gyrus (anteroposterior (AP), -3.3 mm; mediolateral (ML), -1.6 mm; dorsoventral (DV), -3.2 mm) or CA1 layer (AP, -3.3 mm; ML, -1.8 mm; DV, -2.6 mm) of hippocampus. For the inhibition of Flt-1, the neutralizing monoclonal antibody against Flt-1 (R&D Systems) (Feistritzer C, et al., 2004; Ambati et al., 2006) was co-

administered at 10 μg with peptides into CA1 layer. Control animals were injected with control antibody rat IgG.

5.2.5 Immunohistochemical staining and analysis of rat brain

Specific protocols for coronal section (40 μm) preparation and immunohistochemical staining followed published procedures (Ryu et al., 2006, 2007). Briefly, free-floating sections were incubated for 48 hr at 4°C with the following primary antibody: anti-Flt-1 (1:200; Santa Cruz Biotechnology), anti-neuronal nuclei (NeuN, 1:1000; Chemicon), and anti-ionized calcium binding adapter molecule 1 (Iba-1, 1:500; Wako Chemicals). Sections were then incubated with Alexa Fluor 488/594-conjugated secondary antibody (1:200; Molecular Probes) at room temperature for 1 hr. To detect the Flt-1 expressing cell tyes in Aβ-injected hippocampus, sections were incubated for 48 hr at 4°C with anti-Flt-1, in combination with anti-glial fibrillary acidic protein (GFAP, 1:1000; Sigma) or anti-CR3R (OX-42, 1:500; Serotec) as described previously (Choi et al., 2007). The number of Flt-1 or OX-42/GFAP+Flt-1 (+)ve cells in the superior blade of the dentate granule cell layer or Iba-1 or NeuN (+)ve cells in the CA1 region was determined at three equally spaced hippocampal sections, as described (Ryu et al., 2004; Ryu and McLarnon, 2007). To keep the consistency between the selected sections, a rectangular box (0.4 x 0.3 mm) was centered over the CA1 cell layer beginning 1.6 mm lateral to the midline in each image as previously described (Choi et al., 2005; Casolini et al., 2007).

5.2.6 Reverse transcription-PCR in peptide-injected rat hippocampus

Rat brain tissue samples (1, 3, and 7 d post-peptide injection) were also used for RT-PCR analysis using rat specific primers for Flt-1 and β-actin as described previously (Choi et al., 2007). The sequences and expected product sizes of the PCR primers were as follows: rat Flt-1 (sense primer, 5′-TTCCGGACTTTCAACACCTC-3′ and antisense primer, 5′-CCGAATAGCGAGCAGATTTC-3′; 198 bp) and rat β-actin (sense primer, 5′-GTGGGGCGCCCCAGGCACCA-3′ and antisense primer, 5′-GTCCTTAATGTCACGCACGATTTC-3′; 526 bp).

5.2.7 *In Vivo* chemotaxis assay of rat microglia

An enhanced green fluorescent protein (EGFP)-lentivirus construct was generated by transfecting HEK 293T cells with three plasmids: the transfer plasmid pHR'-CMV-EGFP, the packaging plasmid PR8-2, and the envelop plasmid PVSVG. The lentivirus was then generated and concentrated, as described previously (Skarsqard et al., 2005). Rat cultured microglia were prepared from embryonic day-14 Sprague-Dawley rats (Aarum et al., 2003) and infected with lentivirus (with 3-fold higher titers of lentivirus than the seeded microglial cell density). Three days after lentiviral infection, immunostaining of EGFP-labeled microglia were performed with a mixture of primary antibodies: anti-Iba-1 (1:1000; Wako) and anti-enhanced green fluorescent protein (EGFP, 1:200; Invitrogen). Before transplantation, EGFP-labeled microglia were incubated with anti-Flt-1 Ab or control Ab (10 μg, R&D Systems) for 30 min. Stereotaxic cell transplantation was performed as described (Ryu et al., 2004). Cells (2 ul, 1 x 10^5 cells per μl) were transplanted (at 0.5 μl/min) under anesthesia, 3 d after $A\beta_{1-42}$ injection (2 nmol, CA1) into the medial corpus callosum at the following coordinates (AP, -3.3; ML, 0.0; DV, -2.8). Animals were perfused at 7 d post-cell transplantation and double immunohistochemical procedures were performed with primary Ab: anti-EGFP (1:500, Invitrogen) or anti-EGFP in combination with anti-VEGF (1:200, Santa Cruz Biotechnology) or anti-Flt-1 (1:200, Santa Cruz Biotechnology). For quantifications of transplanted EGFP-labeled migrated microglia on the corpus callosum to the side of transplantation, we counted the number of EGFP (+)ve microglia within a rectangle (0.3 x 0.2 mm) on the three different regions (600, 1200, and 1800 μm away from the transplantation site). All quantitative analyses were performed in a blinded manner.

5.2.8 *In Vitro* chemotaxis assay of human microglia

The migration of human microglia *in vitro* was determined using Transwell™ inserts (pore size, 8 μm, Becton Dickinson Labware) and 24-well culture plates (Corning Costar) as previously described (Aarum et al., 2003). Cell-free conditioned medium was collected from microglial cultures stimulated with PBS, $A\beta_{1-42}$ (5 μM), or $A\beta_{42-1}$ (5 μM) for 24 hr and placed in a lower chamber. Human microglia were placed in an upper chamber in serum-free medium and treated (1 hr at 37°C) with anti-Flt-1 neutralizing antibody or control IgG (10 μg/ml, R&D Systems). The transwell plates were incubated for 24 hr at 37°C. Human microglial migration was quantified by counting the number of cells that migrated through the membrane to the lower chamber using an inverted bright-field microscope (Five fields/each well).

5.2.9 Statistical analysis

Results are presented as mean ± SEM. The statistical analysis was performed using a one-way analysis of variance, followed by the Student-Newman-Keuls multiple comparison test or Student's *t* test (GraphPad Prism 3.0; Graph Pad, San Diego, CA) with the significance level set at $p < 0.05$.

5.3 RESULTS

5.3.1 Expression of Flt-1 and VEGF in microglia and brain tissue from ND and AD individuals

An initial aspect of this work was the characterization of expressions of Flt-1, and its ligand VEGF, in microglia and in brain sections obtained from ND and AD individuals. Human microglia obtained from ND and AD tissues were initially analyzed for levels of Flt-1 and VEGF. Representative RT-PCR showed little or no expression of either receptor or ligand in human ND microglia (Fig. 5-1A), however, AD microglia demonstrated markedly increased levels of both factors. Semi-quantification of data is shown in Fig. 5-1A. In total (n = 8 ND cases, n = 6 AD cases), Flt-1 was increased 2.2-fold and VEGF was increased 7.2-fold in AD, compared with ND, human microglia.

We next examined effects of $A\beta_{1-42}$ stimulation of human ND microglia. As shown in Fig. 5-1B, low levels of Flt-1 and VEGF were evident in PBS control with a marked increase for both ligand and receptor induced by peptide stimulation (5 μM for 8 hr). Semi-quantitative analysis is presented in Fig. 5-1B with overall (n = 4 independent samples/group) mRNA levels increased by 2.3-fold (for Flt-1) and by 8-fold (for VEGF) with peptide, compared to control, treatment.

5.3.2 Immunohistochemical staining of Flt-1 and VEGF with microglia in ND and AD brian

We next investigated for association between the VEGF receptor and VEGF itself with microgliosis in ND and AD sections. Representative immunohistochemical staining showed minimal levels of either Flt-1 (upper left panel, Fig. 5-1C) or VEGF (upper left panel, Fig. 5-1D) in ND sections. However, both receptor (lower left panel, Fig. 5-1C) and ligand (lower left panel, Fig. 5-1D) were highly expressed in AD brain sections.

Representative double staining for HLA-DR (+)ve microglia with Flt-1 and VEGF are presented (right panels, Fig. 5-1C and D, respectively), for ND and AD tissue. Both Flt-1 and VEGF showed little merged staining with microglia in ND sections. However, AD brain tissue demonstrated marked levels of association of Flt-1/HLA-DR (lower right panel, Fig. 5-1C) and VEGF/HLA-DR (lower right panel, Fig. 5-1D) in tissue obtained from AD individuals.

Single staining analysis was used to quantify levels of Flt-1 and VEGF and double staining to quantify association of these factors with microglia. (n = 6 ND cases, 7 AD cases). The area

Figure 5-1. Expression of Flt-1 and VEGF in human ND/AD microglia, *in vitro* and in ND/AD tissue. (A) Typical RT-PCR for Flt-1 and VEGF expressions in microglia obtained from ND and AD brain tissue. The bar graphs show semi-quantitative results for relative levels of mRNA for Flt-1 and VEGF from 8 ND and 6 AD individuals. *, $p < 0.05$. (B) Representative expressions of Flt-1 and VEGF in human ND microglia treated with PBS or $A\beta_{1\text{-}42}$ (5 μM for 8 hr). The bar graph presents overall semi-quantitative results for the two factors (n = 4 independent samples/group) *, $p < 0.05$. (C) Marker immunoreactivities (ir) from ND tissue and AD tissue showing representative single staining for Flt-1 and double staining of Flt-1/HLA-DR. Areas of merged double staining are yellow. Scale bar: 150 μm (left panels) and 50 μm (right panels). Overall ir (n = 6 cases from ND, 7 cases from AD) for Flt-1 and numbers of Flt-1 (+)ve microglia. (D) Representative results showing single staining for VEGF and double staining for VEGF/HLA-DR in ND and AD tissue. Scale bar: 150 μm (left panels) and 50 μm (right panels). Quantification (n = 6 cases from ND, 7 cases from AD) of VEGF ir and numbers of VEGF (+)ve microglia. *, $p < 0.05$.

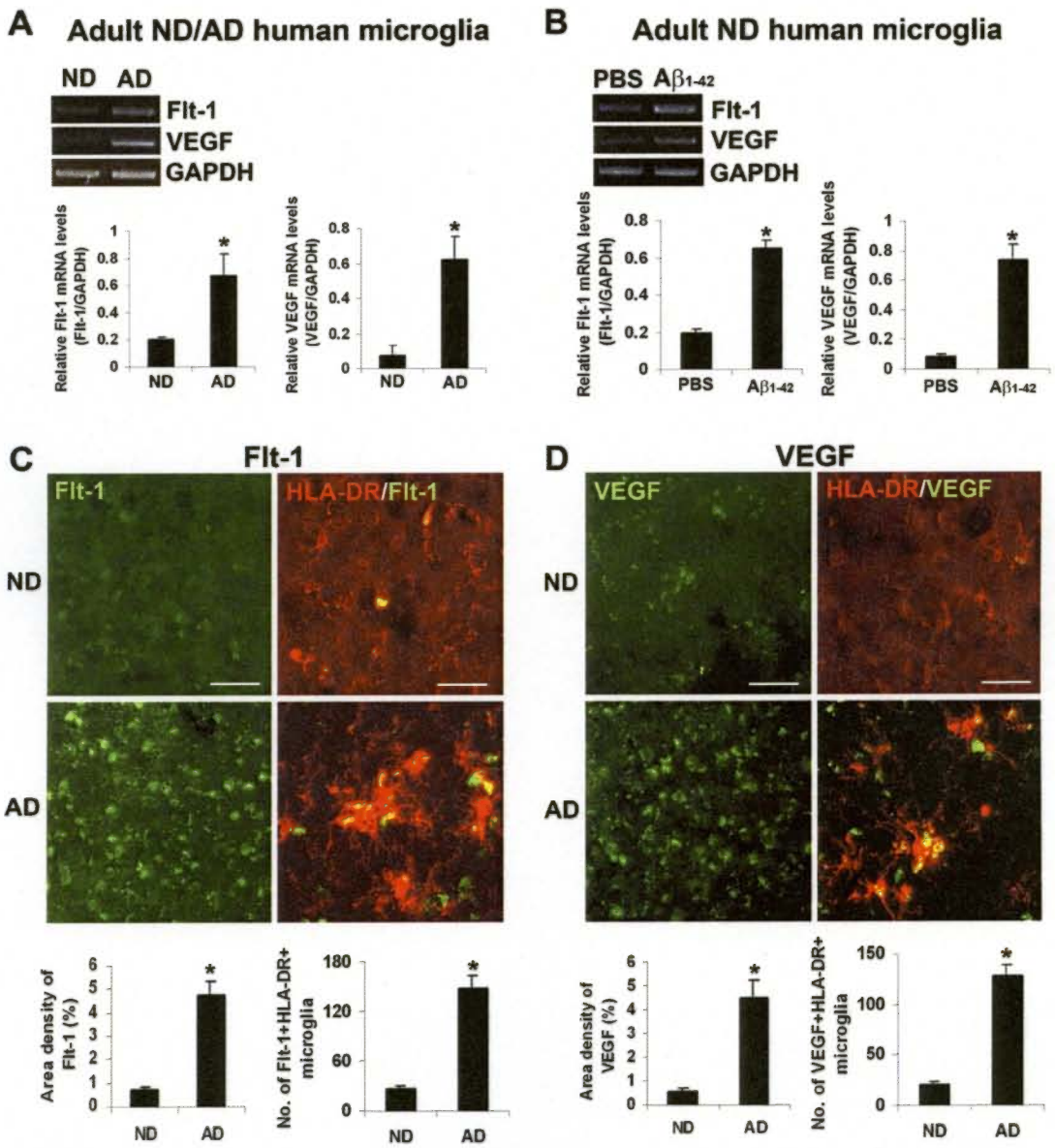
A
Adult ND/AD human microglia
ND AD
Flt-1
VEGF
GAPDH
Relative Flt-1 mRNA levels (Flt-1/GAPDH)
Relative VEGF mRNA levels (VEGF/GAPDH)
B
Adult ND human microglia
PBS Aβ1-42
C
Flt-1
Flt-1
HLA-DR/Flt-1
Area density of Flt-1 (%)
No. of Flt-1+HLA-DR+ microglia
D
VEGF
VEGF
HLA-DR/VEGF
Area density of VEGF (%)
No. of VEGF+HLA-DR+ microglia

density of Flt-1 ir was significantly increased by 5.4-fold in AD, relative to ND, tissue (lower left graph, Fig. 5-1C). A similar magnitude of increase (by 4.6-fold) was measured for the number of microglia expressing Flt-1 (lower right graph, Fig. 5-1C) in AD vs ND tissue. The area density of VEGF was increased 7-fold in AD, compared with ND, brain tissue (lower left graph, Fig. 5-1D). The corresponding increase in the number of microglia associated with VEGF was 5.2-fold in AD vs ND sections (lower right graph, Fig. 5-1D).

5.3.3 Double staining of Flt-1 and VEGF with β-amyloid in AD brain tissue

A relevant question was the possible association of Flt-1 and VEGF with peptide deposition. This point was addressed using immunohistochemical staining to determine localization of receptor and ligand with Aβ in AD brain sections. Representative staining for Flt-1 and VEGF is presented at low magnification in AD sections (upper panels, Fig. 5-2). The insets show respective double staining analysis for Flt-1/peptide (lower left panel) and VEGF/peptide (lower right panel). Although quantification of associated staining was not attempted, we observed numerous examples of Flt-1 in association with peptide whereas VEGF exhibited a lower frequency of localization with peptide. Overall, we would estimate that in excess of 75% of Flt-1 ir and about 50% of VEGF ir was associated with peptide in AD brain tissue.

5.3.4 Time-dependency of Flt-1 expression *in vivo*

We initially used RT-PCR to determine time-dependent changes in VEGF receptor-1 (Flt-1) expression following intra-hippocampal injection of $A\beta_{1-42}$. Representative results indicated controls (7 d injections with PBS or reverse peptide $A\beta_{42-1}$) to exhibit minimal levels of the VEGF receptor-1 (Fig. 5-3A). However, $A\beta_{1-42}$ injection was associated with elevated Flt-1, relative to controls, at 1 and 3 d post-peptide with a further increase at a duration of 7 d. Semi-quantitative RT-PCR is presented in the right bar graph of Fig. 5-3A (n = 5 animals/group). Expression of Flt-1 was significantly higher (by 2-fold at 1 d and 1.8-fold at 3 d) for peptide vs PBS control (7 d) injections. The corresponding increase for the longest duration of $A\beta_{1-42}$ injection (7 d) was a 3.7-fold increase in Flt-1 with peptide compared with PBS.

We also employed immunohistochemical staining to examine changes in Flt-1 with duration of peptide injection (1-7 d). Representative staining for controls (7 d injections of either PBS or $A\beta_{42-1}$) demonstrated little or no immunoreactivity (ir) for Flt-1 (upper left and middle panels,

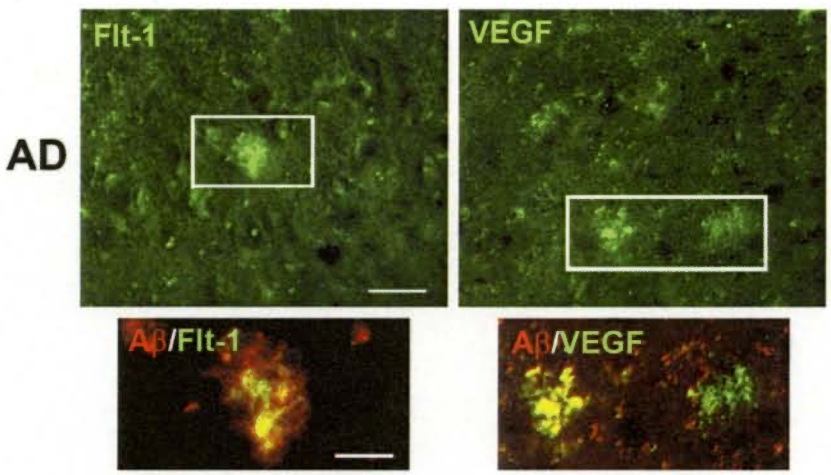

Figure 5-2. Association of Flt-1 and VEGF with beta-amyloid peptide in AD tissue. The top panels show representative Flt-1 ir (left panel) and VEGF ir (right panel) in AD brain tissue: Scale bar 150 µm. The lower panels illustrate higher magnification of double staining for Flt-1/β-amyloid (upper left panel) and VEGF/β-amyloid (upper right panel). Scale bar denotes 25 µm.

Figure 5-3. Time dependency and cellular association of Flt-1 expression in $A\beta_{1-42}$-injected rat hippocampus. (A) Representative Flt-1 mRNA expression following hippocampal injections with controls (PBS and $A\beta_{42-1}$ (7 d)) and $A\beta_{1-42}$ (1, 3, and 7 d). β-actin was used as a reaction standard. The bar graphs show semi-quantitative RT-PCR results for relative levels of Flt-1 mRNA expression (n = 5 animals/group). *p< 0.05 vs. PBS. (B) Representative Flt-1 immunoreactivity following hippocampal injection with PBS (7 d), reverse peptide $A\beta_{42-1}$ (7 d) and $A\beta_{1-42}$ (1, 3, and 7 d). Scale bar: 50 µm. The bar graph shows number of Flt-1 (+)ve cells for PBS and $A\beta_{42-1}$ controls (7 d) and the time-dependence of Flt-1 expression for the different times of peptide injections (n = 6 animals/group). *, p< 0.05 vs. PBS. (C) Double staining for astrocytes (GFAP marker) and microglia (OX-42 marker) following 7 d injections of PBS and for $A\beta_{1-42}$. Representative staining patterns are for Flt-1/GFAP and Flt-1/OX-42. Scale bar: 30 µm. Quantification of number of Flt-1 (+)ve cells for the different markers in PBS and peptide-injected brain (n = 6 animals/group). *, p< 0.05 vs. PBS; # for comparison of OX-42 vs. GFAP marker.

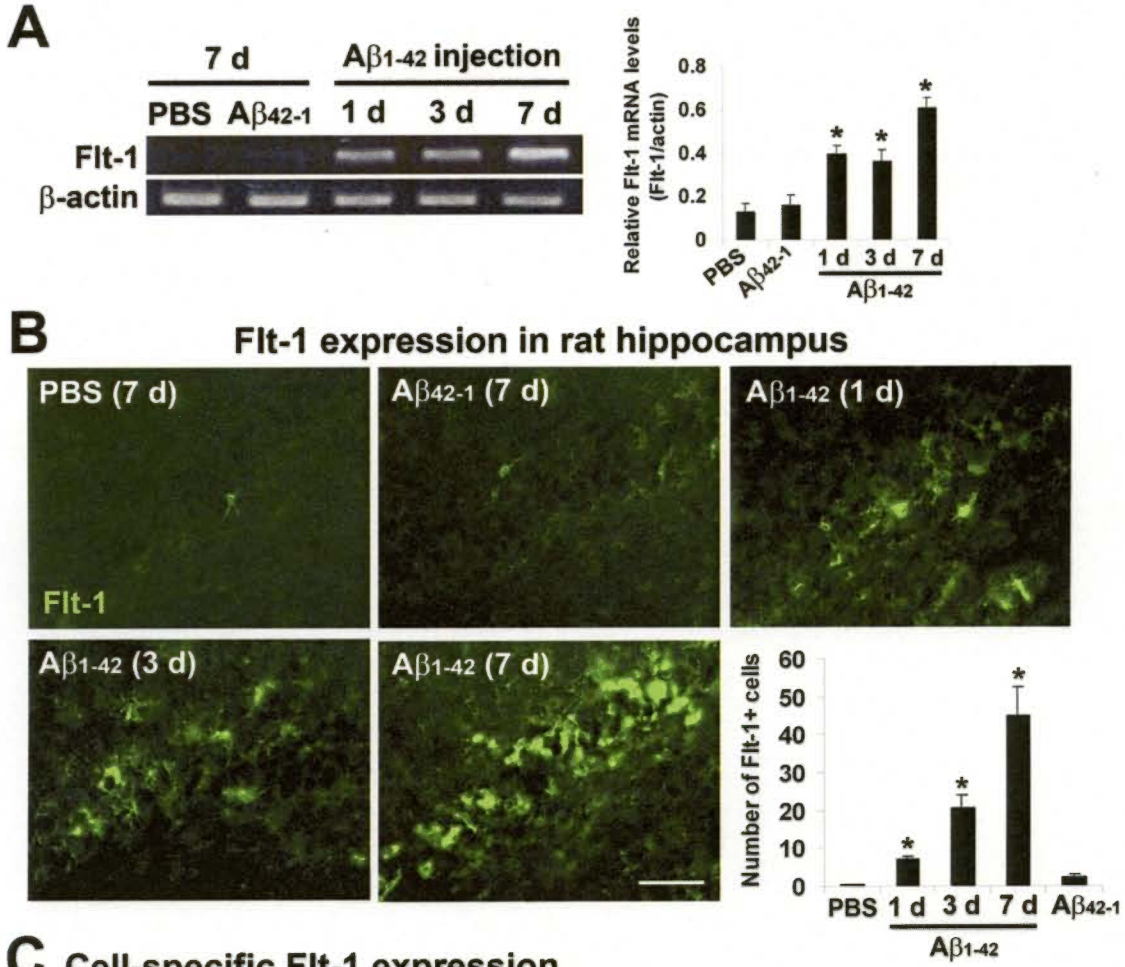
A
7 d
Aβ1-42 injection
PBS
Aβ42-1
1 d
3 d
7 d
Flt-1
β-actin
Relative Flt-1 mRNA levels (Flt-1/actin)
0.8
0.6
0.4
0.2
0
PBS
Aβ42-1
1 d
3 d
7 d
Aβ1-42
B
Flt-1 expression in rat hippocampus
PBS (7 d)
Flt-1
Aβ42-1 (7 d)
Aβ1-42 (1 d)
Aβ1-42 (3 d)
Aβ1-42 (7 d)
Number of Flt-1+ cells
60
50
40
30
20
10
0
PBS
1 d
3 d
7 d
Aβ42-1
Aβ1-42
C
Cell-specific Flt-1 expression
PBS (7 d)
GFAP/Flt-1
PBS (7 d)
OX-42/Flt-1
Aβ1-42 (7 d)
GFAP/Flt-1
Aβ1-42 (7 d)
OX-42/Flt-1
Number of Flt-1+ cells
50
40
30
20
10
0
GFAP
OX-42
GFAP
OX-42
PBS
Aβ1-42

Fig. 5-3B). However, $A\beta_{1-42}$ injection caused a progressive time-dependent increase in levels of Flt-1 (upper right and lower panels, Fig. 5-3B). Overall (n = 6 animals/group), significant increases in Flt-1 were determined at 1 d, 3 d and 7 d post-peptide injections (by 3-fold, 11-fold and 25-fold, respectively, relative to PBS 7 d injection) (lower right bar graph, Fig. 5-3B). These results are consistent with RT-PCR data with the exception that immunostaining analysis showed progressive increases in Flt-1 at early times after peptide injection.

5.3.5 Cell-dependent expressions of Flt-1

We next used double staining to examine the specific cells expressing Flt-1. These experiments were carried out at a single time point of 7 d post-$A\beta_{1-42}$ injection and used GFAP and OX-42 as respective markers for astrocytes and microglia. The results (Fig. 5-3C) showed minimal Flt-1/GFAP double staining in PBS control (upper left panel) with an elevated astrocyte expression of Flt-1 marker in peptide-injected brain (lower left panel) primarily due to the increase in Flt-1 ir. In a similar manner, low levels of merged Flt-1/OX-42 staining were evident in PBS control (upper right panel, Fig. 5-3C). However, peptide-injected hippocampus demonstrated a considerable proportion of microglia in association with the Flt-1 (lower right panel). Quantification of data is presented in the right bar graph of Fig. 5-3C (n = 6 animals/group). Low levels of Flt-1 ir were associated with GFAP (+)ve astrocytes or OX-42 (+)ve microglia in PBS control. However, following peptide injection GFAP/Flt-1 ir was increased by 5.2-fold and OX-42/Flt-1 ir was increased by 14.5-fold, relative to controls. Both increases were significant, however, association of Flt-1 was significantly higher with microglia compared with astrocytes.

5.3.6 Effects of anti-Flt-1 Ab on microglial responses and neuronal viability

The findings of marked increases of Flt-1 levels in microglia induced by peptide prompted investigation on effects of receptor modulation on microgliosis. Additionally, since $A\beta_{1-42}$ injection leads to a loss of hippocampal neurons (Ryu et al., 2004, 2006; Ryu and McLarnon, 2007), we also examined inhibition of Flt-1 as a putative neuroprotective strategy. These experiments employed an anti-Flt-1 neutralizing antibody (anti-Flt-1 Ab) in conjunction with Iba-1 (microglial marker) and NeuN (neuronal marker) in $A\beta_{1-42}$-injected (7 d) rat brain.

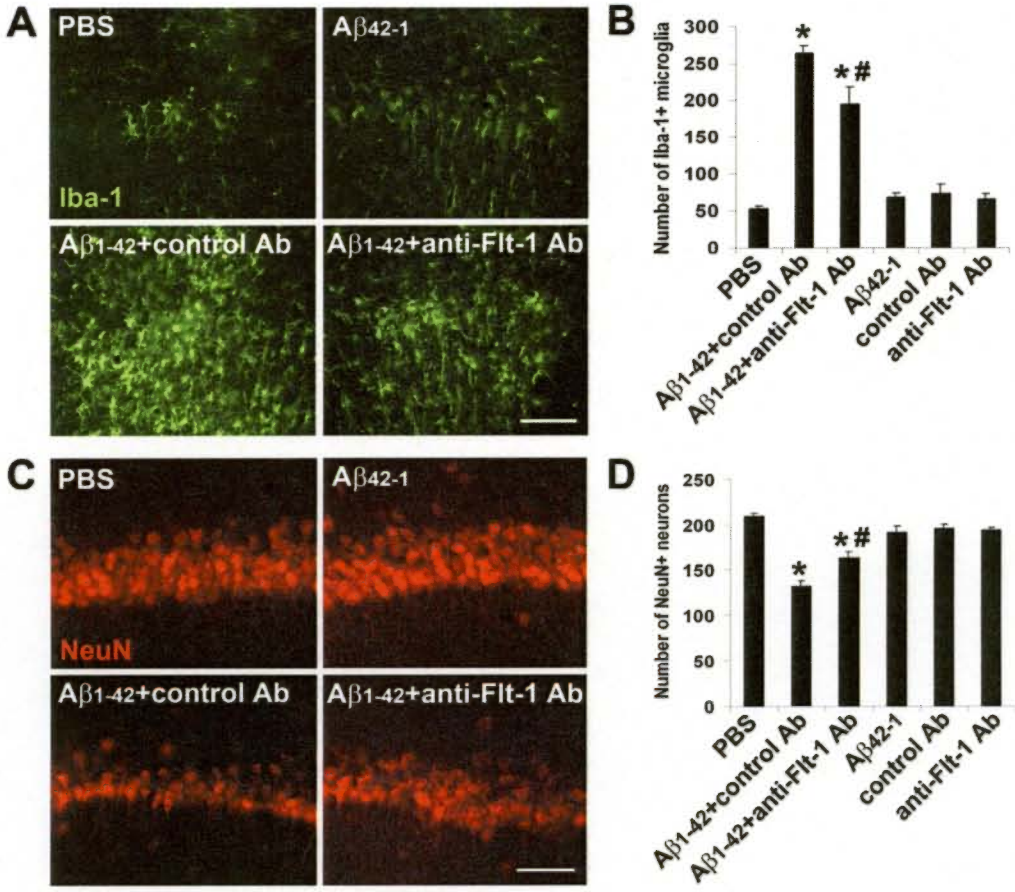

Figure 5-4. Effects of anti-Flt-1 antibody (Ab) on Iba-1 (microglial marker) and NeuN expression *in vivo*. (A) Representative Iba-1 immunoreactivity (ir) following 7 d intra-hippocampal injection for the following: PBS, $A\beta_{42-1}$, $A\beta_{1-42}$ plus control Ab and $A\beta_{1-42}$ plus anti-Flt-1 Ab. Scale bar: 50 µm. (B) Numbers of Iba-1 (+)ve microglia for the different injections (n = 6 animals/group). *, $p< 0.05$ for comparison of PBS vs. $A\beta_{1-42}$ and # for comparison of $A\beta_{1-42}$ plus control Ab vs. $A\beta_{1-42}$ plus anti-Flt-1 Ab. (C) Representative NeuN ir with 7 d injections for PBS, $A\beta_{42-1}$, $A\beta_{1-42}$ plus control Ab, and $A\beta_{1-42}$ plus anti-Flt-1 Ab. Scale bar: 50 µm. (D) Numbers of NeuN cells for the different injections (n = 6 animals/group). *, $p < 0.05$ for PBS vs. $A\beta_{1-42}$; #, $p < 0.05$ for $A\beta_{1-42}$ vs. $A\beta_{1-42}$ plus anti-Flt-1 Ab.

Representative microglial ir (upper panels, Fig. 5-4A) indicated relatively low levels of cell staining in controls (7 d injections of PBS or reverse $A\beta_{42-1}$). However, the $A\beta_{1-42}$ -injected hippocampus demonstrated a diffuse and high level of Iba-1 staining (lower left panel) which was reduced in the presence of anti-Flt-1 Ab with peptide (lower right panel). Overall (n = 6 animals/group), the number of Iba-1 (+)ve microglia was increased 4-fold in $A\beta_{1-42}$, compared to PBS, injected animals (Fig. 5-4B). Treatment with anti-Flt-1 Ab significantly reduced microgliosis (by 26%) compared with $A\beta_{1-42}$ injection alone (Fig. 5-4B).

Representative NeuN ir indicated an intact layer of CA1 pyrimidal neurons in controls (PBS or $A\beta_{42-1}$) (Fig. 5-4C, upper panels). The number of NeuN (+)ve cells was markedly diminished following $A\beta_{1-42}$ injection (lower left panel). However, if anti-Flt-1 Ab treatment was applied to peptide-injected animals, numbers of NeuN (+)ve neurons were increased (lower right panel). Overall (n = 6 animals/group), the number of hippocampal neurons was reduced by 37% with $A\beta_{1-42}$, compared to PBS, injection (Fig. 5-4D). Application of anti-Flt-1 Ab was effective in conferring neuroprotection whereby numbers of neurons were significantly increased (by 23%) compared to control Ab injection (Fig. 5-4D).

5.3.7 Microglial chemotactic responses *in vitro*

The up-regulation of Flt-1 in the peptide-injected hippocampus (Fig. 5-3A,B) and association with OX-42 (+)ve cells (Fig. 5-3C) could reflect chemotactic responses of microglia. Experiments were designed to examine this possibility *in vitro* and *in vivo*. A schematic diagram (Fig. 5-5A) indicates the method used to measure *in vitro* migration of human microglia. Microglial cells were initially subjected to 24 hr exposure for the following treatments; PBS, $A\beta_{1-42}$, and reverse peptide $A\beta_{42-1}$. Supernatants from the treated microglia were then applied to a transwell chamber (lower chamber) for the measurement of migration. Microglia in the upper chamber were preincubated with control Ab or with anti-Flt-1 Ab (10 μg/ml for 1 hr), prior to the chemotactic assay. The bar graph in Fig. 5-5B summarizes the results from n = 5 experiments. Microglial chemotaxis increased 4-fold with $A\beta_{1-42}$ treatment, relative to PBS control. Inclusion of anti-Flt-1 Ab with $A\beta_{1-42}$ peptide, significantly diminished microglial mobility by 37% compared to the application of peptide alone. Numbers of migrating microglia were similar for controls and for anti-Flt-1 Ab applied alone.

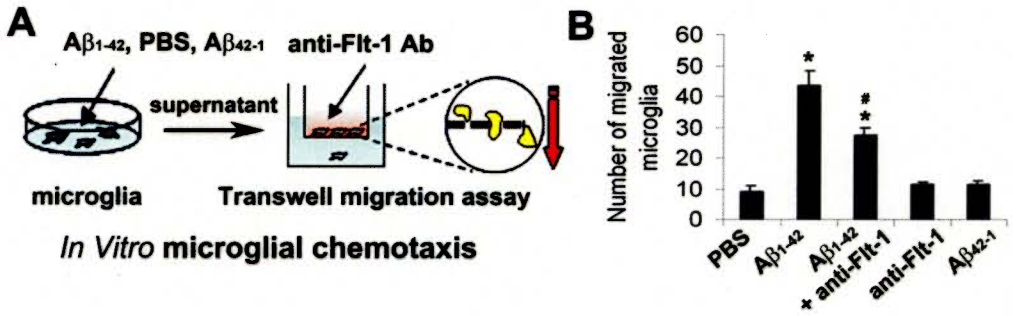

Figure 5-5. Migration of human microglia, *in vitro*. (A) Schematic diagram for the treatment of microglia with PBS, $A\beta_{1\text{-}42}$, or $A\beta_{42\text{-}1}$ and supernatant application, in the absence and presence of anti-Flt-1 Ab, in the transwell microglial migration assay. (B) The bar graph shows the number of migrating microglia with the different treatments and the effects of anti-Flt-1 Ab on migration (n = 5 samples/group). * denotes $p < 0.05$ for peptide vs. PBS treatment, and # denotes $p < 0.05$ for effects of anti-Flt-1 Ab on migration with peptide application.

5.3.8 Microglial chemotactic responses *in vivo*

To examine chemotactic responses *in vivo*, we used the procedures schematically diagrammed in Fig. 5-6A (upper panel). Rat microglia were first isolated from rat brain and then infected with a lentivirus-expressing enhanced green fluorescent protein (EGFP). Fig. 5-6A (lower panels) shows representative *in vitro* double staining (EGFP and Iba-1) for the cells prior to injection; co-localization of EGFP with the microglial marker Iba-1 was evident for all cells examined. The EGFP-microglia were incubated with control or anti-Flt-1 Ab (10 μg/ml for 30 min) and then stereotaxically injected into $A\beta_{1-42}$-injected rat brain (at 3 d post-peptide injection) at the location shown (denoted *). Three areas were designated for the counting of EGFP-microglia (labeled 1 to 3 in Fig. 5-6A), at sites between injected EGFP-microglia and peptide.

The number of EGFP (+)ve microglia in the different areas were measured in three groups of animals; $A\beta_{1-42}$ plus microglia incubated with control Ab; $A\beta_{1-42}$ plus microglia incubated with anti-Flt-1 Ab or reverse peptide $A\beta_{42-1}$ plus microglia incubated with control Ab. Animals receiving reverse peptide injection (upper panel, Fig. 5-6B) showed high levels of EGFP-microglia in area 1 adjacent to transplantation site but minimal migration of cells to areas 2 or 3 nearer to peptide. Representative immunostaining showed a different pattern of chemotaxis with $A\beta_{1-42}$ injection (middle panel, Fig. 5-6B) whereby considerable levels of EGFP (+)ve microglia were evident in both areas 2 and 3. Animals receiving anti-Flt-1 Ab with peptide (lower panel, Fig. 5-6B) exhibited similar levels of EGFP ir in area 1 as for the other treatments. However, anti-Flt-1 Ab was effective in decreasing numbers of migrating microglia in areas more proximal to peptide, compared to animals receiving control antibody treatment.

The quantification for *in vivo* chemotaxis of EGFP (+)ve microglia is presented in Fig. 5-6C. Overall (n = 6 animals/group), no differences in numbers of EGFP (+)ve microglia were measured in area 1 for the different treatments. In area 2, anti-Flt-1 Ab treatment significantly reduced the number of EGFP (+)ve cells (by 57%) relative to peptide-injection. The corresponding decrease in area 3 was 87%, representing a significant reduction by anti-Flt-1 Ab in the migration of EGFP-labelled microglia induced by peptide stimulation.

Double immunostaining of the EGFP-microglia-injected hippocampus was also examined to determine association between injected cells and markers for Flt-1 and VEGF. Representative double staining for EGFP (+)ve microglia and Flt-1 are shown in the left panels of Fig. 5-6D, with merged staining indicating considerable regions of overlap of the markers. Similarly, the association of VEGF with EGFP (+)ve microglia was also demonstrated (right panels, Fig. 5-6D).

Overall, we estimate that in excess of 90% of EGFP-microglia exhibited expression of Flt-1 and VEGF.

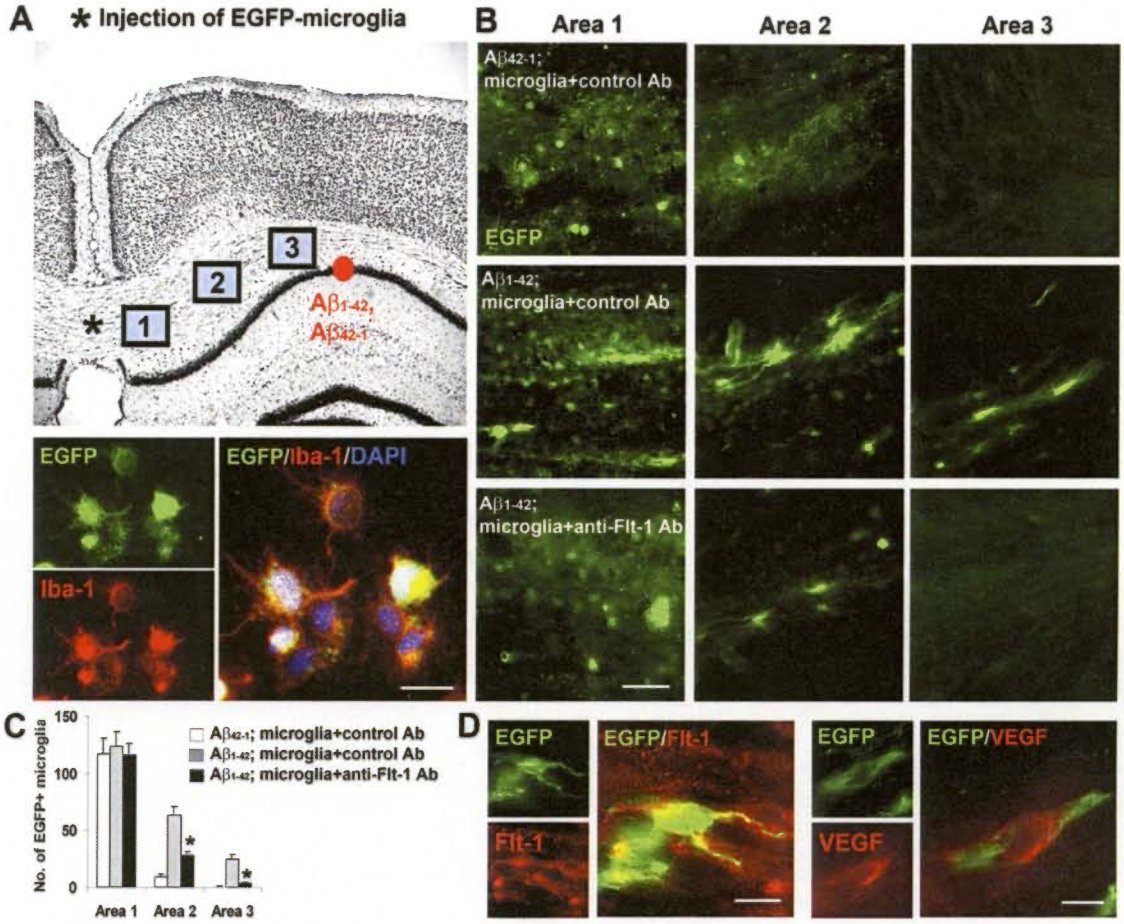

Figure 5-6. Chemotactic responses of EGFP-labeled microglia, *in vivo*. (A) upper panel, schematic diagram showing *in vivo* locations of EGFP-labeled microglial transplantation (*) and $A\beta_{1-42}$ or reverse peptide injection (red circle). The three areas chosen for the analysis of EGFP cell migration are shown (refer to text). Lower panels show representative double staining for EGFP (upper left panel) and for Iba-1 (lower left panel), and merged staining for both markers (right panel). Scale bar: 20 µm. (B) Representative EGFP microglial staining in the three areas for: $A\beta_{42-1}$ plus microglia incubated with control Ab (upper panels), $A\beta_{1-42}$ plus microglia incubated with control Ab (middle panels) and $A\beta_{1-42}$ plus microglia incubated with anti-Flt-1 Ab (lower panels). Scale bar: 50 µm. (C) The bar graph shows the numbers of EGFP-labeled microglia in areas 1 to 3, for the three protocols (n = 6 animals/group). * denotes $p < 0.05$ for the effects of anti-Flt-1 Ab on microglial chemotaxis in peptide-injected hippocampus. (D) Representative single and double staining for EGFP/Flt-1 (left panels) and for EGFP/VEGF (right panels). Scale bar: 20 µm.

5.4 DISCUSSION

Chronic inflammation is integral to AD pathology, however, specific mechanisms underlying inflammatory responses are not well understood (Mrak and Griffin, 2007). A critical and early component of inflammatory response is an increased microglial mobility and chemotactic activity to Aβ peptide deposition in AD brain. Our results suggest that the VEGF receptor subtype Flt-1 serves as a microglial chemotactic receptor to mobilize these immune cells in proximity to peptide deposits yielding localized and amplified inflammatory microenvironments in AD brain. Importantly, such microenvironments may be neurotoxic since we provide evidence that Flt-1-dependent mobilization of microglia is associated with neurodegeneration.

The conclusions stated above are supported by the findings that Flt-1 are up-regulated under three independent experimental conditions; in AD cortical brain tissue, following intra-hippocampal injection of $A\beta_{1-42}$ in rat brain and after peptide stimulation of human microglia. This work has directly demonstrated involvement of Flt-1 in mediating microglial chemotactic responses *in vivo* and *in vitro*, in response to peptide stimulation. Importantly, anti-Flt-1 Ab was found effective in inhibiting mobility of EGFP-labelled microglia induced by $A\beta_{1-42}$ injection into rat hippocampus and attenuating mobility of cultured microglia responding to a transwell insert of peptide. Previous work, using the murine microglial cell line (BV-2), has reported increased cell migration in response to VEGF (Forstreuter et al., 2002). Since VEGF is also a potent factor for induction of neovasculature, the present data also suggest microglial chemokine activity may be associated with vascular remodeling in AD brain, a point discussed below.

An important finding was that microglia obtained from AD brain samples exhibited significantly higher expressions and levels of Flt-1 and ligand VEGF relative to ND brain tissue. Double staining showed little or no localization of either Flt-1 or VEGF with HLA-DR (+)ve microglia in ND sections. A very different result was obtained in AD brain tissue where considerable Flt-1 and VEGF ir was associated with microglia. These data could indicate that in AD, enhanced Flt-1 and VEGF expression contributes to microglial autocrine and paracrine processes. Thus, β-amyloid peptide not only induces chemotaxis in AD brain but also acts to amplify responses resulting in microgliosis. Our results also demonstrate considerable extents of Flt-1 and VEGF ir co-localized with peptide. Since both factors are associated with microglia (Fig. 5-1), these data imply clusters of mobile microglial cells in proximity to peptide deposits.

In vivo, intra-hippocampal injection of $A\beta_{1-42}$ caused a time-dependent (1-7 d) increase in expression of Flt-1 as measured using RT-PCR or immunohistochemical staining (Fig. 5-3).

Double staining analysis demonstrated a predominant association of Flt-1 with microglia, however, a smaller extent of Flt-1 localization to astrocytes was also evident. At 7 d post-peptide injection, significant increases of microgliosis and neuronal damage were measured relative to controls (injection of PBS or reverse peptide, $A\beta_{42-1}$). A novel finding was that the inclusion of anti-Flt-1 Ab with peptide, inhibited microgliosis and conferred partial neuroprotection. These results suggest blocking peptide-induced microglial migration as a rationale strategy to attenuate neuronal damage in AD brain.

To examine functional roles of Flt-1 *in vivo*, EGFP-labeled microglia were transplanted into rat hippocampus previously injected with $A\beta_{1-42}$, or reverse $A\beta_{42-1}$, peptide. Three areas, differentially located between sites of microglial transplantation and peptide injection, were used to quantify microglial mobility. In the presence of reverse peptide, no net migration of EGFP-microglia away from the transplantation site was evident. However, with $A\beta_{1-42}$ as a chemotactic stimulus, microglia exhibited increased mobility into parenchymal areas directed towards the peptide-injection site. Treatment of peptide-injected brain with anti-Flt-1 Ab was highly effective in reducing the numbers of migrating EGFP-microglia in all three regions between sites of microglial transplantation and peptide injection. Double staining analysis showed considerable extents in overlaps of EGFP microglial marker with both Flt-1 and VEGF.

Anti-Flt-1 Ab was also effective in inhibiting the migration of human microglia *in vitro,* where supernatants (conditioned medium) from cells exposed to PBS, $A\beta_{1-42}$ and $A\beta_{42-1}$ were employed as stimulants. Under control conditions, neither PBS nor reverse peptide were effective in the induction of microglial mobility. With $A\beta_{1-42}$ as a stimulus, a markedly increased migration was evident (by 4-fold) relative to PBS; this enhanced migration was reduced with inclusion of anti-Flt-1 Ab treatment with peptide. However, anti-Flt-1 Ab was only partially effective in the inhibition of microglial chemotactic response. This latter result could reflect that under the experimental conditions of this assay, factors in the conditioned medium, other than VEGF, could also contribute to the increased mobility of microglia.

The possibility that accumulation of peptide could serve as foci for the induction of microglial-mediated inflammatory paracrine responses involving VEGF is an important consideration in the pathology of AD. Previous work has reported elevated levels of VEGF in AD brain (Kalaria et al., 1998). Since VEGF is a highly potent vascular mediator, our results suggest the possibility of vascular remodeling near sites of microgliosis, elevated VEGF and peptide deposits. It has been pointed out that vascular angiogenic factors are elevated in AD

pathology (Vagnucci and Li, 2003; Pogue and Lukiw, 2004), however, despite this finding there is little evidence for formation of new blood vessels in AD diagnosed individuals. Instead, vasculature in AD brain exhibits considerable morphological abnormalities and increased permeability and leakage of BBB (Prat et al., 2001; de la Torre, 2002; Fiala et al., 2002; Zlokovic, 2005; Zipser et al., 2007). Our results could help account for this discrepancy. The lack of neovascularization in AD brain, despite elevated levels of angiogenic inducers, may be explained by a progressive and concomitant increase in an inflammatory environment causing newly formed blood vessels to degenerate.

Deposition of amyloid beta peptide is a critical stimulus for inflammation in AD brain (Combs et al., 2001; Lue et al., 2001). We postulate that peptide deposits act as foci for assimilating clusters of mobile activated microglia and serving as sites for vascular remodeling in sustaining inflammatory environments. Microglial Flt-1 and VEGF are suggested as primary, but clearly not as sole, factors in maintaining chronic inflammatory responses dealing with removal of unwanted peptide. Although intra-hippocampal peptide injection represents an acute insult, the procedure exacerbates inflammatory responses and likely compresses inflammation in this animal model into a much shorter timeframe (days) compared with the slow progression of inflammation (years) evident in AD brain. This point is testable in future studies using transgenic mouse models of AD where it is predicted that aged animals (months) will exhibit Flt-1 and VEGF microglial-dependent chemotactic processes with anti-Flt-1 Ab effective in inhibiting microgliosis and conferring neuroprotection.

5.5 REFERENCES

Aarum J, Sandberg K, Haeberlein SL, Persson MA (2003) Migration and differentiation of neural precursor cells can be directed by microglia. Proc Natl Acad Sci U S A 100:15983-15988.

Akiyama H, Mori H, Saido T, Kondo H, Ikeda K, McGeer PL (1999) Occurrence of the diffuse amyloid beta-protein (Abeta) deposits with numerous Abeta-containing glial cells in the cerebral cortex of patients with Alzheimer's disease. Glia 25:324-331.

Ambati BK, Nozaki M, Singh N, Takeda A, Jani PD, Suthar T et al. (2006) Corneal avascularity is due to soluble VEGF receptor-1. Nature 443:993-997.

Arai T, Miklossy J, Klegeris A, Guo JP, McGeer PL (2006) Thrombin and prothrombin are expressed by neurons and glial cells and accumulate in neurofibrillary tangles in Alzheimer disease brain. J Neuropathol Exp Neurol 65:19-25.

Barleon B, Sozzani S, Zhou D, Weich HA, Mantovani A, Marme D (1996) Migration of human monocytes in response to vascular endothelial growth factor (VEGF) is mediated via the VEGF receptor flt-1. Blood 87:3336-3343.

Bates DO, Lodwick D, Williams B (1999) Vascular endothelial growth factor and microvascular permeability. Microcirculation. 6:83-96.

Casolini P, Domenici MR, Cinque C, Alemà GS, Chiodi V, Galluzzo M, Musumeci M, Mairesse J, Zuena AR, Matteucci P, Marano G, Maccari S, Nicoletti F, Catalani A (2007) Maternal exposure to low levels of corticosterone during lactation protects the adult offspring against ischemic brain damage. J Neurosci 27:7041-7046.

Choi SH, Lee DY, Kim SU, Jin BK (2005) Thrombin-induced oxidative stress contributes to the death of hippocampal neurons in vivo: role of microglial NADPH oxidase. J Neurosci 25:4082-4090.

Choi HB, Ryu JK, Kim SU, McLarnon JG (2007) Modulation of the purinergic P2X7 receptor attenuates lipopolysaccharide-mediated microglial activation and neuronal damage in inflamed brain. J Neurosci 27:4957-4968.

Combs CK, Karlo JC, Kao SC, Landreth GE (2001) beta-Amyloid stimulation of microglia and monocytes results in TNFalpha-dependent expression of inducible nitric oxide synthase and neuronal apoptosis. J Neurosci 21:1179-1188.

de la Torre JC (2002) Vascular basis of Alzheimer's pathogenesis. Ann N Y Acad Sci 977:196-215.

De Bandt M, Ben Mahdi MH, Ollivier V, Grossin M, Dupuis M, Gaudry M, Bohlen P, Lipson KE, Rice A, Wu Y, Gougerot-Pocidalo MA, Pasquier C (2003) Blockade of vascular endothelial growth factor receptor I (VEGF-RI), but not VEGF-RII, suppresses joint destruction in the K/BxN model of rheumatoid arthritis. J Immunol 171:4853-4859.

Feistritzer C, Kaneider NC, Sturn DH, Mosheimer BA, Kahler CM, Wiedermann CJ (2004) Expression and function of the vascular endothelial growth factor receptor FLT-1 in human eosinophils. Am J Respir Cell Mol Biol 30:729-735.

Ferrara N, Chen H, Davis-Smyth T, Gerber HP, Nguyen TN, Peers D, Chisholm V, Hillan KJ, Schwall RH (1998) Vascular endothelial growth factor is essential for corpus luteum angiogenesis. Nat Med. 4:336-340.

Ferrara N, Gerber HP, LeCouter J (2003) The biology of VEGF and its receptors. Nat Med 9:669-676.

Fiala M, Liu QN, Sayre J, Pop V, Brahmandam V, Graves MC, Vinters HV (2002) Cyclooxygenase-2-positive macrophages infiltrate the Alzheimer's disease brain and damage the blood-brain barrier. Eur J Clin Invest 32: 360-371.

Franciosi S, Ryu JK, Choi HB, Radov L, Kim SU, McLarnon JG (2006) Broad-spectrum effects of 4-aminopyridine to modulate amyloid beta1-42-induced cell signaling and functional responses in human microglia. J Neurosci 26:11652-11664.

Feistritizer C, Kaneider NC, Sturn DH, Mosheimer BA, Kahler CM and Wiedermann CJ (2004) Expression and function of the vascular endothelial growth factor receptor Flt-1 in human eosinophils. Am J Respir Cell Mol Biol 30:729-735.

Forstreuter F, Lucius R, Mentlein R (2002) Vascular endothelial growth factor induces chemotaxis and proliferation of microglial cells. J Neuroimmunol 132:93-98.

Guo JP, Arai T, Miklossy J, McGeer PL (2006) Abeta and tau form soluble complexes that may promote self aggregation of both into the insoluble forms observed in Alzheimer's disease. Proc Natl Acad Sci U S A 103:1953-1958.

Hardy J, Selkoe DJ (2002) The amyloid hypothesis of Alzheimer's disease: progress and problems on the road to therapeutics. Science 297:353-356.

Hoshino M, Takahashi M, Aoike N (2001) Expression of vascular endothelial growth factor, basic fibroblast growth factor, and angiogenin immunoreactivity in asthmatic airways and its relationship to angiogenesis. J Allergy Clin Immunol 107:295-301.

Insausti R, Tuñón T, Sobreviela T, Insausti AM, Gonzalo LM (1995) The human entorhinal cortex: a cytoarchitectonic analysis. J Comp Neurol 355:171-198.

Kalaria RN, Cohen DL, Premkumar DR, Nag S, LaManna JC, Lust WD (1998) Vascular endothelial growth factor in Alzheimer's disease and experimental cerebral ischemia. Brain Res Mol Brain Res 62:101-105.

Leung DW, Cachianes G, Kuang WJ, Goeddel DV, Ferrara N (1989) Vascular endothelial growth factor is a secreted angiogenic mitogen. Science 246:1306-1309.

Lue LF, Rydel R, Brigham EF, Yang LB, Hampel H, Murphy GM Jr, Brachova L, Yan SD, Walker DG, Shen Y, Rogers J (2001) Inflammatory repertoire of Alzheimer's disease and nondemented elderly microglia in vitro. Glia 35:72-79.

Matsunaga Y, Saito N, Fujii A, Yokotani J, Takakura T, Nishimura T, Esaki H, Yamada T (2002) A pH-dependent conformational transition of Abeta peptide and physicochemical properties of the conformers in the glial cell. Biochem J 361:547-556.

McLarnon JG, Ryu JK, Walker DG, Choi HB (2006) Upregulated expression of purinergic P2X(7) receptor in Alzheimer disease and amyloid-beta peptide-treated microglia and in peptide-injected rat hippocampus. J Neuropathol Exp Neurol 65:1090-1097.

Millauer B, Wizigmann-Voos S, Schnurch H, Martinez R, Moller NP, Risau W, Ullrich A (1993) High affinity VEGF binding and developmental expression suggest Flk-1 as a major regulator of vasculogenesis and angiogenesis. Cell 72:835-846.

Mrak RE, Griffin WS (2007) Common inflammatory mechanisms in Lewy body disease and Alzheimer disease. J Neuropathol Exp Neurol 66:683-686.

Murakami M, Iwai S, Hiratsuka S, Yamauchi M, Nakamura K, Iwakura Y, Shibuya M (2006) Signaling of vascular endothelial growth factor receptor-1 tyrosine kinase promotes rheumatoid arthritis through activation of monocytes/macrophages. Blood 108:1849-1856.

Pogue AI, Lukiw WJ (2004) Angiogenic signaling in Alzheimer's disease. Neuroreport 15:1507-1510.

Prat A, Biernacki K, Wosik K. Antel JP (2001) Glial cell influence on the human blood-brain barrier. Glia 36: 145-155.

Ryu JK, Franciosi S, Sattayaprasert P, Kim SU, McLarnon JG (2004) Minocycline inhibits neuronal death and glial activation induced by beta-amyloid peptide in rat hippocampus. Glia 48:85-90.

Ryu JK, Kim J, Cho SJ, Hatori K, Nagai A, Choi HB, Lee MC, McLarnon JG, Kim SU (2004) Proactive transplantation of human neural stem cells prevents degeneration of striatal neurons in a rat model of Huntington disease. Neurobiol Dis 16:68-77.

Ryu JK, McLarnon JG (2006) Minocycline or iNOS inhibition block 3-nitrotyrosine increases and blood-brain barrier leakiness in amyloid beta-peptide-injected rat hippocampus. Exp Neurol 198:552-557.

Ryu JK, McLarnon JG (2007) Thalidomide inhibition of perturbed vasculature and glial-derived tumor necrosis factor-α in an animal model of inflamed Alzheimer's disease brain. Neurobiol Dis doi:10.1016/j.nbd.2007.08.019.

Ryu JK, Tran KC, McLarnon JG (2007) Depletion of neutrophils reduces neuronal degeneration and inflammatory responses induced by quinolinic acid in vivo. Glia 55:439-451.

Skarsgard ED, Huang L, Reebye SC, Yeung AY, Jia WW (2005) Lentiviral vector-mediated, in vivo gene transfer to the tracheobronchial tree in fetal rabbits. J Pediatr Surg 40:1817-1821.

Sköld MK, von Gertten C, Sandberg-Nordqvist AC, Mathiesen T, Holmin S (2005) VEGF and VEGF receptor expression after experimental brain contusion in rat. J Neurotrauma. 22:353-367.

Spires TL, Meyer-Luehmann M, Stern EA, McLean PJ, Skoch J, Nguyen PT, Bacskai BJ, Hyman BT (2005) Dendritic spine abnormalities in amyloid precursor protein transgenic mice demonstrated by gene transfer and intravital multiphoton microscopy. J Neurosci 25:7278-7287.

Tran KC, Ryu JK, McLarnon JG (2005) Induction of angiogenesis by platelet-activating factor in the rat striatum. Neuroreport 16:1579-1583.

Vagnucci AH, Li WW (2003) Alzheimer's disease and angiogenesis. Lancet. 361:605-608.

Walker DG, Link J, Lue LF, Dalsing-Hernandez JE, Boyes BE (2006) Gene expression changes by amyloid beta peptide-stimulated human postmortem brain microglia identify activation of multiple inflammatory processes. J Leukoc Biol 79:596-610.

Yano K, Liaw PC, Mullington JM, Shih SC, Okada H, Bodyak N, Kang PM, Toltl L, Belikoff B, Buras J, Simms BT, Mizgerd JP, Carmeliet P, Karumanchi SA, Aird WC (2006) Vascular endothelial growth factor is an important determinant of sepsis morbidity and mortality. J Exp Med 203:1447-1458.

Zand L, Ryu JK, McLarnon JG (2005) Induction of angiogenesis in the beta-amyloid peptide-injected rat hippocampus. Neuroreport 16:129-132.

Zipser BD, Johanson CE, Gonzalez L, Berzin TM, Tavares R, Hulette CM, Vitek MP, Hovanesian V, Stopa EG (2007) Microvascular injury and blood-brain barrier leakage in Alzheimer's disease. Neurobiol Aging 28:977-986.

CHAPTER 6: SUMMARY AND CONCLUSIONS, SCHEMATIC DIAGRAM, SIGNIFICANCE AND FUTURE DIRECTIONS OF RESEARCH AND CONCLUDING REMARKS

6.1 OVERALL SUMMARY AND CONCLUSIONS

Chronic inflammation is an ongoing process associated with many types of sustained insults and injuries. This study suggests that chronic inflammation may be a specific causative process in the progressive loss of hippocampal and cortical neurons in AD. A critical question to ask is how inflammation might be linked to the progressive neuronal loss and the cognitive decline in AD. The studies presented in this thesis have attempted to answer this question using a spectrum of *in vivo* and *in vitro* methods for characterizing microglial signaling in inflamed AD brain. In particular, this research has focused on the interactions of microglia and the vasculature as a basis for chronic inflammation using $A\beta_{1-42}$ intrahippocampal injection as an *in vivo* animal model of inflamed AD brain. In addition, *in vitro* experiments were carried out using RT-PCR and chemotactic assays to study functional responses of microglial activation following $A\beta_{1-42}$ stimulation. The central hypothesis of this research is that $A\beta_{1-42}$-induced microglial activation causes vascular remodeling associated with angiogenic activity and BBB leakiness which sustain chronic inflammation. Furthermore, my data suggests that chronic inflammation contributes to neuronal damage. Pharmacological modulations of interactions between reactive microglia and perturbed vasculature were investigated for their potential use in therapeutic intervention to decrease chronic inflammation and provide neuroprotection in the animal model. A series of linked experimental studies, summarized below, were performed to test the hypothesis.

6.1.1 *Aβ-induced gliosis and perturbation of BBB*

First, I investigated the effect of *in vivo* $A\beta_{1-42}$ injection on inflammatory responses and intactness of BBB using immunohistochemical methods. Intrahippocampal administration of $A\beta_{1-42}$ caused upregulation of peroxynitrite formation in glia, microglia and astrocytes. Pharmacological inhibition of glial-derived reactive nitrogen species with the broad-spectrum anti-inflammatory agent minocycline or the selective iNOS inhibitor 1400W was highly effective in decreasing levels of nitrotyrosine. Immunohistochemical results showed IgG permeability through BBB was markedly increased with $A\beta_{1-42}$ injection and both minocycline and 1400W were highly effective in restoring the integrity of the BBB. My conclusion from

these results is that glial activation and the consequent increase in oxidative stress mediate the deleterious effect of $A\beta_{1-42}$ on BBB integrity.

6.1.2 *Thalidomide inhibits Aβ-induced microglial and vascular responses*

The results discussed above indicate that $A\beta_{1-42}$ deposition could have significant effects on integrity of BBB and involve glial activation. These findings suggested the utility of pharmacological modulation of glial-vasculature interactions with a modulator of inflammation and vasculature. I chose thalidomide since the compound has been shown to exhibit anti-angiogenic actions on vascular processes. Double immunofluorescent staining indicated that $A\beta_{1-42}$-induced microglial activation was associated with altered vascular function. The latter included upregulation of vascular matrix protein laminin, which suggested formation of new blood vessels (angiogenesis). In addition, by infusing FITC-labeled albumin in animals with intrahippocampal peptide injection, I was able to demonstrate albumin fluorescence in brain parenchyma in proximity to blood vessels. These data strongly suggest a weakened BBB in a peptide-injected animal model of AD. Thalidomide treatment was found effective in decreasing angiogenic activity, reducing albumin fluorescence intensity indicating increased intactness of BBB and attenuating activation of microglia. Thalidomide applied *in vitro*, to human adult microglia reduced TNF-α expression induced by cell exposure to $A\beta_{1-42}$. These studies established that $A\beta_{1-42}$-induced glial activation could alter vascular function and that thalidomide could serve as an immunomodulatory agent acting to modify $A\beta_{1-42}$-induced inflammation. Furthermore, thalidomide showed neuroprotection *in vivo* and which was associated with reduced microgliosis and vascular alterations. The overall results of this work indicate perturbations in vasculature as an integral component of inflammatory response following intra-hippocampal injection of $A\beta_{1-42}$ peptide.

6.1.3 *Microglial reactivity and leak BBB in AD*

The findings from the previous studies point to vascular remodeling and plasma protein extravasation as a component of inflammatory response in peptide-injected rat hippocampus. This possibility was examined by measurement of the levels of extravasated plasma protein fibrinogen in AD and ND (nondemented) brain tissues and *in vivo* in $A\beta_{1-42}$ injected rat hippocampus. Immunohistochemical analysis showed enhanced immunoreactivity (ir) of parenchymal fibrinogen and also populations of reactive and proliferating microglia in brain

tissue from AD patients compared with ND individuals. Infiltration of fibrinogen, extents of microgliosis and neuronal viability in rat hippocampus were then measured after intrahippocampal injection of $A\beta_{1-42}$ peptide. A particular focus of these experiments was the study of effects of pharmacological modulations targeting reduction in levels of fibrinogen (using the defibrinogenating compound ancrod) or inhibition of microglial activation (using the monoclonal antibody, anti-Mac-1). The increased leakiness of BBB induced by peptide stimulation was decreased with depletion of fibrinogen with ancrod. Microglial activation and neuronal injury were significantly reduced in rat hippocampus after ancrod treatment. A novel additional finding was the increased microglial activation and proliferation and enhanced BBB damage with fibrinogen injection with peptide. Under these conditions, the microglial inhibitor anti-Mac-1 Ab was effective to attenuate the changes in gliosis and vascular processes. The results of this study support the notion that extravasation of the plasma protein fibrinogen as an inflammatory component in AD brain.

6.1.4 *VEGF receptor Flt-1 mediates microglial chemotactic inflammatory responses in AD*

The previous studies suggested microglial inflammatory responses induced by peptide contribute to vascular abnormalities and neuronal damage. An important question concerning increased microglial reactivity induced by peptide deposits was addressed by measuring in vitro and in vivo chemotactic responses of microglia to $A\beta_{1-42}$. One potential chemotactic factor is VEGF (vascular endothelial growth factor) which also serves as an angiogenic stimulus. Intra-hippocampal injection of $A\beta_{1-42}$ caused an increased level of VEGF receptor-1 (Flt-1) expression in activated microglia. Treatment using the neutralizing antibody (anti-Flt-1) decreased peptide-induced microgliosis. An interesting finding was that neuronal loss was also significantly decreased by inhibition of Flt-1 in microglia. *In vitro*, a transwell migration assay showed anti-Flt-1 treatment reduced peptide-induced chemotactic microglial migration. Additionally, immunohistochemical analysis, using a specific anti-GFP antibody for transplanted GFP-labeled microglia, showed that treatment of peptide-injected brain with anti-Flt-1 Ab was highly effective in reducing the numbers of migrating GFP-microglia. Disease-related change of Flt-1 expression was examined in AD brain using RT-PCR and immunohistochemical analysis. The results showed human adult microglia obtained from AD patients exhibit significantly higher mRNA and protein expression levels of Flt-1 and ligand VEGF relative to ND brain tissue.

Overall, these data suggest that upregulated expression of Flt-1 could contribute to microglial chemotactic responses in the chronic inflammatory processes of AD.

The results summarized above demonstrate that $A\beta_{1-42}$-induced increases in microglial reactivity have significant impact on angiogenic activity and vascular permeability. These findings establish perturbed blood vessels as a critical component of inflammatory responses which help sustain increases in microglial activation. Pharmacological compounds directed at specific components of microglial-vascular interactions were found to inhibit inflammation and provide neuroprotection.

6.2 SCHEMATIC FLOW DIAGRAM OF CHRONIC INFLAMMATION

A summary schematic diagram that incorporates the findings of the studies described above is shown in Figure 6. In the diagram, Aβ is the stimulus to initially enhance microglial mobility leading to localized cell clustering in proximity to the peptide deposits. Subsequent inflammatory responses include interactions between microglia and vasculature which leads to vascular remodeling comprising neovascularization and BBB leakiness. Increased BBB permeability leads to infiltration of plasma proteins and possibly other immune cells such as macrophages and neutrophils. The overall processes result in a chronic inflammatory microenvironment consisting of activated microglia and a milieu of proinflammatory factors. When the inflammatory response is maintained, an assemblage of inflammatory mediators are released, such as reactive oxygen and nitrogen species from the activated microglia, to ultimately contribute to the slow, progressive neurodegeneration seen in the AD brain. The general hypothesis is that reciprocal interactions occur between activated microglia and perturbed vasculature in Aβ-injected brain to drive the chronic inflammatory responses.

This schematic flow chart is consistent with risk factor enhancement characteristic of AD pathology. For example, as noted in the introduction, many vascular risk factors have been reported including hypertension, hypercholesterolemia, diabetes mellitus and smoking. Presumably these risk factors contribute to abnormalities in vasculature which amplify immune responses. Furthermore, aging is a primary risk factor which could promote inflammation in AD brain. Blood vessels in aged AD individuals show a spectrum of abnormalities which could be manifest as the latter stages of vascular remodeling which resulted from initial neovascularization and leakiness to plasma proteins. By necessity, the summary schematic flow chart shown in Fig. 6 represents a simplified overview of chronic inflammation in AD.

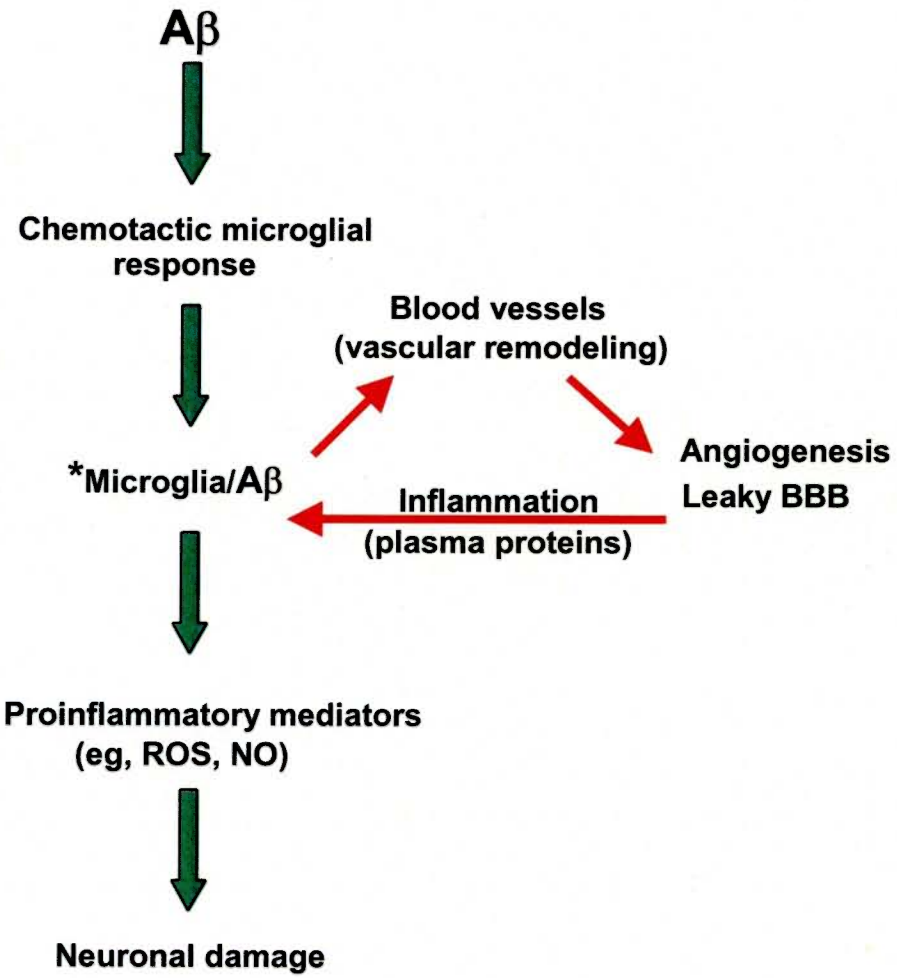

Figure 6. Schematic flow chart for Aβ-mediated chronic inflammation and neuronal damage in AD pathology. * Pool of reactive microglia with Aβ deposits. ROS: reactive oxygen species. NO: nitric oxide.

A number of interactive processes have not been included which could contribute to inflammation in AD. For example, direct effects of Aβ peptide on astrocytes and endothelial cells are not included in the diagram. As noted below, future studies need to address other interactions and other inflammatory factors which could contribute to sustaining chronic inflammation.

6.3 SIGNIFICANCE OF WORK

At present, it is not well understood how chronic inflammation is linked to neuronal damage in AD. Indeed, the limited utility of anti-inflammatory compounds such as NSAIDs have led to questions concerning whether chronic inflammation even plays a significant role in AD pathology. The present results would argue that NSAIDs may be relatively ineffective since they do not modify microglial-vasculature interactions. The studies presented in this thesis provide novel *in vivo* and *in vitro* findings that link chronic inflammatory responses, angiogenic activity, BBB intactness, and neuronal viability, in conditions that resemble those of the AD brain. These results should lead to a greater understanding of how chronic inflammation in the AD brain causes neuronal damage. The development of multidrug therapy, aimed at multiple mechanisms in the chronic inflammation of AD pathology, may be more efficacious than therapy aimed at inhibiting a single pathway. Overall, the findings reported in this thesis suggest that pharmacological inhibition of microglial-vasculature interactions and microglial chemotactic responses as novel strategies for protecting neurons in AD brain.

6.4 OUTLINE OF FUTURE WORK

The findings of this thesis suggest that microglial inflammatory responses are putative causative components in the progressive loss of hippocampal neurons in AD. In addition, the results provide a framework for future studies for addressing the mechanisms by which microglial-vascular interactions are linked to neuroprotection in AD. An important area of study is the use of transgenic animal models of AD. A number of these models show aged transgenic animals to exhibit considerable extents of chronic inflammation. Proposed studies would include measurements of pharmacological modulation of microglial and vascular responses and interactions in transgenic animal models of AD as maneuvers for decreasing neuronal damage and enhancing cognitive performance. Additional analysis, using specific markers for the integrity of BBB in AD brain, is required. An important question to be answered is does the neovascularization we observe following peptide injection represent an early stage of vascular

remodeling which subsequently presents as abnormal vessels in an environment of chronic inflammation in AD.

It is important to point out that some microglial responses may have beneficial effects in AD (Wyss-Coray, 2006; Simard and Rivest, 2006). In particular, these studies suggest microglial acute responses may be beneficial. However, at this time it is unclear if acute and chronic inflammatory responses lead to respective, primary helpful and harmful, effects. In addition, a great deal of ongoing work is directed in evaluation of the effects of directly inducing inflammatory responses using peptide vaccination. The rationale is that passive or active vaccination could clear plaque deposits by causing an immune response. At present, this approach has led to both favorable and unfavorable outcomes for AD patients (Ferrer et al., 2004; Masliah et al., 2005).

6.5 CONCLUDING REMARKS

AD is a devastating neurodegenerative disease affecting large numbers of elderly people. Although the impact of AD on patients, their families, and society in general is likely to increase as the population ages, current treatment options are limited because of the lack of understanding in the pathophysiology of AD. A basic requirement is to first understand the mechanisms underlying disease progression before potential therapeutic targets can be found for AD treatment. The work discussed in this thesis contributes to ongoing efforts aimed at understanding and characterizing the mechanisms leading to chronic inflammation of AD. A better understanding of the underlying mechanisms of chronic inflammation as well as intervention with pharmacological agents to reduce cell activation and vascular abnormalities will constitute an important step forward in treatment of AD individuals.

6.6 REFERENCES

Wyss-Coray T. 2006. Inflammation in Alzheimer disease: driving force, bystander or beneficial response? Nat Med 12:1005-1015.

Simard AR, Rivest S. 2006. Neuroprotective properties of the innate immune system and bone marrow stem cells in Alzheimer's disease. Mol Psychiatry 11:327-335.

Ferrer I, Boada Rovira M, Sánchez Guerra ML, Rey MJ, Costa-Jussá F. 2004. Neuropathology and pathogenesis of encephalitis following amyloid-beta immunization in Alzheimer's disease. Brain Pathol 14:11-20.

Masliah E, Hansen L, Adame A, Crews L, Bard F, Lee C, Seubert P, Games D, Kirby L, Schenk D. 2005. Abeta vaccination effects on plaque pathology in the absence of encephalitis in Alzheimer disease. Neurology 64:129-131.

CHAPTER 7: APPENDIX

A copy of the UBC animal care committee approval letter and research approval letter from UBC clinical research ethics board

The University of British Columbia

ANIMAL CARE CERTIFICATE

PROTOCOL NUMBER: **A02-0277**

INVESTIGATOR OR COURSE DIRECTOR: **McLarnon, J.G.**

DEPARTMENT: **Pharmacology/Therapeutics**

PROJECT OR COURSE TITLE: **Studies on the role of microglia in beta-amyloid injected hippocampus: Implication in Alzheimer's disease**

ANIMALS: **Rats 228**

START DATE: **03-03-01** APPROVAL DATE: **April 26, 2004**

FUNDING AGENCY: **Alzheimer Society of Canada**

The Animal Care Committee has examined and approved the use of animals for the above experimental project or teaching course, and have been given an assurance that the animals involved will be cared for in accordance with the principles contained in Care of Experimental Animals - A Guide for Canada, published by the Canadian Council on Animal Care.

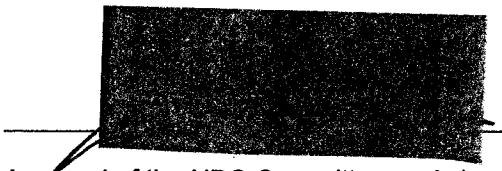

Approval of the UBC Committee on Animal Care by one of:
Dr. W.K. Milsom, Chair
Dr. J. Love, Director, Animal Care Centre
Ms. L. Macdonald, Manager, Animal Care Committee

This certificate is valid for one year from the above start or approval date (whichever is later) provided there is no change in the experimental procedures. Annual review is required by the CCAC and some granting agencies.

A copy of this certificate must be displayed in your animal facility.

Office of Research Services and Administration
102, Agronomy Road, Vancouver, V6T 1Z3
Phone: 604-827-5111 FAX: 604-822-5093

The University of British Columbia
Office of Research Services,
Clinical Research Ethics Board – Room 210, 828 West 10th Avenue, Vancouver, BC
V5Z 1L8

Certificate of Expedited Approval: Renewal

Clinical Research Ethics Board Official Notification

PRINCIPAL INVESTIGATOR	DEPARTMENT	NUMBER
McLarnon, J.G.	Pharmacology/Therapeutics	C99-0298

INSTITUTION(S) WHERE RESEARCH WILL BE CARRIED OUT
UBC Campus

CO-INVESTIGATORS:

SPONSORING AGENCIES
Alzheimer Society of Canada

TITLE: Effects of Beta Amyloid on Currents and Ca2+ in Human Microglia

APPROVAL RENEWAL DATE	TERM (YEARS)	AMENDMENT:	AMENDMENT APPROVED:
May 12 2004	1		

CERTIFICATION:
In respect of clinical trials:
1. The membership of this Research Ethics Board complies with the membership requirements for Research Ethics Boards defined in Division 5 of the Food and Drug Regulations.
2. The Research Ethics Board carries out its functions in a manner consistent with Good Clinical Practices.
3. This Research Ethics Board has reviewed and approved the clinical trial protocol and informed consent form for the trial which is to be conducted by the qualified investigator named above at the specified clinical trial site. This approval and the views of the this Research Ethics Board have been documented in writing.

The Chair of the UBC Clinical Research Ethics Board has reviewed the documentation for the above named project. The research study, as presented in the documentation, was found to be acceptable on ethical grounds for research involving human subjects and was approved for renewal by the UBC Clinical Research Ethics Board.

The CREB approval for renewal of this study expires one year from the date of renewal.

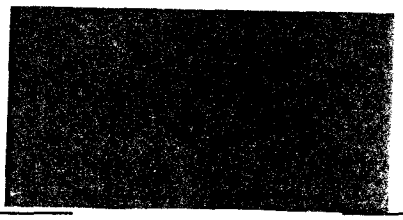

Approval of the Clinical Research Ethics Board by one of:
Dr. P. Loewen, Chair
Dr. Alain Gagnon, Associate Chair
Dr. James McCormack, Associate Chair